European Journal of Taxonomy 1006: 1–58
https://doi.org/10.5852/ejt.2025.1006.2989

europeanjournaloftaxonomy.eu
ISSN 2118-9773
2025 · Mamani V. *et al.*

Received: 3 December 2024 • *Accepted: 7 April 2025* • *Published: 1 August 2025*

Topic editor: Magalie Castelin • *Section editor: Arnaud Henrard* • *Desk editor: Pepe Fernández*

Monograph

urn:lsid:zoobank.org:pub:E4FAF05B-5420-42B0-AB8D-5870FD3E370A

Notes on African Biantinae with sexual dimorphism in leg II: five new *Metabiantes* species and redescription of *Clinobiantes paradoxus* (Opiliones: Laniatores: Biantidae)

Vanesa MAMANI [1,*], Merlijn JOCQUÉ [2] & Abel PÉREZ-GONZÁLEZ [3]

[1,3]División Aracnología, Museo Argentino de Ciencias Naturales "Bernardino Rivadavia", Av. Angel Gallardo 470, C1405DJR, Buenos Aires, Argentina.
[1]Departamento de Biodiversidad y Biología Experimental, Facultad de Ciencias Exactas y Naturales, Universidad de Buenos Aires, Av. Int. Güiraldes s/n, Ciudad Universitaria, C1428EHA, Buenos Aires, Argentina.
[2]Aquatic and Terrestrial Ecology (ATECO), Royal Belgian Institute of Natural Sciences (RBINS), Vautierstraat 29, 1000 Brussels, Belgium.

[*]Corresponding author: lic988vane@gmail.com
[2]Email: merlijnjocque@gmail.com
[3]Email: abelaracno@gmail.com

Abstract. This study deals with a group of African biantines harvestmen (Biantidae: Biantinae) that exhibit a unique sexual dimorphism on legs II, where the males possess a widened femur II and metatarsus II armed with ventral rows of triangular tubercles. *Clinobiantes paradoxus* Roewer, 1927, is redescribed and illustrated, including detailed illustrations and descriptions of the male and female genital morphology based on an examination of type material, with a lectotype designated herein. In addition, five new species of *Metabiantes* Roewer, 1915, also with dimorphic legs II, from tropical African countries are described and illustrated in detail: *M. elongatus* sp. nov., *M. serratus* sp. nov., and *M. kivuensis* sp. nov. from Democratic Republic of the Congo, *M. herculeus* sp. nov. from Tanzania, and *M. kaurii* sp. nov. from Mozambique. These findings enhance our knowledge within *Metabiantes* diversity, provide new insights into the distribution of Biantidae in tropical Africa, and highlight the morphological diversity associated with sexual dimorphism in the group.

Keywords. Harvestmen, taxonomy, leaf-litter-dwelling, canopy-dwelling, Central Africa.

Mamani V., Jocqué M. & Pérez-González A. 2025. Notes on African Biantinae with sexual dimorphism in leg II: five new *Metabiantes* species and redescription of *Clinobiantes paradoxus* (Opiliones: Laniatores: Biantidae). *Eusropean Journal of Taxonomy* 1006: 1–58. https://doi.org/10.5852/ejt.2025.1006.2989

Introduction

Biantinae Thorell, 1889, comprises 17 genera and 136 valid species (Kury *et al.* 2022). It is the most diverse subfamily within Biantidae Thorell, 1889, predominantly found in the Afrotropical and Indomalayan regions (Kury & Pérez-González 2007; Gong *et al.* 2018). Among the 11 Biantinae genera recorded in continental Africa, *Clinobiantes* Roewer, 1927, and *Metabiantes* Roewer, 1915, are two morphologically similar and poorly defined genera.

With 40 described species, *Metabiantes* is the most diverse genus of the subfamily. In contrast, *Clinobiantes*, with the only described species, *Clinobiantes paradoxus* Roewer, 1927, is one of the numerous monotypic biantid genera (Kury *et al.* 2022). The taxonomic delineation between *Metabiantes* and *Clinobiantes* remains ambiguous, highlighting the broader need for a systematic revision of African biantids. *Metabiantes* could currently be considered a 'basket genus', where lesser-defined and unrelated species are grouped. Originally, *Metabiantes* was erected by Roewer (1915) and defined by the absence of armature on mesotergal areas III and IV, the patella of the pedipalp possessing one mesodistal spine, and the tibia armed ventrally with two mesal and two ectal spines. *Clinobiantes* also erected by Roewer (1927), was differentiated from *Metabiantes* by the presence of armature in areas III and IV. However, this is not a valid diagnosis because the actual concept of *Metabiantes* includes species with (e.g., *M. insulanus* (Roewer, 1949), *M. leighi* (Pocock, 1902), *M. zuluanus* Lawrence, 1937, etc.) and without (e.g., *M. pusulosus* (Loman, 1898), *M. convexus* Roewer, 1949, *M. parvulus* Kauri, 1985, etc.) armature in mesotergal areas III and IV. These taxonomic inconsistencies hinder the formulation of a reliable diagnosis for both genera, underscoring the need to reassess their validity and establish a new diagnosis based on well-defined discriminant characteristics. However, achieving this goal requires a more comprehensive taxonomic and systematic review.

One of the most remarkable morphological characteristics of *Clinobiantes paradoxus* is the pronounced sexual dimorphism in the enlarged leg II of males. This dimorphism has also been observed in other biantid genera, including *Metabiantes* and *Biantessus* Roewer, 1949.

In *Metabiantes*, sexual dimorphism in leg II has been recorded in the type species, *Metabiantes pusulosus*, as well as unequivocally in four additional species: *M. machadoi* Lawrence, 1957, *M. obscurus* Kauri, 1961, *M. zuluanus* Lawrence, 1937, and *M. zuurbergianus* Kauri, 1961. Specimens (other than types or topotypes) of two species of *Metabiantes* – *M. convexus* Roewer, 1949, and *M. leighi* (Pocock, 1902) – have been recorded with this dimorphism, although further confirmation is required. For *Biantessus*, sexual dimorphism in leg II has been reported in *B. nigrotarsus* (Lawrence, 1933) and *B. vertebralis* (Lawrence, 1933). In all these species, the secondary sexual characteristic involves the male metatarsus II, which is sometimes thickened and consistently armed with ventral rows of tubercles (Lawrence 1937b). However, other podomeres may exhibit various morphological modifications among these species. For instance, male tibia II may be incrassate and ventrally armed with tubercles (e.g., *Biantessus nigrotarsus* and *Metabiantes zuluanus*) or incrassate and unarmed (e.g., *Metabiantes machadoi*). Notably, a swollen trochanter II has been observed in males of *Metabiantes pusulosus* and *Metabiantes zuluanus*, while a widened femur II has been reported in males of *Clinobiantes paradoxus* and *Metabiantes machadoi* (Loman 1898; Roewer 1927; Lawrence 1957; Kauri 1961). These variations in morphological features contribute to the complexity and diversity of the biantid genera. Despite the significant taxonomic importance of conspicuous morphology associated with the enlarged and sexually dimorphic legs II, the functional significance of these modifications remains unclear. A plausible hypothesis is that they play a role in mating behavior, intraspecific competition, or species recognition. Given the taxonomic inconsistencies in *Metabiantes* and *Clinobiantes*, further examination of male dimorphic traits could provide valuable insights into species boundaries and evolutionary relationships within Biantidae.

This work provides a revised description and detailed illustration of *Clinobiantes paradoxus*, based on a comprehensive review of the syntypes, along with the description of five new species of *Metabiantes* exhibiting sexual dimorphism in leg II, to enhance taxonomic understanding and the knowledge of diversity in certain biantids, particularly those displaying this unique type of sexual dimorphism in leg II.

Material and methods

Specimen repositories

The specimens examined in this study are deposited in the following institutions:

MACN = Museo Argentino de Ciencias Naturales "Bernardino Rivadavia", Buenos Aires, Argentina (M.J. Ramírez)
RMCA = Musée royal de l'Afrique centrale in Tervuren, Belgium (D. Van den Spiegel)
SMF = Senckenberg Naturmuseum und Forschungsinstitut, Frankfurt, Germany (P. Jäger)

Specimen preparations

Specimens were examined using a Leica M205A stereo microscope, and different focal plane pictures were taken with a Leica DF295 digital camera. Illustrations were performed on a Leica M165C stereoscopic microscope, equipped with a camera lucida. Male genitalia were prepared using glycerin as a clearing agent, following Acosta *et al.* (2007), and were drawn using a camera lucida attached to an Olympus BH-2 microscope. To expand male genitalia, it was placed firstly in hot lactic acid, followed by distilled water (Schwendinger & Martens 2002). Specimens intended for scanning electron microscopy (SEM) underwent sonication to remove particularly stubborn particles of dirt; they were submerged in a 5:1 (water: neutral detergent) solution, and ultrasound (Mini ULTRAsonik™ Ney) was applied. The cleaning progress was monitored every 20 seconds to ensure thorough cleanliness. Subsequently, the specimens were dissected, and for SEM samples, their appendages, bodies, and genitalia were dehydrated via 80%–90%–96%–100% ethanol series and affixed to aluminum stubs using conductive adhesive copper tape. The SEM samples were sputter-coated with 10 nm of gold and examined and photographed using both a Philips XL30 TMP New Look SEM microscope and a Zeiss GeminiSEM 360 microscope at MACN.

Drawings were vectorized, and plates were prepared in CorelDRAW Graphics Suite 2023 (ver. 24.3.0). The distribution map was created by SimpleMappr (Shorthouse 2010). Morphological nomenclature follows Kury & Pérez-González (2007), Kury & Medrano (2016), Wolff *et al.* (2016), Pérez-González & Werneck (2018), and Gnaspini & Rodrigues (2011), with minor modifications. Specifically, for the ovipositor, we refer to the sensilla as 'setae' and the sagittal groove as 'furcal groove'. The two apical lobes of the ovipositor are herein referred to as 'furca', as we consider them homologous to the ovipositor furca in Cyphophthalmi Simon, 1879 and Eupnoi Hansen & Sørensen, 1904 (Shultz & Pinto-da-Rocha 2007). Some new conventions were adopted here to describe the morphology of the penis. The medial cleft on the apical edge of the pars distalis is herein referred to as 'U-shaped cleft'. The laminar projections of the conductors are divided into three parts: 'dorsal fold', 'ventral fold', and 'lateral projection'. The male dimorphism concept (i.e., major males and minor males) follows Buzatto & Machado (2014) and herein is used as a putative condition because it was not quantitatively tested. Measurements are given in millimeters (mm).

Abbreviations used in the figures

As = astragalus
Ca = calcaneus
Co = conductor
DF = dorsal fold

FG = furcal groove
Fu = furca
L = lobe
LP = lateral projection
P = projection
PB = pars basalis
PD = pars distalis
S = seta
SrA = seminal receptacle area
St = stylus
Ti = titillator
Tr = truncus
VF = ventral fold

Results

Taxonomy

Class Arachnida Lamarck, 1801
Order Opiliones Sundevall, 1833
Suborder Laniatores Thorell, 1876
Infraorder Grassatores Kury, 2002
Superfamily Samooidea Sørensen, 1886
Family Biantidae Thorell, 1889
Subfamily Biantinae Thorell, 1889

Genus ***Clinobiantes*** Roewer, 1927

Clinobiantes Roewer, 1927: 302. Type species by monotypy: *Clinobiantes paradoxus* Roewer, 1927.

Clinobiantes – Roewer 1949: 249. — Staręga 1992: 323.

Includes species

Monotypic.

Distribution

Cameroon (Southwest Province), Equatorial Guinea (Corisco Island).

Remarks

Santos & Prieto (2009) recorded a *Clinobiantes* sp. for Equatorial Guinea, but the identity of this species has not been clarified yet.

Clinobiantes paradoxus Roewer, 1927
Figs 1, 3–6; Table 1

Clinobiantes paradoxus Roewer, 1927: 302, fig. 17.

Clinobiantes paradoxus – Staręga 1992: 323.

Type material

Lectotype here designated
CAMEROON • ♂; Bibundi; SMF 9900064 (examined) (Fig. 2).

Paralectotype
CAMEROON • ♀; same data as for lectotype; SMF 9900064 (examined) (Fig. 2).

Remarks

A second female is morphologically different and not conspecific with the male lectotype of *Clinobiantes paradoxus* or the female paralectotype herein designated (Fig. 2).

Redescription

Male (lectotype, SMF 9900064)
Body measurements. Total body length 2.48, carapace length 0.76, scutum magnum length 2.17, carapace maximum width 1.36, abdominal scutum maximum width 1.8. Appendage measurements in Table 1.

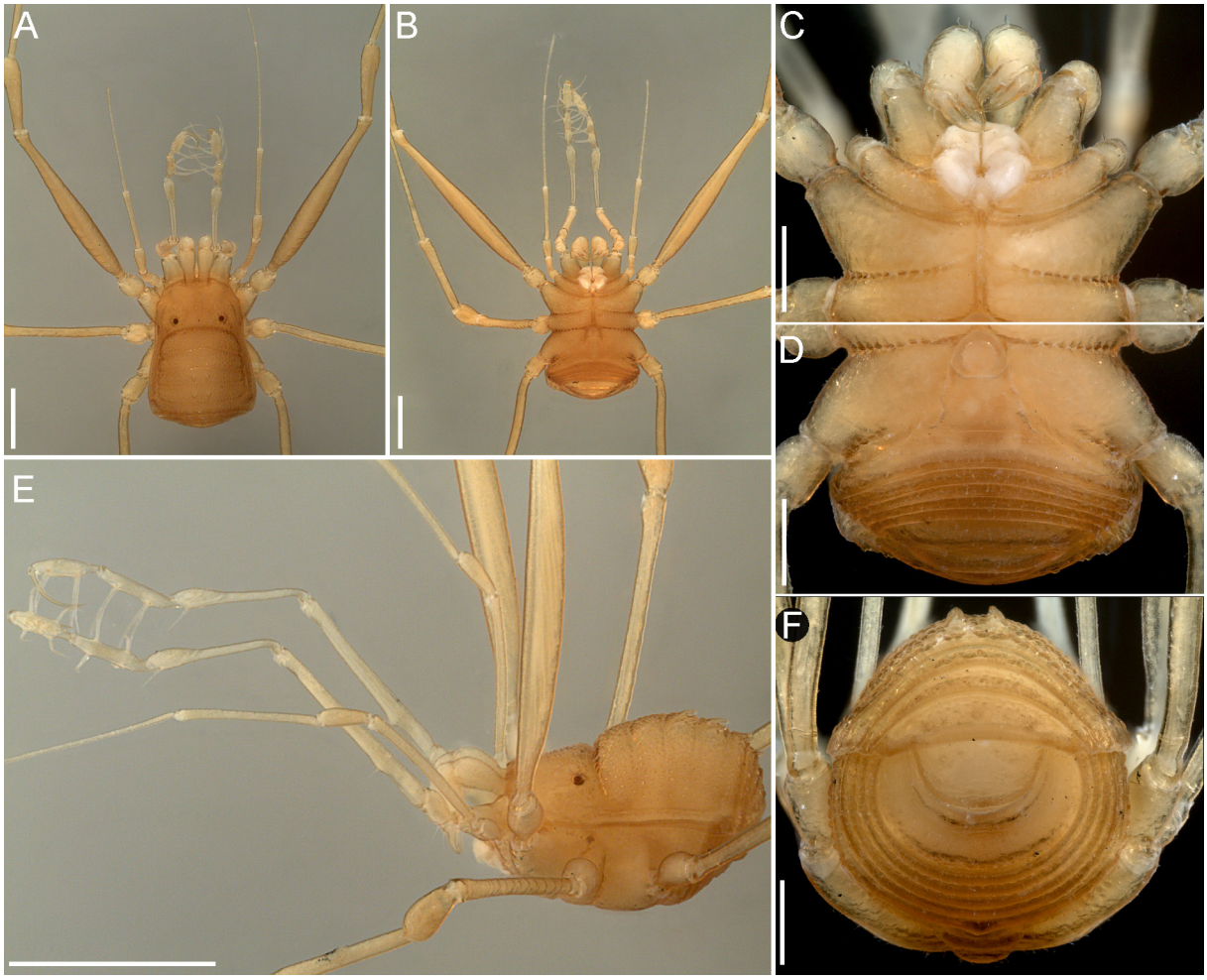

Fig. 1. *Clinobiantes paradoxus* Roewer, 1927, lectotype, ♂ (SMF 9900064), habitus photos. **A**. Dorsal view. **B**. Ventral view. **C**. Ventral view with detail of coxae I–III. **D**. Ventral view with detail of coxa IV and free sternites. **E**. Lateral view. **F**. Posterior view. Scale bars: A–B = 1 mm; C–D, F = 500 µm; E = 2 mm.

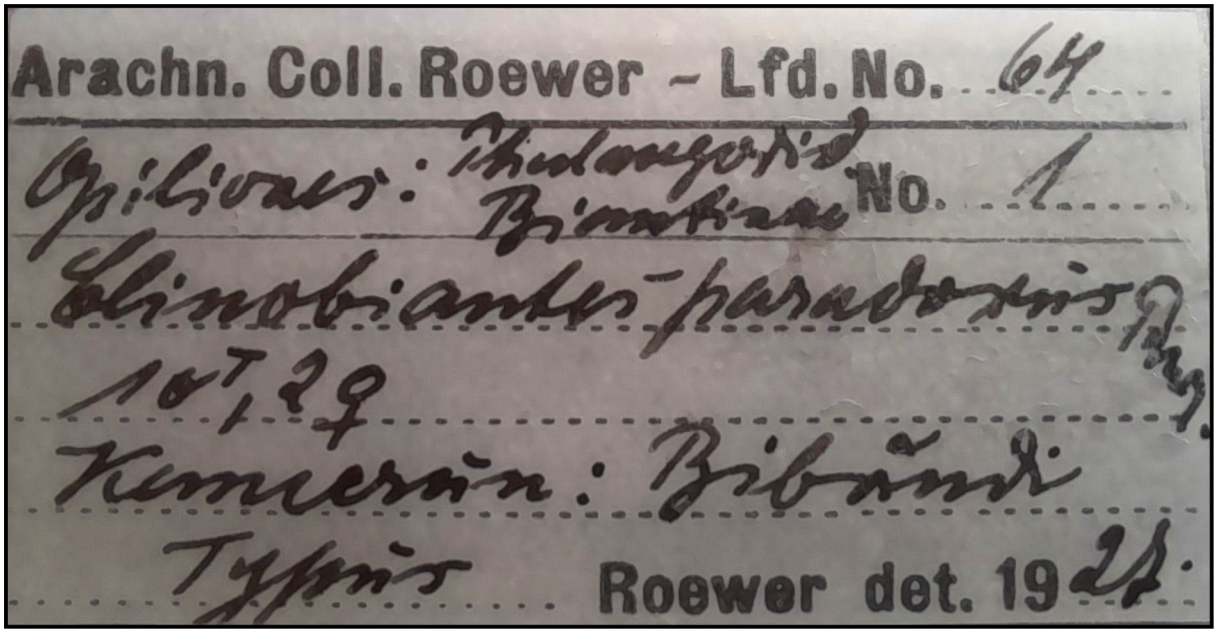

Fig. 2. Label accompanying the types *Clinobiantes paradoxus* Roewer, 1927 (SMF 9900064). Label text: Arachn. Coll. Roewer – Lfd. No.64, Opiliones: Phalangodid, Biantinae No.1, *Clinobiantes paradoxus* Rwr. 1♂, 2♀, Kamerun: Bibundi, Typus, Roewer det. 1927.

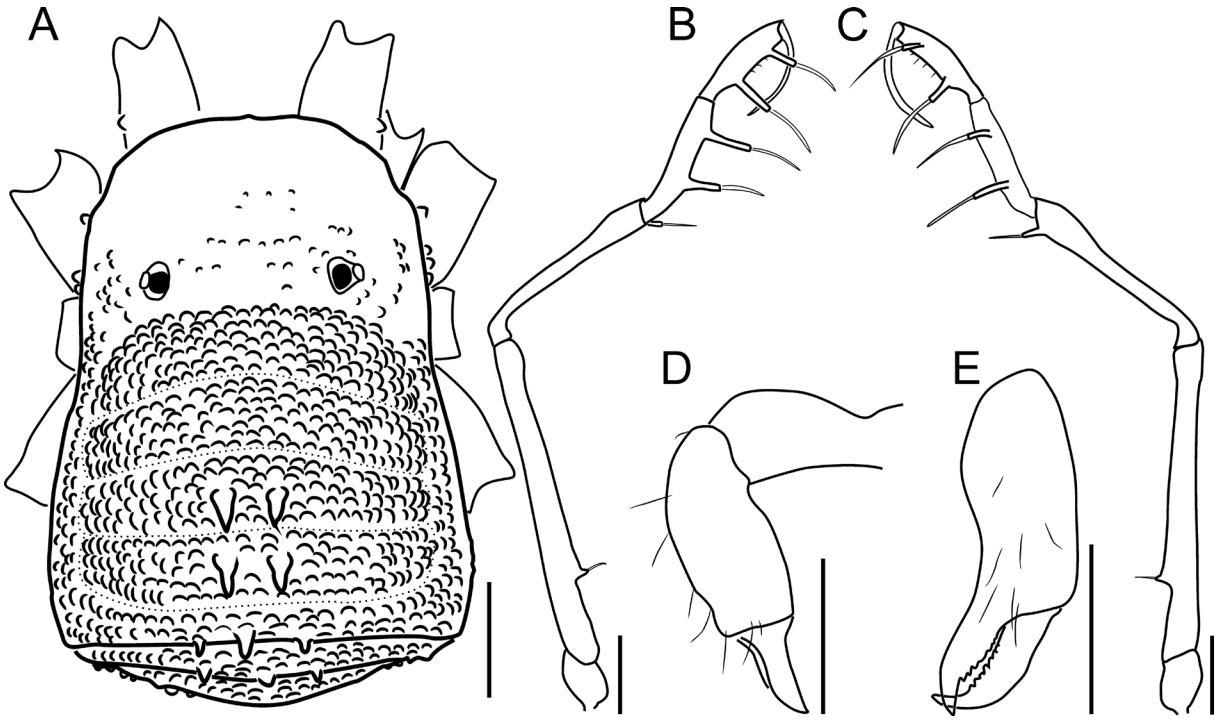

Fig. 3. *Clinobiantes paradoxus* Roewer, 1927, lectotype, ♂ (SMF 9900064), drawings of habitus, pedipalp, and chelicera. **A**. Habitus, dorsal view. **B–C**. Right pedipalp. **B**. Ectal view. **C**. Mesal view, **D–E**. Left chelicera. **D**. Ectal view. **E**. Frontal view. Scale bars = 500 µm.

Dorsum. Outline slightly hourglass-shaped (almost rectangular) with Eta (η) shape, with a very slight constriction at sulcus I level (Figs 1A, 3A). Carapace granulated, wider than long, anterior border slightly convex and unarmed (Figs 1A, 3A). Cheliceral sockets not marked (Figs 1A, 3A). Eyes separated near sulcus I (Figs 1A, 3A); interocular area granulated (Figs 1E, 3A). Carapace in lateral view straight at anterior region and slightly higher posteriorly (Fig. 1E). Abdominal scutum in lateral view convex (Fig. 1E). Sulcus I deep and well-marked, in dorsal view curved to the anterior body region (Figs 1A, E, 3A). Mesotergal areas coarsely granulated and well-defined, with sulci II–V marked but shallower than sulcus I; medially sulci II–III slightly curved to the anterior body region; sulci IV–V straight (Figs 1A, E, 3A). Mesotergal areas III–IV medially with two conical and pointed tubercles, strongly inclined backward (Figs 1A, E–F, 3A). Mesotergal area V granulated, medially with three conical and pointed tubercles. Lateral borders of abdominal scutum with rows of granules (Figs 1A, E, 3A). Free tergites granulated; free tergite I medially with three small conical tubercles (Figs 1A, E, 3A).

Venter. Coxa I with some setiferous tubercles in anterior margin (Fig. 1C); coxa II incrassated, of same size as (or slightly larger than) coxa IV (Fig. 1B–D); anteroposterior borders of coxa III with a row of strong granules connecting with coxae II and IV, respectively (Fig. 1B–D). Posterior border of spiracular area and free sternites I–V with a row of granules; anal operculum with few granules (Fig. 1D, F). Spiracles not concealed (Fig. 1B, D).

Chelicera. Basichelicerite unarmed, with an elongated and slightly marked bulla (Figs 1E, 3D). Cheliceral hand with sparse setae (Fig. 3D–E). Fixed and movable fingers with small triangular-shaped teeth (Fig. 3E).

Pedipalp. Coxa elongated (i.e., remarkably longer than trochanter), proximally with one dorsoectal and one ectoventral granule (Figs 1A, C, 3A). Femur straight, proximally with a slight ventral narrowing followed by a small ventral spine (Figs 1E, 3B–C). Patella elongated, club-shaped, with a distal

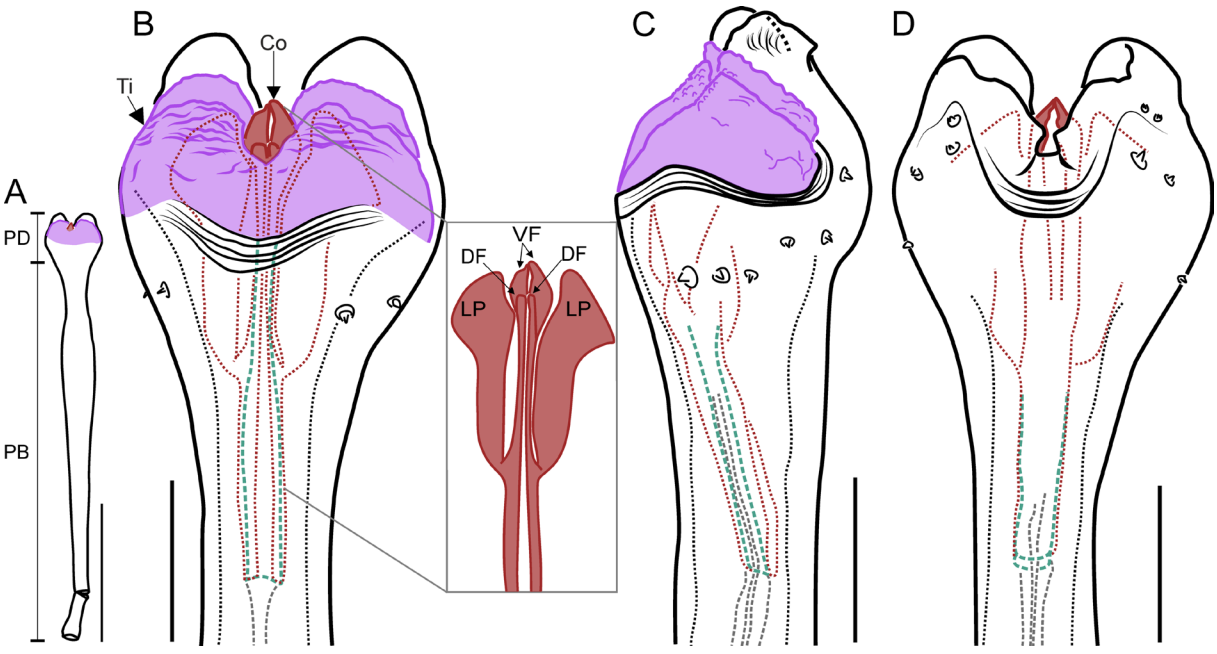

Fig. 4. *Clinobiantes paradoxus* Roewer, 1927, lectotype, ♂ (SMF 9900064), penis drawings. **A–B**. Dorsal view (detail of conductors within box). **C**. Lateral view. **D**. Ventral view. Stylus in green, conductors in brownish red, titillators in magenta. Abbreviations: Co = conductor; DF = dorsal fold; LP = lateral projection; PB = pars basalis; PD = pars distalis; Ti = titillator; VF = ventral fold. Scale bars: A = 500 µm; B–D = 100 µm.

ventromesal spine (Figs 1E, 3B–C). Tibia with two ventromesal and two ventroectal long spines (Fig. 3B–C). Tarsus with two ventromesal and two ventroectal long spines (Figs 1E, 3B–C).

Legs. Femur II fusiform dorsally swollen (Figs 1A, B, 6B). Tibia II slender, slightly distally swollen, with ventral small triangular tubercles (Fig. 6D). Metatarsus II with a ventrally swollen astragalus bearing two rows of triangular tubercles; astragalus-calcaneus boundary marked by a strong constriction, and slightly

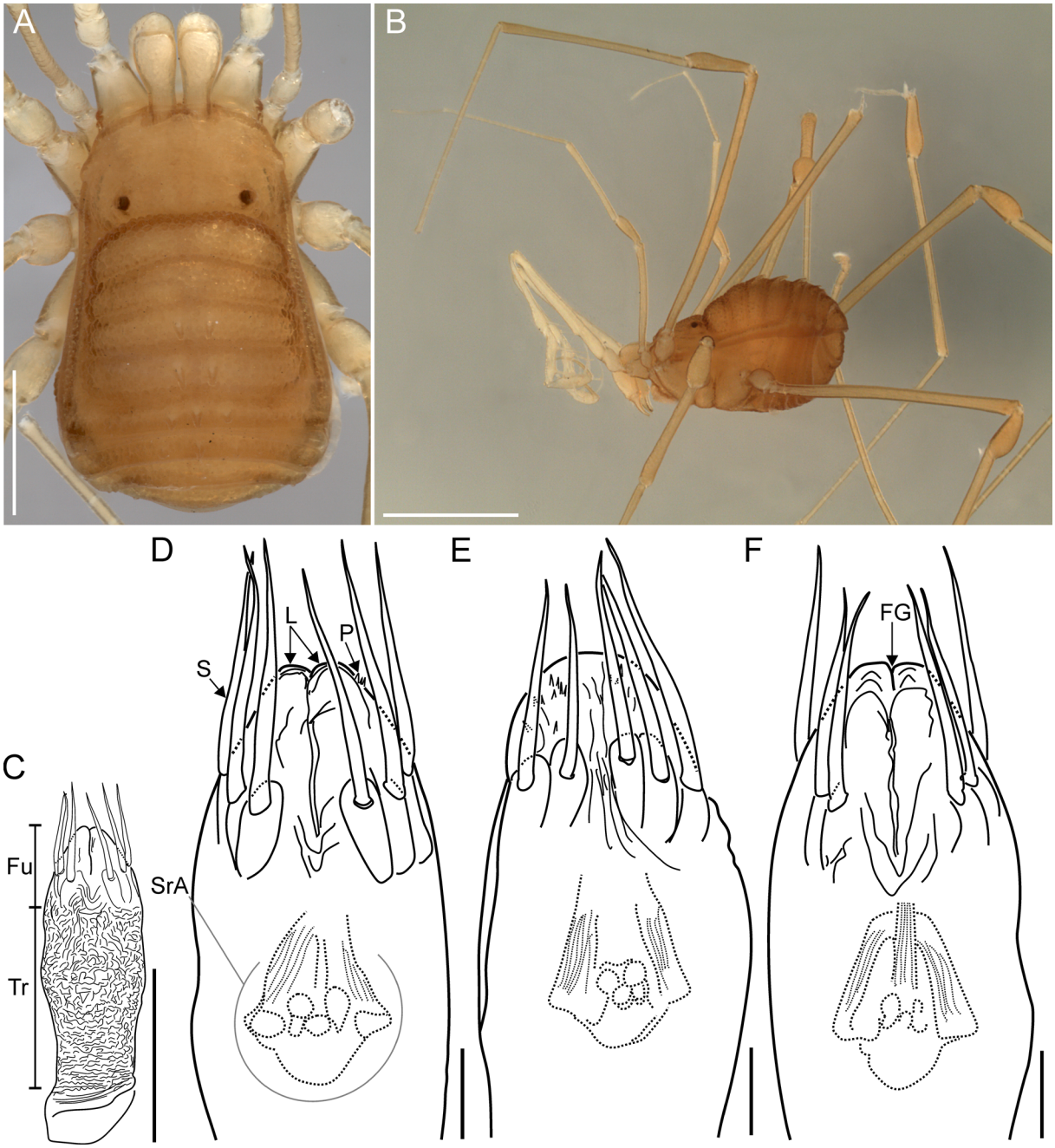

Fig. 5. *Clinobiantes paradoxus* Roewer, 1927, paralectotype, ♀ (SMF 9900064). **A–B**. Habitus photos. **A**. Dorsal view. **B**. Lateral view. **C–F**. Ovipositor drawings. **C–D**. Dorsal view. **E**. Lateral view. **F**. Ventral view. Abbreviations: FG = furcal groove; Fu = furca; L = lobe; P = projection; S = seta; SrA = seminal receptacle area; Tr = truncus. Scale bars: A = 1 mm; B = 2 mm; C = 500 µm; D–F = 100 µm.

thickened calcaneus giving a peculiar form to the distal part of the metatarsus (Fig. 6F). Tarsi III–IV with a dense scopula. Tarsal formula: 3(2):5(3):5:5.

Color (in 80% ethanol). Body and appendages uniformly yellowish-brown (Figs 1A–F, 6B, D, F).

Male genitalia. Penis with clearly defined boundaries between pars basalis and pars distalis (Fig. 4A). Pars basalis tubular, basally thin, broadens medially, with distal constriction (Fig. 4A). Pars distalis swollen, with maximum width at titillator level (Fig. 4A–B, D). Apical edge laminar (i.e., dorsoventrally flat) with a medial U-shaped cleft dividing it into two rounded halves (Fig. 4B, D); halves less chitinous apically, and could possibly be inflated by hemolymph pressure (Fig. 4C–D). Pars distalis with a distal depression in the ventromedial region (Fig. 4D). Each side of pars distalis armed with short, conical microsetae arranged irregularly, extending from the dorsolateral to the ventrodistal region (Fig. 4B–D). Capsula externa with two broad titillators covering most capsula interna (Fig. 4B–C). Capsula interna with two complex conductors and one stylus, basally fused. Each conductor with two medial laminar folds apically, one short dorsal and one ventral longer, visible ventrally within the U-shaped cleft; each conductor also with one broad lateral projection (Fig. 4B); stylus tubular, with its free tip fully covered by conductors (Fig. 4B–D).

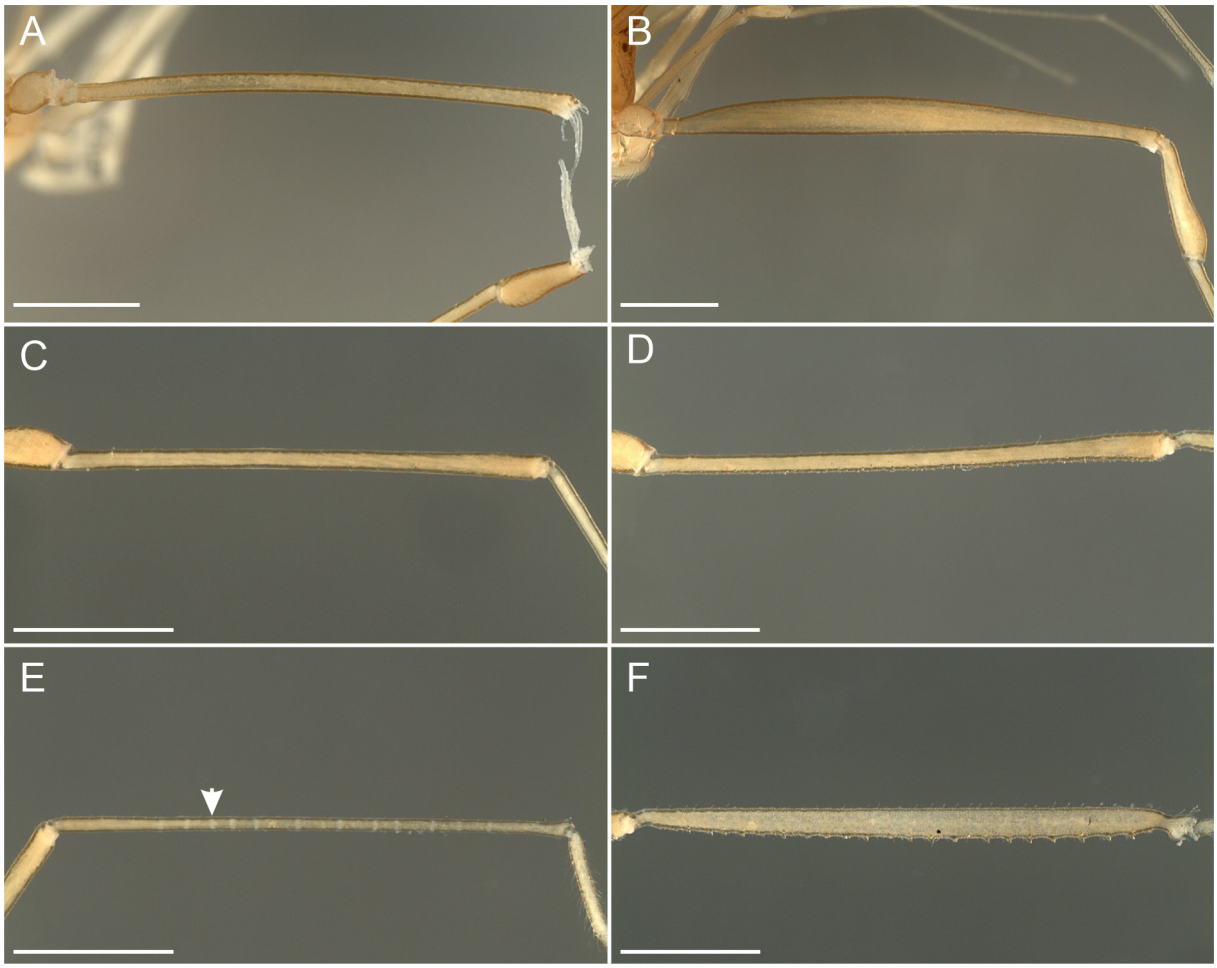

Fig. 6. *Clinobiantes paradoxus* Roewer, 1927, sexual dimorphism, right legs II photos. **A, C, E**. Paralectotype, ♀ (SMF 9900064). **B, D, F**. Lectotype, ♂ (SMF 9900064). **A–B**. Femur, retrolateral view. **C–D**. Tibia, retrolateral view. **E–F**. Metatarsus, retrolateral view. Arrow indicates a pseudoarticular ring. Scale bars = 1 mm.

Table 1. Appendage measurements (in mm) of *Clinobiantes paradoxus* Roewer, 1927. ***** = lectotype. Abbreviations: Fe = femur; Mt = metatarsus; Pa = patella; T = total; Ta = tarsus; Ti = tibia; Tr = trochanter.

		Tr	Fe	Pa	Ti	Mt	Ta	T
♂ SMF 9900064*	Pedipalp	0.37	1.94	1.29	0.79	–	0.67	5.06
	Leg I	0.32	1.54	0.52	1.39	2.01	1.21	6.99
	Leg II	0.52	5.17	1.25	3.84	4.02	2.24	17.04
	Leg III	0.44	2.64	0.68	1.78	3.25	1.04	9.83
	Leg IV	0.41	3.85	0.76	2.46	4.46	1.21	13.15
♀ SMF 9900064	Pedipalp	0.40	1.97	1.17	0.79	–	0.63	4.96
	Leg I	0.32	1.60	0.52	1.29	1.89	1.14	6.76
	Leg II	0.44	4.02	1.06	3.00	3.20	2.07	13.79
	Leg III	0.39	2.47	0.67	1.69	3.08	1.07	9.37
	Leg IV	0.50	3.47	0.87	2.20	4.39	1.21	12.64

Female (paralectotype, SMF 9900064)

Body measurements. Total body length 2.82, carapace length 0.76, scutum magnum length 2.31, maximum carapace width 1.38, abdominal scutum maximum width 1.88. Appendage measurements in Table 1.

Body. Female resembles male in armature of scutum magnum, but with tubercles of mesotergal areas III–IV, posterior border, and free tergite I slightly smaller (Fig. 5A–B vs Fig. 1E). Leg II with femur, tibia, and metatarsus neither swollen nor armed (Fig. 6A, C, E vs Fig. 6B, D, F); metatarsus II thin and unarmed, with pseudoarticular rings (Fig. 6E vs Fig. 6F). Tarsal formula 3(2):5(3):5:5.

Female genitalia. Ovipositor cylindrical (Fig. 5C), distally bearing two lobes (furca) (Fig. 5C–D, F). Each furcal lobe with five long, pointed setae (Fig. 5E) – three dorsal and two ventral – resulting in a total of six setae on the dorsal region (Fig. 5D) and four on the ventral region (Fig. 5F). External surface of furcal lobes with several short, pointed projections, irregularly distributed (Fig. 5E). Receptacle chambers located near the base of the furcal groove (Fig. 5D–F).

Distribution

Known only from the type locality (Fig. 40).

Genus ***Metabiantes*** Roewer, 1915

Metabiantes Roewer, 1915: 28. Type species : *Biantes pusulosus* Loman, 1898, by subsequent designation of Roewer 1949: 248.

Spinibiantes Roewer, 1915: 27. Type species: *Hinzuanius leighi* Pocock 1902, by monotypy. Synonymy established by Lawrence (1931: 354).

Biantiplus Roewer, 1949: 250. Type species: *Metabiantes zuluanus* Lawrence, 1937, by original designation. Synonymy established by Kauri (1961: 40).

Metabiantes – Roewer 1923: 133; 1949: 248; 1961: 44. — Lawrence 1931: 354; 1949: 17; 1957: 60; 1962: 22; 1963: 282. — Kauri 1961: 17; 1985: 73. — Staręga 1992: 365.

Spinibiantes – Roewer 1923: 140; 1949: 249.

Included species

Metabiantes armatus Lawrence, 1962, *M. barbertonensis* Lawrence, 1963, *M. basutoanus* Kaury, 1961, *M. caracticus* Kaury, 1961, *M. convexus* Roewer, 1949, *M. elongatus* sp. nov., *M. filipes* (Roewer, 1912), *M. flavus* Lawrence, 1949, *M. hanstroemi* Kauri, 1961, *M. herculeus* sp. nov., *M. incertus* Kauri, 1961, *M. insulanus* (Roewer, 1949), *M. jeanneli* (Roewer, 1913), *M. kakololius* Kauri, 1985, *M. kaurii* sp. nov., *M. kivuensis* sp. nov., *M. kosibaiensis* Kauri, 1961, *M. lawrencei* Starega, 1992, *M. leighi* (Pocock, 1902), *M. litoralis* Kauri, 1961, *M. longipes* (Kauri, 1985), *M. machadoi* Lawrence, 1957, *M. meraculus* (Loman, 1898), *M. minutus* Kauri, 1985, *M. montanus* Kauri, 1985, *M. obscurus* Kauri, 1961, *M. parvulus* Kauri, 1985, *M. perustus* Lawrence, 1963, *M. pumilio* Roewer, 1927, *M. punctatus* (Sørensen, 1910), *M. pusulosus* (Loman, 1898), *M. rudebecki* Kauri, 1961, *M. serratus* sp. nov., *M. stanleyi* Kauri, 1985, *M. submontanus* Kauri, 1985, *M. teres* Lawrence, 1963, *M. teretipes* Lawrence, 1962, *M. traegardhi* Kauri, 1961, *M. trifasciatus* Roewer, 1915, *M. ulindinus* Kauri, 1985, *M. unicolor* (Roewer, 1912), *M. urbanus* Kauri, 1961, *M. varius* Kauri, 1961, *M. zuluanus* Lawrence, 1937, and *M. zuurbergianus* Kauri, 1961.

Distribution

Afrotropical: Angola, Cameroon, Democratic Republic of the Congo, Equatorial Guinea*, Kenya, Lesotho, Mozambique, São Tomé and Príncipe, South Africa, Tanzania, and Uganda.

Remarks

* Santos & Prieto (2009) recorded *Metabiantes* spp. for Equatorial Guinea (Muni River, Motora River (Mitong), Congüe River, and Etembue), but the identity of this species has not been clarified yet.

Metabiantes elongatus sp. nov.
urn:lsid:zoobank.org:act:CCA055CD-6549-420A-BD70-415692EE1280
Figs 7–14; Table 2

Diagnosis

Metabiantes elongatus sp. nov. differs from the rest of the species of the genus (except *M. serratus* sp. nov., *M. litoralis*, and *M. zuluanus*) by the following combination of characteristics: presence of two tubercles on mesotergal areas III–V (Figs 7A, 8A, 13A) and, in males, having a slender femur II (Figs 10A, 14B, D) and metatarsus II with tubercles on the ventral region (Figs 10E, 14H). *Metabiantes elongatus* and *M. serratus* share a remarkably similar male genital morphology but *M. elongatus* can be easily differentiated from *M. serratus* in lacking tubercles on free tergites I–II (Fig. 7C vs Figs 33C, 34C) and in possessing a thinner femur II (Figs 10A, 14B, D vs Figs 36A–B, 39B, D), unswollen tibia (Figs 10C, 14F vs Figs 36C, 39F), and unswollen metatarsus of leg II (Figs 10E, 14H vs Figs 36E, 39H). Additionally, *M. elongatus* lacks a pronounced constriction at astragalus-calcaneus junction in metatarsus of leg II as observed in *M. serratus* (Fig. 10E–F vs Fig. 36E–F). *Metabiantes elongatus* can be differentiated from *M. litoralis* by having granules on free tergites instead of the presence of a row of small tubercles in *M. litoralis* (Fig. 7C vs Kauri 1961: fig. 33a–b). Males of *Metabiantes elongatus* have a non-enlarged trochanter II (Fig. 7A). In contrast, males of *M. zuluanus* exhibit a remarkably swollen trochanter II (Lawrence 1937a: fig. 26a). Regarding male genital morphology, *M. elongatus* has a penis with a deeper U-shaped cleft of lamina apicalis, wider titillators, and remarkably smaller basal setae, easily differentiated from the penis of *M. litoralis* and *M. zuluanus* with a shallow cleft, narrow titillators, and bigger basal setae (Figs 11B–D, 12A–C vs Kauri 1961: figs 22a–b, 34a–b).

Etymology

The species epithet is derived from the Latin word '*longatus*', meaning 'elongate' and refers to the elongated femur II in males of this species.

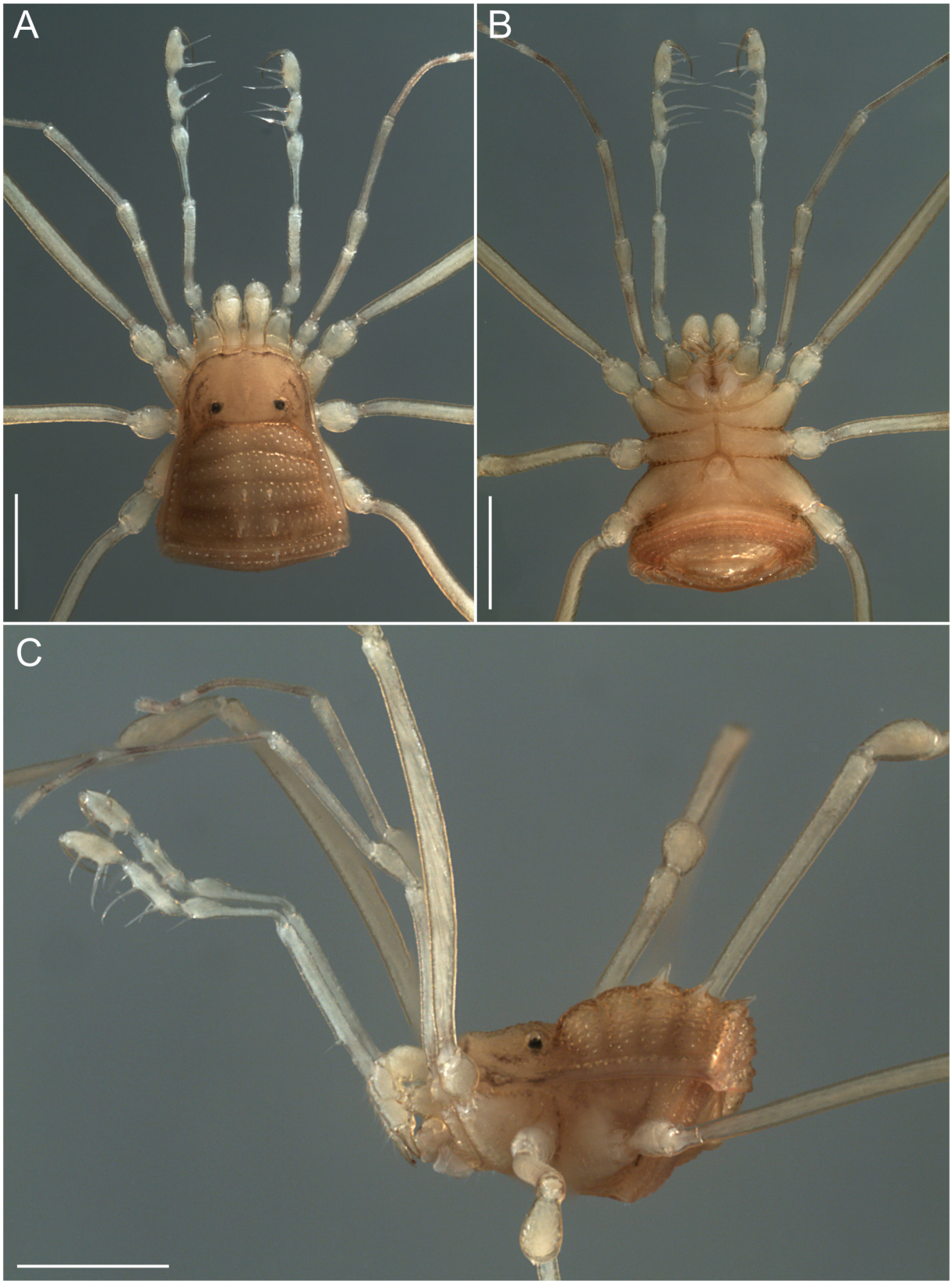

Fig. 7. *Metabiantes elongatus* sp. nov., holotype, ♂ (BE_RMCA_ARA.Opi.219865), habitus photos. **A**. Dorsal view. **B**. Ventral view. **C**. Lateral view. Scale bars = 1 mm.

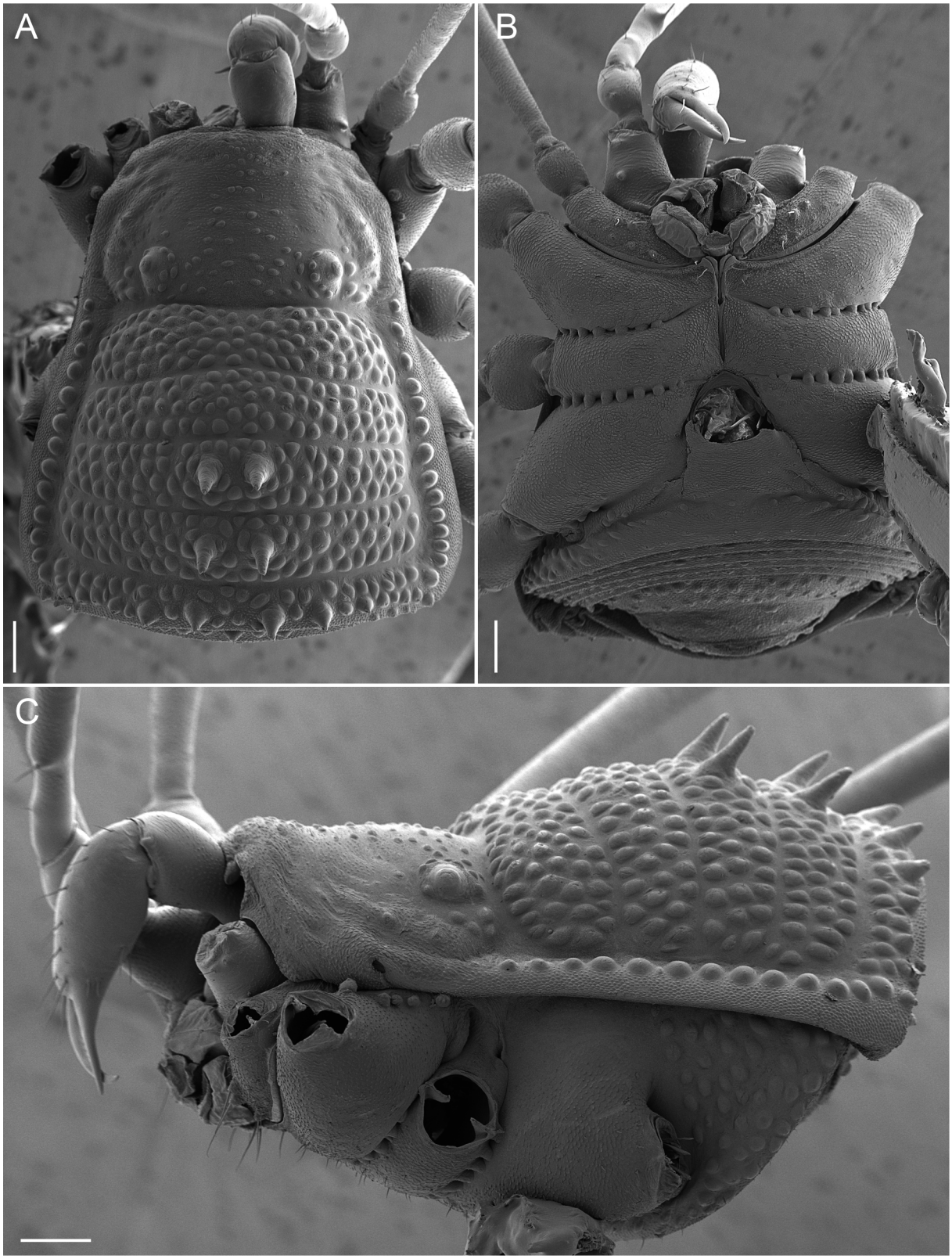

Fig. 8. *Metabiantes elongatus* sp. nov., paratype, ♂ (MACN-Ar 45430), scanning electron micrographs of habitus. **A**. Dorsal view. **B**. Ventral view. **C**. Lateral view. Scale bars = 200 µm.

Type material

Holotype

CONGO • ♂; Bas-Congo, Mayombe, Luki Forest Reserve; 5.63333° S, 13.06667° E; 12 Nov. 2006; D. De Bakker and J.P. Michiels leg.; primary rainforest; fogging; RMCA, BE_RMCA_ARA.Opi.219865.

Paratypes

CONGO • 1 ♂, 1 ♀; same data as for holotype; RMCA, BE_RMCA_ARA.Opi.247662 • 1 ♂ (SEM voucher); same data as for holotype; MACN-Ar 45425 • 1 ♂ (SEM voucher); same data as for holotype; MACN-Ar 45430 • 9 ♂♂ (1 photo voucher), 13 ♀♀ (1 photo voucher, 2 SEM vouchers); same data as for holotype; MACN-Ar 45440 • 9 ♂♂, 6 ♀♀; same data as for holotype; 13 Nov. 2006; RMCA, BE_RMCA_ARA.Opi.219866 • 10 ♂♂, 16 ♀♀; same data as for holotype; 5 Nov. 2006; RMCA, BE_RMCA_ARA.Opi.219858.

Description

Male (holotype, BE_RMCA_ARA.Opi.219865)

Body measurements. Total body length 1.95, carapace length 0.66, scutum magnum length 1.84, carapace maximum width 1.08, abdominal scutum maximum width 1.62. Appendage measurements in Table 2.

Dorsum. Outline slightly hourglass-shaped with Eta (η) shape, with a very slight constriction located at sulcus I level (Figs 7A, 8A). Carapace with scattered granules, wider than long; anterior border slightly convex and unarmed (Figs 7A, 8A). Cheliceral sockets not marked (Fig. 8A). Eyes separated near sulcus I; interocular area with scattered granules (Figs 7A, C, 8A, C). Carapace in lateral view straight at anterior region and slightly higher posteriorly (Figs 7C, 8C). Sulcus I deep and complete, medially slightly curved toward the posterior body region (Fig. 8A). Mesotergal areas I–IV granulated and well-defined, with sulci II–IV marked but shallower than sulcus I; medially sulcus II slightly curved to the anterior body region; sulci III–V straight (Fig. 8A). Mesotergal areas III–IV medially with two conical and pointed setiferous tubercles (Figs 7A, 8A). Mesotergal area V with two irregular rows of granules and four medial tubercles in the posterior margin (Fig. 8A). Lateral margins with a row of granules (Figs 7A, 8A). Ozopore with an oval and narrow orifice with a descending channel that extends toward the ventroposterior region (Fig. 8C). Free tergites granulated (Fig. 7C).

Venter. Coxa I with few, small, medial setiferous granules; coxa II incrassated, slightly smaller than coxa IV (Figs 7B, 8B); anteroposterior borders of coxa III with a row of strong granules connecting with coxae II and IV, respectively (Fig. 8B). Posterior border of spiracular area, free sternites I–V with a row of granules; anal operculum granulated (Fig. 8B) Spiracles not concealed (Fig. 8B).

Chelicera. Basichelicerite unarmed with slightly marked bulla (Fig. 9G). Cheliceral hand with sparse setae (Fig. 9G–H). Fixed finger with spaced, triangular-shaped teeth; movable finger with a row of small, rounded teeth (Fig. 9H).

Pedipalp. Coxa elongated (i.e., remarkably longer than trochanter), proximally with three granules – one dorsoectal, one ectal (Fig. 8A), and one ventroectal (Fig. 8B). Trochanter with one small ventroectal setiferous granule (Fig. 8B). Femur straight, proximally with a strong ventral narrowing followed by a small ventromesal spine (Fig. 9A–B); ventrally with scattered pores and surface texture with scales-like appearance (Fig. 9B, D). Patella elongated, club-shaped, and armed with a short mesodistal spine (Fig. 9A). Tibia with two ventroectal and two long ventromesal spines (Fig. 9A, C); tibia ventrally with scattered pores and scales-like surface (Fig. 9E). Tarsus with two ventromesal and two ventroectal spines; proximal spines longer than distal spines (Fig. 9A, C). Setae of spines with a basal portion smooth, then with scattered microtrichia (Fig. 9C, E); microtrichia with a wide base and rounded tip (Fig. 9F).

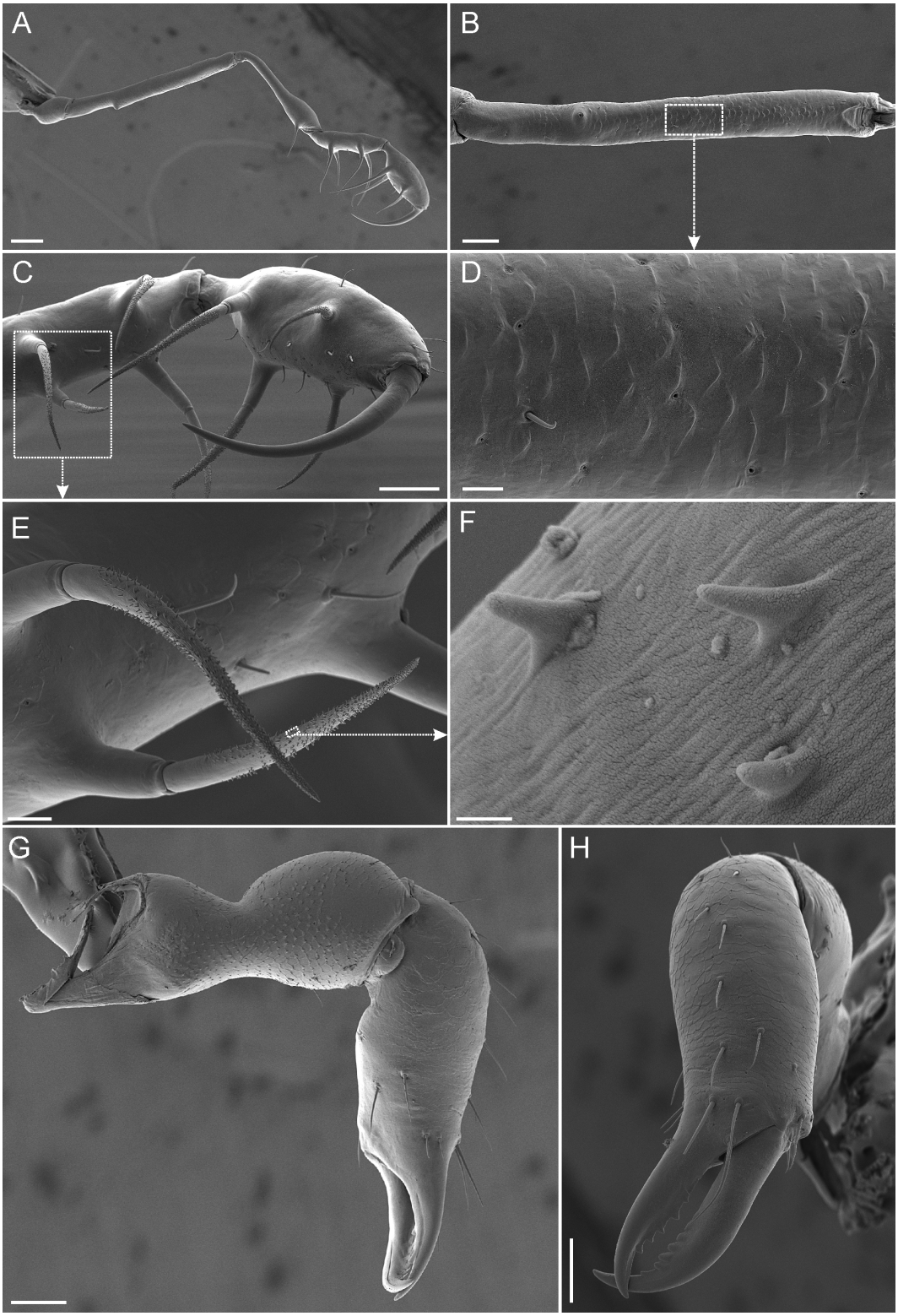

Fig. 9. *Metabiantes elongatus* sp. nov., scanning electron micrographs of pedipalp and chelicera. **A–F**. Paratype, ♂ (MACN-Ar 45425), left pedipalp. **A**. Mesal view. **B**. Femur, ventral view. **C**. Tibia and tarsus, ventral view. **D**. Detail of femur, ventral view. **E**. Detail of proximal spines on tibia. **F**. Detail of microtrichia. **G–H**. Paratype, ♂ (MACN-Ar 45430), left chelicera. **G**. Mesal view. **H**. Frontal view. Scale bars: A = 200 μm; B–C, G–H = 100 μm; D–E = 20 μm; F = 1 μm.

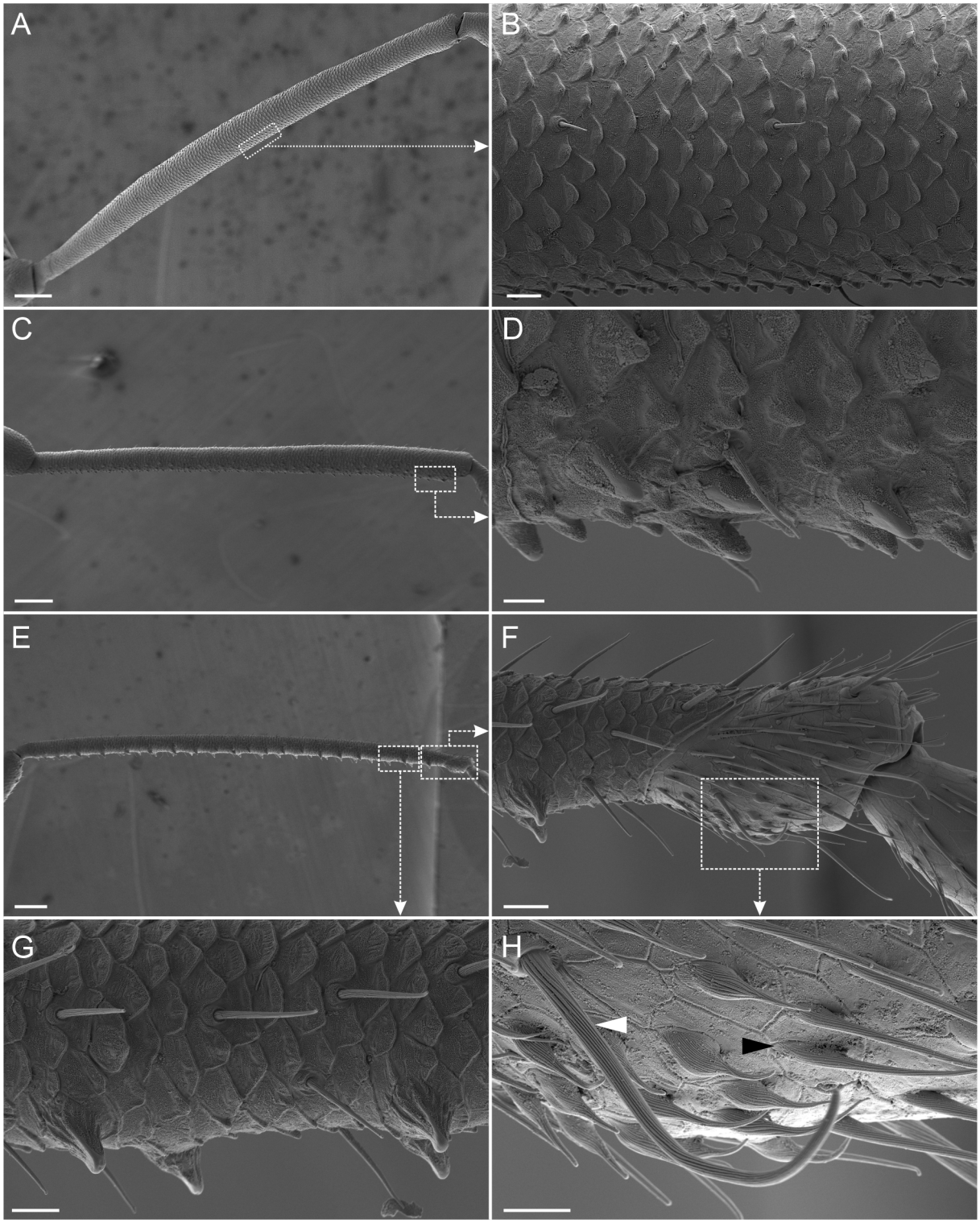

Fig. 10. *Metabiantes elongatus* sp. nov., paratype, ♂ (MACN-Ar 45425), scanning electron micrographs of left leg II. **A**. Femur, prolateral view. **B**. Detail of femur surface. **C**. Tibia, prolateral view. **D**. Detail of tibia surface. **E**. Metatarsus, prolateral view. **F**. Distal metatarsus with division between astragalus and calcaneus visible. **G**. Detail of astragalus surface. **H**. Detail of calcaneus surface. Black triangle indicates a trichome; white triangle indicates a sensillum chaeticum. Scale bars: A, C, E = 200 μm; B, G = 20 μm; D, H = 10 μm; F = 30 μm.

Table 2. Appendage measurements (in mm) of *Metabiantes elongatus* sp. nov. * = holotype. Abbreviations: Fe = femur; Mt = metatarsus; Pa = patella; T = total; Ta = tarsus; Ti = tibia; Tr = trochanter.

		Tr	Fe	Pa	Ti	Mt	Ta	T
♂ RMCA 219865*	Pedipalp	0.27	1.11	0.67	0.51	–	0.44	3.00
	Leg I	0.20	1.20	0.41	0.99	1.29	0.79	4.88
	Leg II	0.36	2.80	0.74	2.37	2.62	1.41	10.30
	Leg III	0.31	1.75	0.46	1.33	2.23	0.75	6.83
	Leg IV	0.40	2.42	0.67	1.70	3.10	0.90	9.19
♀ MACN-Ar 45440	Pedipalp	0.25	1.12	0.65	0.50	–	0.45	2.97
	Leg I	0.17	1.20	0.40	0.92	1.17	0.72	4.58
	Leg II	0.32	2.70	0.60	2.13	2.42	1.43	9.90
	Leg III	0.29	1.64	0.45	1.19	2.09	0.75	6.41
	Leg IV	0.30	2.32	0.62	1.58	2.96	0.89	8.67

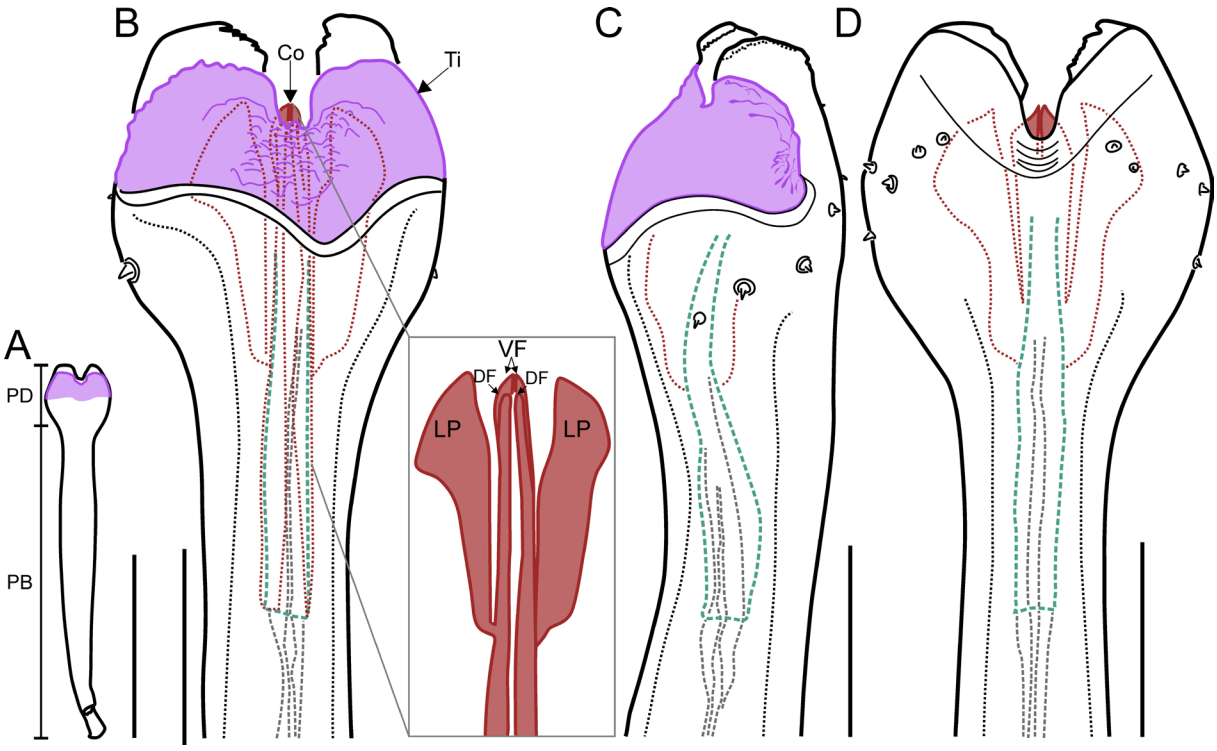

Fig. 11. *Metabiantes elongatus* sp. nov., holotype, ♂ (BE_RMCA_ARA.Opi.219865), penis drawings. **A–B**. Dorsal view (detail of conductors within the box). **C**. Lateral view. **D**. Ventral view. Stylus in green, conductors in brownish red, titillators in magenta. Abbreviations: Co = conductor; DF = dorsal fold; LP = lateral projection; PB = pars basalis; PD = pars distalis; Ti = titillator; VF = ventral fold. Scale bars: A = 500 µm; B–D = 100 µm.

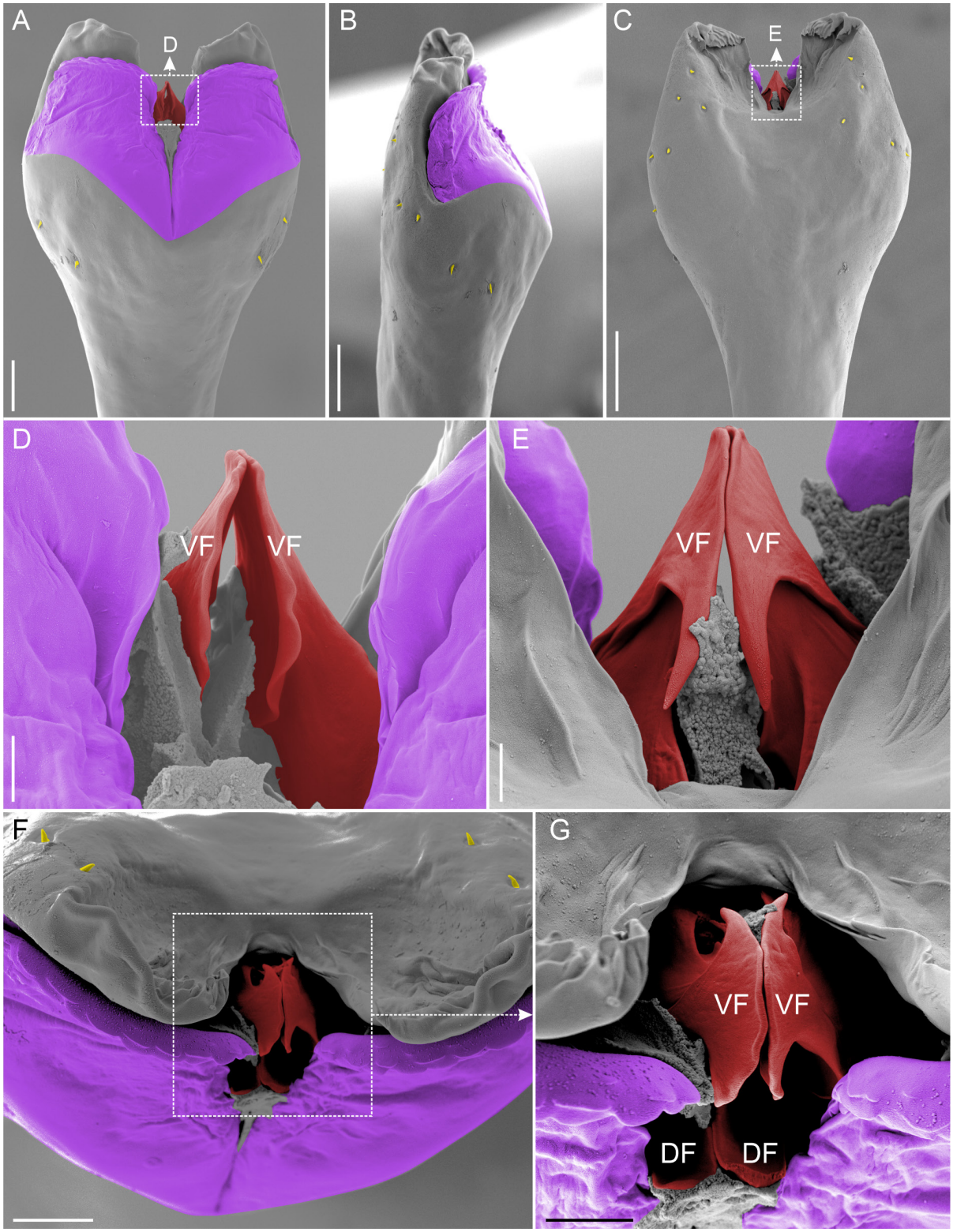

Fig. 12. *Metabiantes elongatus* sp. nov., paratype, ♂ (MACN-Ar 45430), scanning electron micrographs of penis. **A**. Dorsal view. **B**. Lateral view. **C**. Ventral view. **D**. Detail of conductors, dorsal view. **E**. Detail of conductors, ventral view. **F**. Anterior view. **G**. Details of conductors, anterior view. Conductors in red, titillators in magenta, microsetae in yellow. Abbreviations: DF = dorsal fold; VF = ventral fold. Scale bars: A = 30 µm; B = 40 µm; C = 50 µm; D = 5 µm; E, G = 10 µm; F = 20 µm.

Legs. Coxa II with a dorsal row of granules (Fig. 8C). Femur II elongated and slightly fusiform, swelling dorsally, slightly more pronounced, unarmed (Figs 7C, 10A–B, 14D). Tibia II elongated ventrally with small triangular-shaped tubercles (Figs 10C–D, 14F). Metatarsus II with elongated astragalus, armed with equidistant transverse rows of triangular-shaped tubercles (Figs 10E–G, 14H). Calcaneus occupies a reduced distal portion of the metatarsus; calcaneus with scattered long sensilla chaetica and trichomes distributed along all surfaces, with higher density on the ventral region; trichomes of variable length with a wider ovate-shaped base and pointed tip (Fig. 10F, H). Tarsi III–IV with a dense scopula. Tarsal formula: 3(2):5(4):5:5.

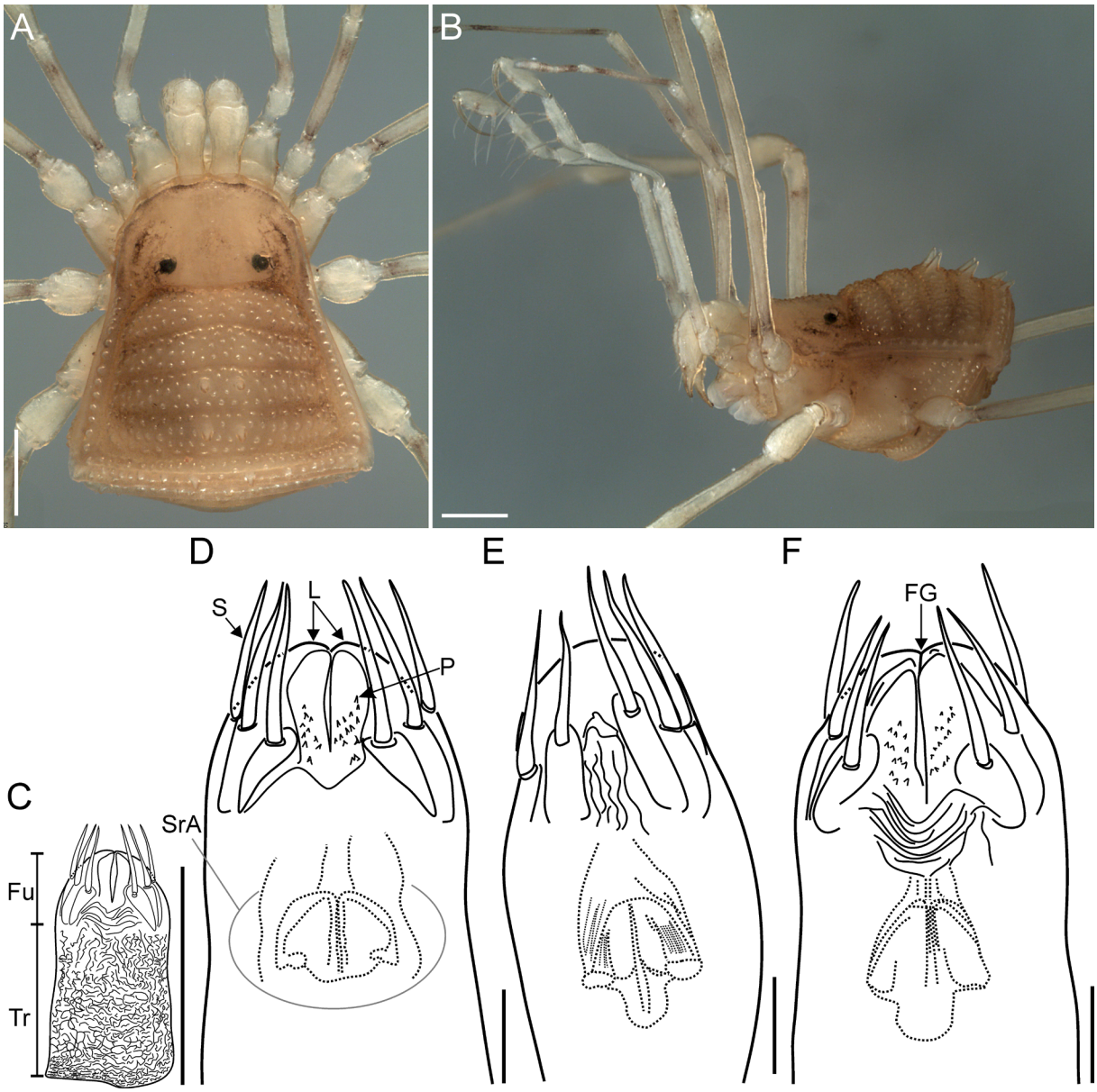

Fig. 13. *Metabiantes elongatus* sp. nov., paratype, ♀ (MACN-Ar 45440). **A–B**. Habitus photos. **A**. Dorsal view. **B**. Lateral view. **C–F**. Ovipositor drawings. **C–D**. Dorsal view. **E**. Lateral view. **F**. Ventral view. Abbreviations: FG = furcal groove; Fu = furca; L = lobe; P = projection; S = seta; SrA = seminal receptacle area; Tr = truncus. Scale bars: A–C = 500 μm; D–F = 100 μm.

Color (specimen preserved in 80% ethanol). Body brown yellowish; anterior border and lateral margins of carapace, lateral area to eyes until anterolateral margin of mesotergal area I with brown reticulations (Fig. 7A–C). Appendages light brown yellowish; metatarsi and tarsi I–IV darker (Figs 7A–C, 14B, D, F, H).

Male genitalia. Penis with clearly defined boundaries between pars basalis and pars distalis (Fig. 11A). Pars basalis basally thin, broadens medially, with distal constriction (Fig. 11A). Pars distalis swollen with maximum width at titillator level (Figs 11B, D, 12A, C); apical edge laminar (i.e., dorsoventrally flat) with a medial U-shaped cleft dividing it into two rounded halves (Figs 11B, D, 12A, C). Halves apically curved towards ventral side, less chitinous and irregularly deformed, probably signifying that could be inflated by hemolymph pressure (Figs 11C–D, 12B–C, F). Pars distalis with a slight distal depression in the ventromedial region (Figs 11D, 12C, F). Each side of pars distalis armed with short, conical microsetae irregularly arranged, extending basally from dorsolateral to ventrodistal region (Figs 11B–D, 12A–C). Capsula externa with two broad titillators that cover almost all the capsula interna (Figs 11B, 12A). Capsula interna with two complex conductors and one stylus, basally fused. Each conductor with two medial laminar folds apically, one short dorsal and one ventral longer, visible ventrally within the

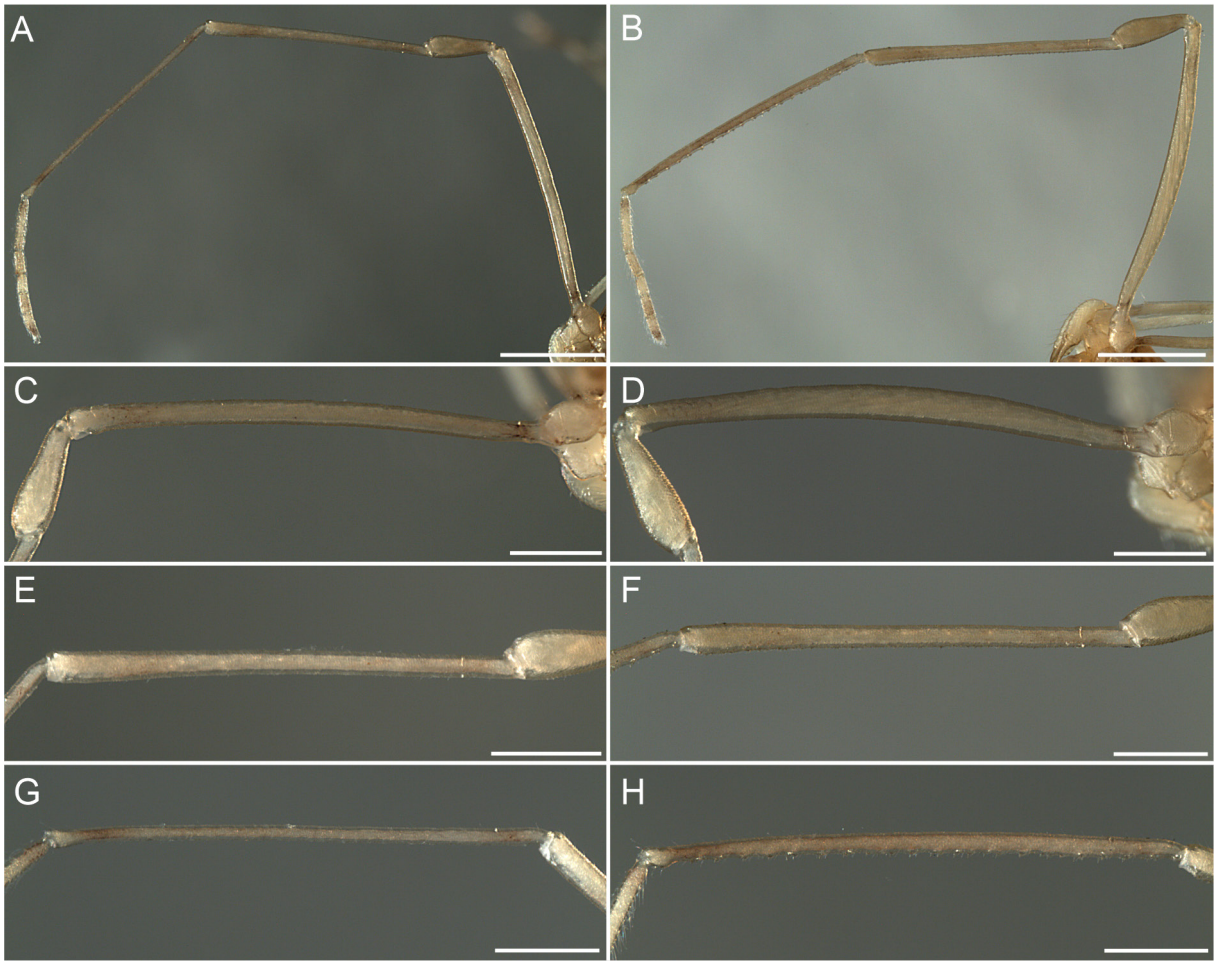

Fig. 14. *Metabiantes elongatus* sp. nov., sexual dimorphism, left legs II photos. **A, C, E, G**. Paratype, ♀ (MACN-Ar 45440). **B, D, F, H**. Holotype, ♂ (BE_RMCA_ARA.Opi.219865). **A–B**. Leg II, retrolateral view. **C–D**. Femur, retrolateral view. **E–F**. Tibia, retrolateral view. **G–H**. Metatarsus, retrolateral view. Scale bars: A–B = 1 mm; C–H = 500 µm.

U-shaped cleft (Figs 11B, D, 12A, C–G). Ventral folds with apical edges in contact, waved, medially free edges dorsally (Fig. 12D) and ventrally folded, with a strongly curved and shorter subapical edge hood-shaped (Fig. 12C, E, G). Each conductor also bearing one broad lateral projection (Fig. 11B, D); stylus tubular, S-shaped in lateral view, with its free tip fully covered by conductors (Fig. 11B–D).

Female (paratype, MACN-Ar 45440)

Body measurements. Total body length 1.97, carapace length 0.67, scutum magnum length 1.81, carapace maximum width 1.04, abdominal scutum maximum width 1.71. Appendage measurements in Table 2.

Body. Resembles that of males in the armature of the scutum magnum (Fig. 13A–B vs Figs 7A, C, 8A, C). Leg II not dimorphic (Fig. 14A); femur II not swollen as in male (Fig. 14A, C vs Fig. 14B, D); tibia II thin as in male but without ventral tubercles (Fig. 14E vs Fig. 14F); metatarsus II thin and unarmed (Fig. 14G vs Fig. 14H). Tarsal formula 3(2):5(4):5:5.

Female genitalia. Ovipositor cylindrical (Fig. 13C), distally bearing two lobes (furca) (Fig. 13C–D, F). Each furcal lobe with five long, pointed setae (Fig. 13E) – three dorsal and two ventral – resulting in a total of six setae on the dorsal region (Fig. 13D) and four on the ventral region (Fig. 13F). External surface of dorsal and ventral furcal lobes medially with several short, pointed projections, irregularly distributed (Fig. 13D, F). Receptacle chambers located near the base of the furcal groove (Fig. 13D–F).

Distribution

Known only from the type locality (Fig. 40).

Metabiantes herculeus sp. nov.

urn:lsid:zoobank.org:act:D394CC39-C444-49BC-8707-824153F3ED9A

Figs 15–20; Table 3

Diagnosis

Metabiantes herculeus sp. nov. differs from its congeners (except *M. kaurii* sp. nov., *M. kivuensis* sp. nov., *M. machadoi*, *M. obscurus*, *M. pusulosus*, and *M. zuurbergianus*) by the following combination of traits: absence of tubercles on mesotergal areas III–V and free tergites; sexually dimorphic male leg II with a thickened femur and patella, a broad tibia, and a metatarsus ventrally armed with tubercles (Figs 17A–F, 20B, D, F, H). Males of *M. herculeus* differ from those of *M. kaurii* and *M. kivuensis* by having ventral tubercles on tibia II, absent in the latter species (Fig. 17C–D vs Figs 23C–D, 28C–D). The penis of *M. herculeus* is distinctive with conductors closely together and lacking lateral projections, unlike the widely separated conductors in *M. kaurii* (Fig. 18B vs Fig. 24B) and the presence of lateral projections in *M. kivuensis* (Fig. 18B vs Fig. 29B). Additionally, the shorter, non-contacting halves of the lamina apicalis in *M. herculeus* contrast with the longer, contacting halves in *M. kaurii* (Fig. 18B, D vs Fig. 24B, D). Unlike *M. kivuensis*, *M. herculeus* lacks a longitudinal division of mesotergal area IV into two halves, which is characteristic of females and major males of *M. kivuensis* (Figs 15A, 16A, 19A vs Figs 25A, 31A). Furthermore, males of *M. herculeus* lack an enlarged trochanter II, distinguishing them from *M. pusulosus* (Fig. 15A vs Kauri 1961: fig. 5a). Also, males of *M. herculeus* are easily distinguished from those of *M. machadoi* by their abruptly thickened femur II (Fig. 17A–B vs Lawrence 1957: fig. 3b) and from those of *M. zuurbergianus* by the presence of ventral tubercles on tibia II (Fig. 17C–D vs Kauri 1961: 25). The penis of *M. herculeus* features a deeper U-shaped cleft of the lamina apicalis, wider titillators, and smaller basal setae, which distinguish it from the shallow cleft, narrow titillators, and larger basal setae in *M. obscurus* and *M. zuurbergianus* (Fig. 18B–D vs Kauri 1961: figs 7a–b, 11a–b). Additionally, the rounded pars distalis with wide titillators in *M. herculeus* differs from the triangular lateral edges of pars distalis and narrow titillators in *M. pusulosus* (Fig. 18B–D vs Kauri 1961: fig. 1a–b).

Etymology

The species name is derived from the Latin word *Hercules*, the Roman counterpart of the Greek hero *Heracles*, the most popular figure in ancient Greek mythology. It can be understood as something related to or characteristic of Hercules, often indicating strength and power qualities, specifically referring to the strongly thickened femur II of the species.

Type material

Holotype

TANZANIA • ♂; Mbeya Region, Tukuyu, Ushirika area, Kayuki tea estate; 9.41667° S, 34.66667° E; 1200 m a.s.l.; 29 Nov. 1991; R. Jocqué leg.; litter; RMCA, BE_RMCA_ARA.Opi.173473.

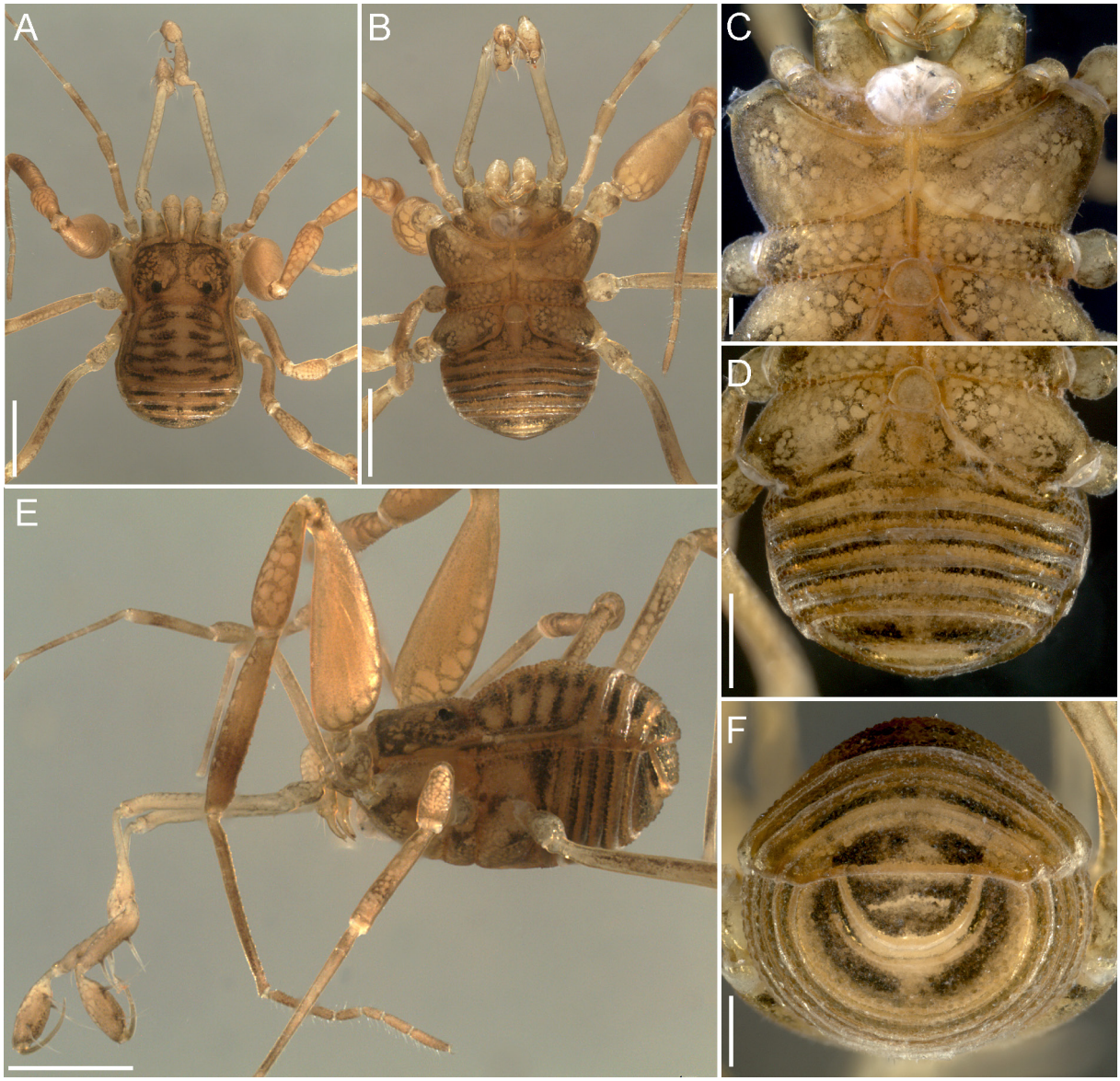

Fig. 15. *Metabiantes herculeus* sp. nov., holotype, ♂ (BE_RMCA_ARA.Opi.173473), habitus photos. **A**. Dorsal view. **B**. Ventral view. **C**. Ventral view with detail of coxae I–IV. **D**. Ventral view with detail of coxa IV and free sternites. **E**. Lateral view. **F**. Posterior view. Scale bars: A–B, E = 1 mm; C = 200 µm; D, F = 500 µm.

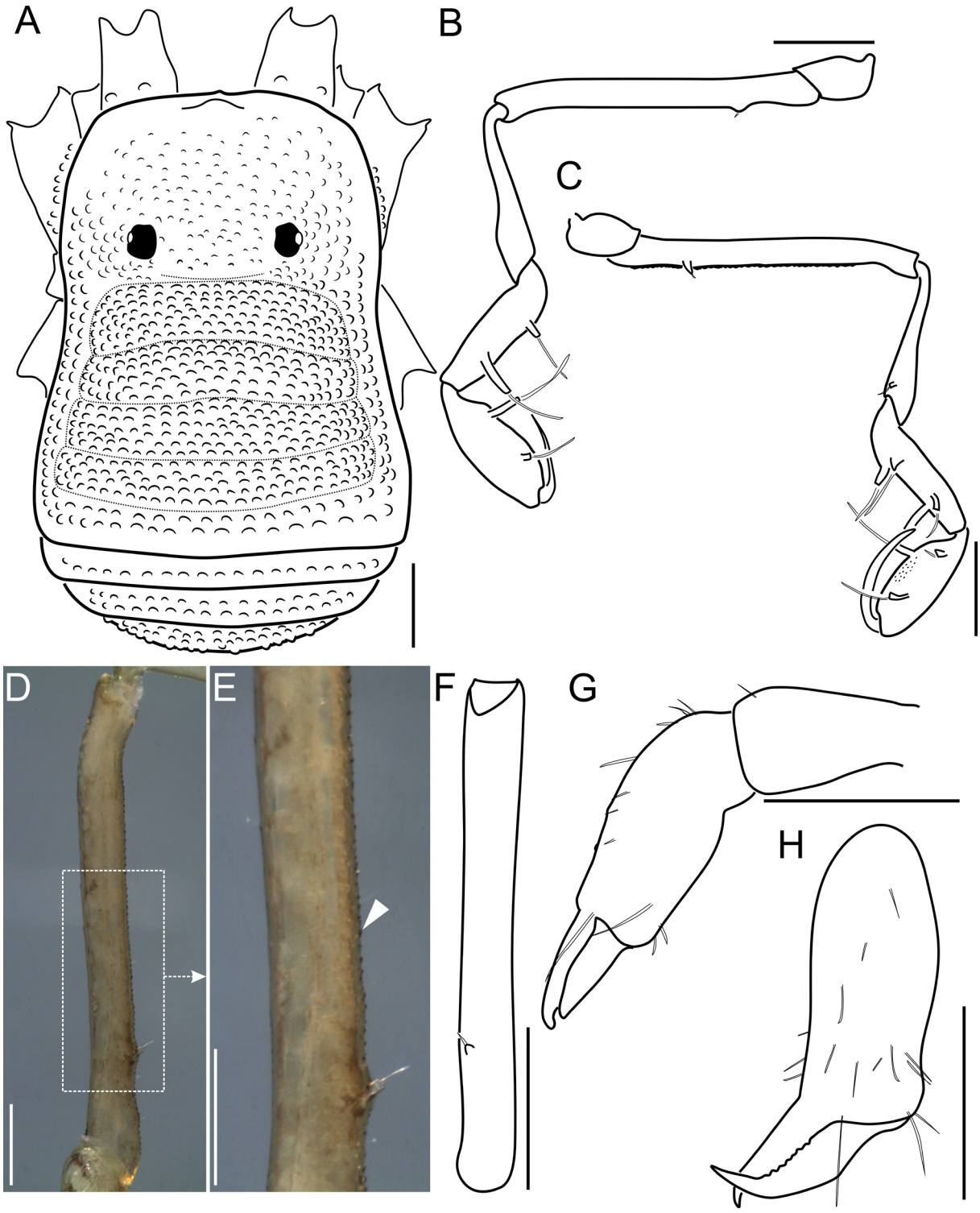

Fig. 16. *Metabiantes herculeus* sp. nov., holotype, ♂ (BE_RMCA_ARA.Opi.173473). **A–C, F–H**. Drawings of habitus, pedipalp, and chelicera. **D–E**. Photos of pedipalp femur. **A**. Habitus, dorsal view. **B–F**. Left pedipalp. **B**. Ectal view. **C**. Mesal view. **D**. Femur, mesal view. **E**. Detail of femur surface. **F**. Femur, ventral view. **G–H**. Left chelicera. **G**. Ectal view. **H**. Frontal view. White triangle indicates a granule. Scale bars: A–C, F–H = 500 µm; D = 250 µm; E = 200 µm.

Paratype

TANZANIA • 1 ♀; same data as for holotype; RMCA, BE_RMCA_ARA.Opi.247663.

Description

Male (holotype, BE_RMCA_ARA.Opi.173473)

Body measurements. Total body length 2.52, carapace length 0.86, scutum magnum length 2.07, carapace maximum width 1.43, abdominal scutum maximum width 1.68. Appendage measurements in Table 3.

Dorsum. Outline slightly hourglass-shaped with Eta (η) shape, with a very slight constriction located at sulcus I level (Figs 15A, 16A); carapace with scattered granules, wider than long, with a small and rounded frontal hump (Figs 15A, 16A); anterior border slightly convex and unarmed (Figs 15A, 16A). Cheliceral sockets not marked (Fig. 16A). Eyes separated near sulcus I; interocular area finely granulated (Figs 15A, E, 16A). Carapace in lateral view straight posterior to frontal hump and becoming slightly higher toward the posterior region (Fig. 15E). Abdominal scutum in lateral view convex (Fig. 15E).

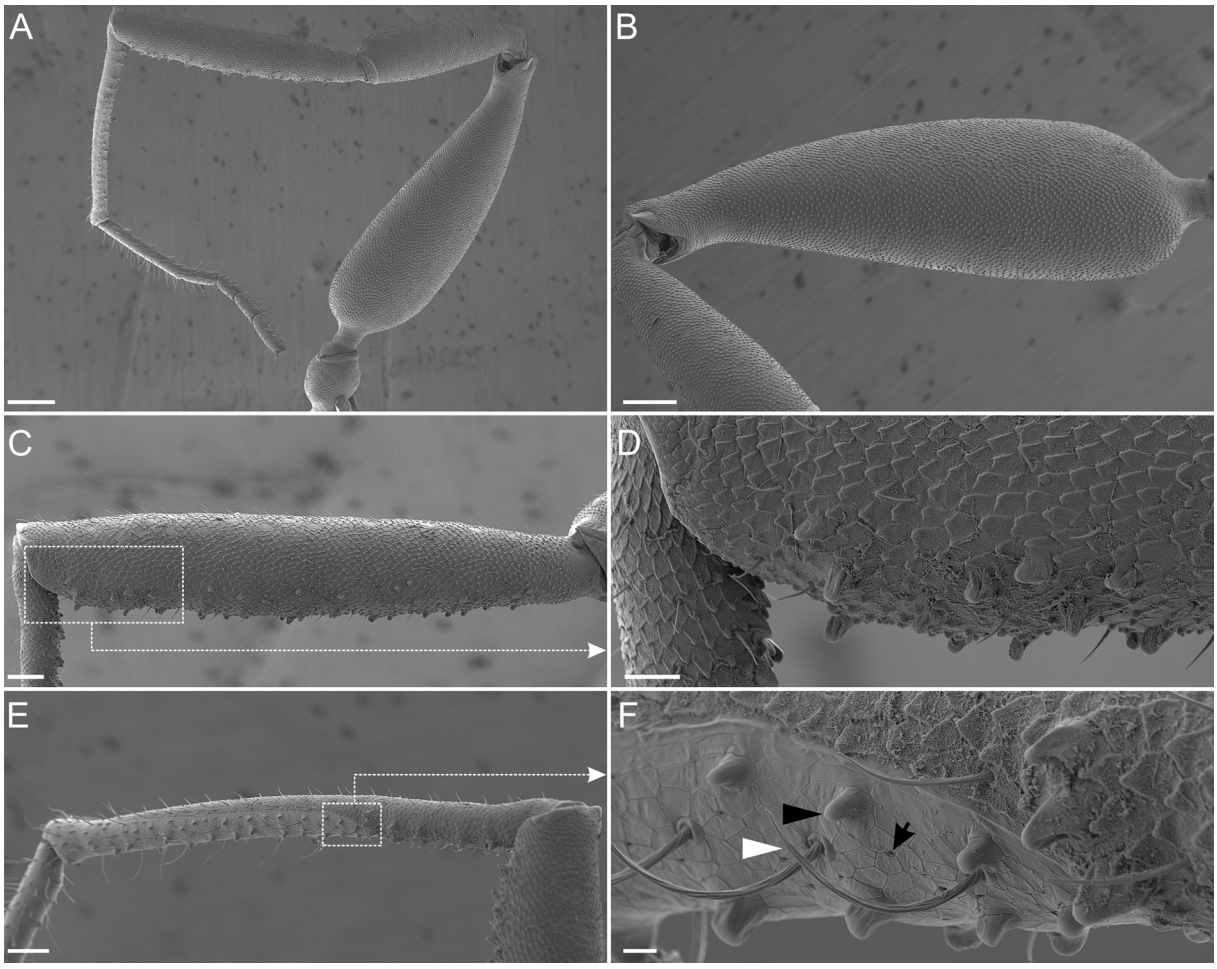

Fig. 17. *Metabiantes herculeus* sp. nov., holotype, ♂ (BE_RMCA_ARA.Opi.173473), scanning electron micrographs of right leg II. **A**. Leg II, retrolateral view. **B**. Femur, prolateral view. **C**. Tibia, prolateral view. **D**. Detail of tibia surface. **E**. Metatarsus, ventroprolateral view. **F**. Detail of astragalus and calcaneus surfaces. Black triangle indicates a trichome; white triangle indicates a sensillum chaeticum; black arrow indicates a glandular opening. Scale bars: A = 300 μm; B = 200 μm; C, E = 100 μm; D = 40 μm; F = 10 μm.

Sulcus I deep and complete (Fig. 16A). Mesotergal areas granulated and well-defined, with sulci II–V marked but shallower than sulcus I; medially sulci II–III slightly curved to anterior body region; sulci IV–V straight (Fig. 16A). Mesotergal area V granulated (Fig. 16A). Lateral margins of abdominal scutum with two rows of granules (Fig. 16A). Free tergites granulated (Figs 15E, 16A).

Venter. Coxa I with few small setiferous granules (Fig. 15C); coxa II incrassated, bigger than coxa IV (Fig. 15B–D); anteroposterior borders of coxa III with a row of strong granules connecting with coxae II and IV, respectively (Fig. 15C–D). Posterior border of spiracular area, free sternites I–V with a row of granules; anal operculum granulated (Fig. 15D–F). Spiracles not concealed (Fig. 15D).

Chelicera. Basichelicerite unarmed, with not marked bulla (Fig. 16G). Cheliceral hand with sparse setae (Fig. 16G–H). Fixed and movable fingers with small triangular-shaped teeth.

Pedipalp. Coxa elongated (i.e., remarkably longer than trochanter), dorsoproximally with one mesal and one ectal granule (Figs 15A, 16A). Trochanter smooth (Fig. 16B–C). Femur straight, proximally with one small ventromesal spine, ventral surface with granules (Fig. 16B–F). Patella elongated, club-shaped, with a small mesodistal spine (Fig. 16B–C). Tibia with two ventroectal and two ventromesal spines; distal ventroectal spine with the highest socket and longest seta (Fig. 16B–C). Tarsus inflated, with oval shape, armed with two ventromesal and two ventroectal spines, proximal spines longer than distal spines (Figs 15E, 16B–C); tarsus ventrally with granules on the medial surface (Fig. 16C).

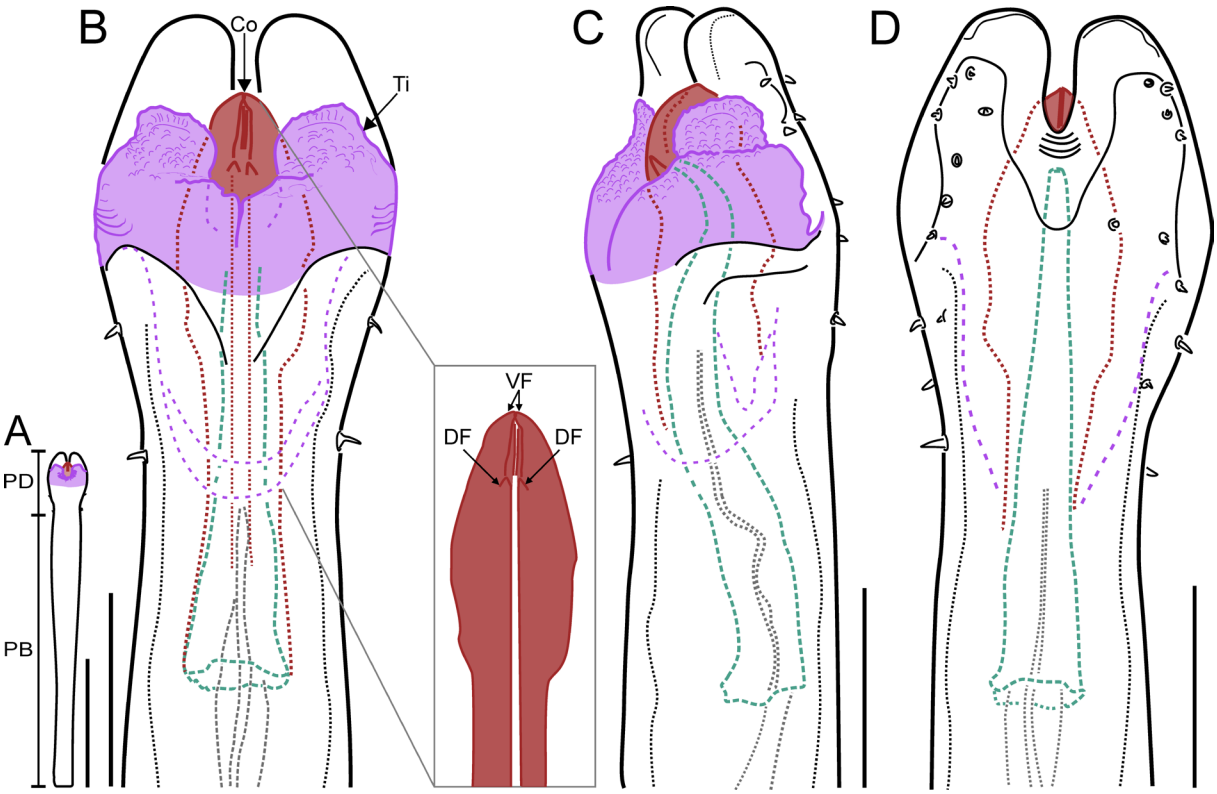

Fig. 18. *Metabiantes herculeus* sp. nov., holotype, ♂ (BE_RMCA_ARA.Opi.173473), penis drawings. **A–B**. Dorsal view (detail of conductors within box). **C**. Lateral view. **D**. Ventral view. Stylus in green, conductors in brownish red, titillators in magenta. Abbreviations: Co = conductor; DF = dorsal fold; PB = pars basalis; PD = pars distalis; Ti = titillator; VF = ventral fold. Scale bars: A = 500 µm; B–D = 100 µm.

Legs. Femur II proximally thin, followed by an abrupt strong thickness, then tapering gradually (Figs 15E, 17A–B, 20B, D). Patella II long, thickened (Figs 17A, 20B). Tibia II widened with ventral small triangular-shaped tubercles (Figs 17C–D, 20F). Metatarsus II with a very long calcaneus that occupies more than half of the ventral metatarsus (Fig. 17E); astragalus short, with equidistant transverse rows of tubercles (Fig. 17E); calcaneus with scattered low and rounded trichomes, long sensilla chaetica and glandular pores on the ventral surface (Fig. 17E–F). Tarsi III–IV with a dense scopula. Tarsal formula: 3(2):5(4):5:5.

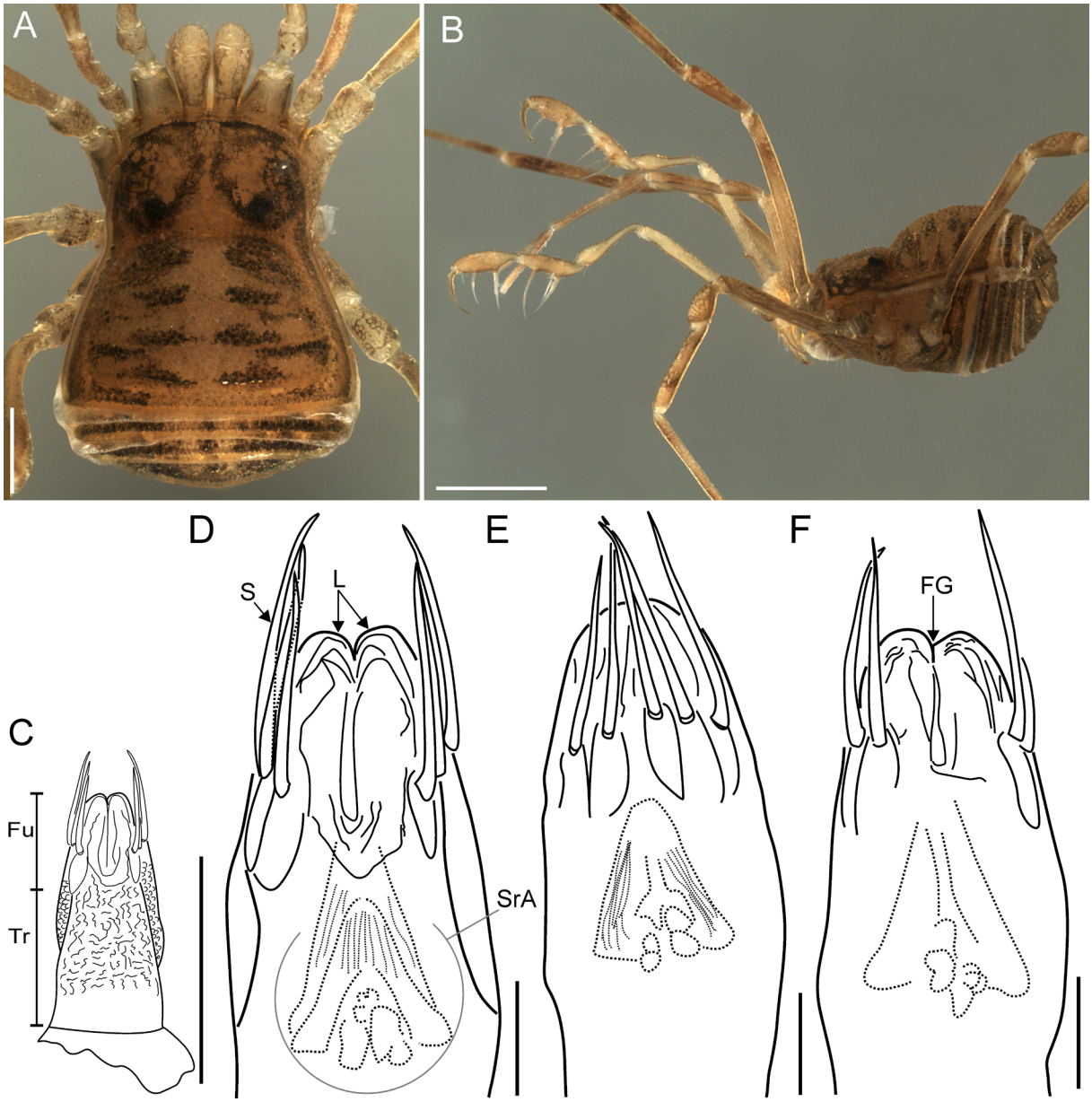

Fig. 19. *Metabiantes herculeus* sp. nov., paratype, ♀ (BE_RMCA_ARA.Opi.247663). **A–B**. Habitus photos. **A**. Dorsal view. **B**. Lateral view. **C–F**. Ovipositor drawings. **C–D**. Dorsal view. **E**. Lateral view. **F**. Ventral view. Abbreviations: FG = furcal groove; Fu = furca; L = lobe; S = seta; SrA = seminal receptacle area; Tr = truncus. Scale bars: A, C = 500 µm; B = 1 mm; D–F = 100 µm.

Color (specimen preserved in 80% ethanol). Body brown-yellowish (Fig. 15A, C–E); carapace, coxae I–IV, and appendages with brown reticulations (Figs 15A–E); lateroanterior, lateral, and lateroposterior borders of mesotergal areas dark brown; mesotergal areas I–III with two medial dark brown patches, closer in mesotergal area III; mesotergal area IV with one posterior medial dark brown patch; mesotergal area V with two lateral dark brown patches; free tergites I–II with two lateral dark brown patches and one medial rounded spot; free tergite III dark brown (Fig. 15A, E); posterior border of spiracular area and free sternites I–IV with a line of dark brown patches (Fig. 15B–F); anal operculum dark brown (Fig. 15F).

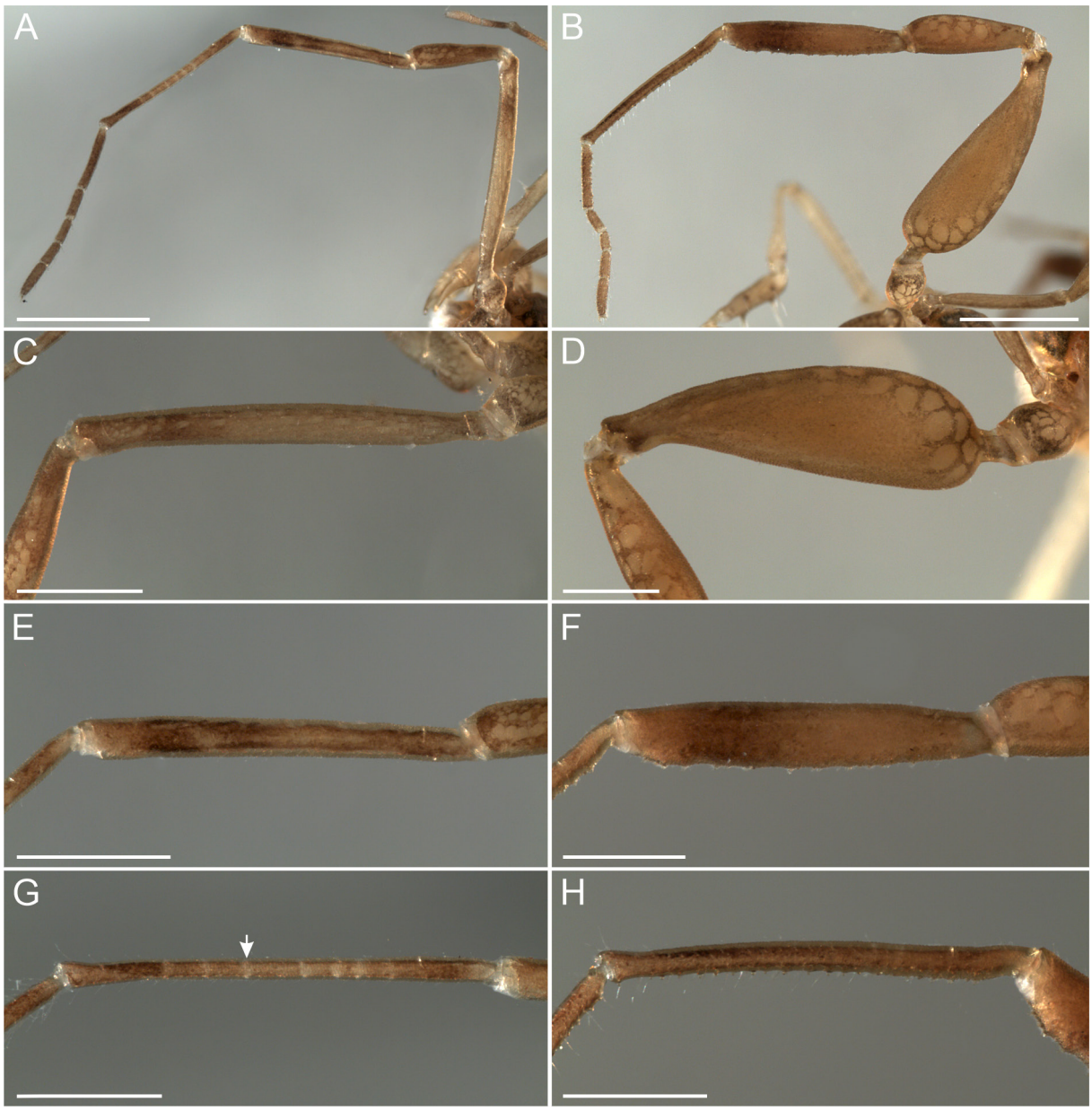

Fig. 20. *Metabiantes herculeus* sp. nov., sexual dimorphism, left legs II photos. **A, C, E, G**. Paratype, ♀ (BE_RMCA_ARA.Opi.247663). **B, D, F, H**. Holotype, ♂ (BE_RMCA_ARA.Opi.173473). **A–B**. Leg II, retrolateral view. **C–D**. Femur, retrolateral view. **E–F**. Tibia, retrolateral view. **G–H**. Metatarsus, retrolateral view. Arrow indicates a pseudoarticular ring. Scale bars: A–B = 1 mm; C–H = 500 µm.

Table 3. Appendage measurements (in mm) of *Metabiantes herculeus* sp. nov. ***** = holotype. Abbreviations: Fe = femur; Mt = metatarsus; Pa = patella; T = total; Ta = tarsus; Ti = tibia; Tr = trochanter.

		Tr	Fe	Pa	Ti	Mt	Ta	T
♂ RMCA 173473*	Pedipalp	0.34	1.41	0.81	0.70	–	0.70	3.96
	Leg I	0.29	1.12	0.44	0.77	1.12	0.84	4.58
	Leg II	0.44	2.05	1.14	1.51	1.53	1.59	8.26
	Leg III	0.33	0.14	0.61	1.17	1.75	0.85	4.85
	Leg IV	0.37	1.94	0.68	1.50	2.29	1.06	7.84
♀ RMCA 247663	Pedipalp	0.29	1.21	0.63	0.58	–	0.55	3.26
	Leg I	0.26	0.94	0.39	0.66	0.95	0.77	3.97
	Leg II	0.31	1.64	0.73	1.27	1.44	1.45	6.84
	Leg III	0.37	1.22	0.45	0.86	1.44	0.83	5.17
	Leg IV	0.35	1.54	0.57	1.20	1.92	0.98	6.56

Male genitalia. Penis with clearly defined boundaries between pars basalis and pars distalis (Fig. 18A). Pars basalis basally thin, broadens medially, with distal constriction (Fig. 18A). Pars distalis slightly swollen with maximum width at titillator level (Fig. 18B). Apical edge laminar (i.e., dorsoventrally flat) with a medial U-shaped cleft that divides it into two rounded and elongated halves (Fig. 18B, D); these halves are apically less chitinous and could possibly be inflated by hemolymph pressure (Fig. 18D). Pars distalis with a distal depression in the ventromedial region (Fig. 18D). Each side of pars distalis armed with short, conical microsetae irregularly arranged, extending basally from the dorsolateral to the ventroapical side (Fig. 18B–D). Capsula externa with two broad titillators separated by a dorsal cleft basally narrow (Fig. 18B). Capsula interna formed by two conductors and one stylus, basally fused. Each one with two laminar folds apically, one small pointed dorsal fold and one longer ventral fold, ventrally visible within the U-shaped cleft; stylus tubular, and irregular S-shaped in lateral view with its free tip fully covered by conductors (Fig. 18B–D).

Female (paratype, BE_RMCA_ARA.Opi.247663)

Body measurements. Total body length 2.16, carapace length 0.67, scutum magnum length 1.83, carapace maximum width 1.12, abdominal scutum maximum width 1.64. Appendage measurements in Table 3.

Body. Female resembles male in the armature of the scutum magnum (Fig. 19A–B vs Fig. 15A, E) but differs from male by having a thinner pedipalp tarsus (Fig. 19B vs Fig. 15E). Also, female differs by having a thin leg II (Fig. 20A vs Fig. 20B); femur and patella II thin (Fig. 20A, C vs Fig. 20B, D); tibia II thin and unarmed (Fig. 20E vs Fig. 20F); metatarsus II and basitarsus thin and unarmed, with pseudoarticular rings (Fig. 20A, G vs Fig. 20B, H). Tarsal formula 3(2):5(4):5:5.

Female genitalia. Ovipositor cylindrical (Fig. 19C), distally bearing two long lobes (furca) (Fig. 19C–D, F). Each furcal lobe with five long, pointed setae (Fig. 19E) – three dorsally and two ventrally – resulting in a total of six setae on the dorsal region (Fig. 19D) and four on the ventral region (Fig. 19F). Receptacle chambers located near the base of the furcal groove (Fig. 19D, F).

Distribution

Known only from the type locality (Fig. 40).

Metabiantes kaurii sp. nov.
urn:lsid:zoobank.org:act:44F823B9-361E-4C7C-B792-D685D7DEC49F
Figs 21–24; Table 4

Diagnosis

Metabiantes kaurii sp. nov. differs from its congeners (except *M. herculeus* sp. nov., *M. kivuensis* sp. nov., *M. machadoi*, *M. obscurus*, *M. pusulosus*, and *M. zuurbergianus*) by the following combination of traits: absence of tubercles on mesotergal areas III–V and free tergites; sexually dimorphic male leg II with a thickened femur, a broad tibia, and a metatarsus ventrally armed with tubercles (Figs 21A, 22A, 23B, D, F). Male of *M. kaurii* differs from *M. herculeus* by the absence of ventral tubercles on tibia II, present in the latter species (Fig. 23C–D vs Fig. 17C–D). The penis of *M. kaurii* is distinctive with widely separated conductors and lacking lateral projections, unlike the close-together conductors in *M. herculeus* (Fig. 24B vs Fig. 18B) and the presence of lateral projections in *M. kivuensis* (Fig. 24B vs Fig. 29B). Additionally, the longer, contacting halves of the lamina apicalis in *M. kaurii* contrast with the shorter, non-contacting halves in *M. herculeus* (Fig. 24B, D vs Fig. 18B, D). Unlike *M. kivuensis*, *M. kaurii* lacks a longitudinal division of mesotergal area IV into two halves, which is characteristic of females and major males of *M. kivuensis* (Figs 21A, 22A vs Figs 25A, 31A). Furthermore, the male of *M. kaurii* lacks an enlarged trochanter II, distinguishing it from those of *M. pusulosus* (Fig. 21A vs Kauri 1961: fig. 5a). Also, the male of *M. kaurii* is distinguished from that of *M. machadoi* by its abruptly thickened femur II (Fig. 23A vs Lawrence 1957: fig. 3b). The penis of *M. kaurii* features a deeper U-shaped cleft of the lamina apicalis, wider titillators, and smaller basal setae, which distinguish it from the shallow cleft, narrow titillators, and larger basal setae in *M. obscurus* and *M. zuurbergianus* (Fig. 24B–D vs Kauri 1961: figs 7a–b, 11a–b). Additionally, the slight triangular lateral edges of the pars distalis and wide titillators in *M. kaurii* differ from the stronger triangular lateral edges of the pars distalis and narrow titillators in *M. pusulosus* (Fig. 24B–D vs Kauri 1961: fig. 1a–b).

Etymology

The species epithet is a patronym, honoring the Estonian arachnologist Hans Kauri (1906–1999) for his contributions to opilionology, particularly that of the African fauna.

Type material

Holotype
MOZAMBIQUE • ♂; Niassa; 12.38278° S, 35.33369° E; 1724 m a.s.l.; 14 Nov. 2006; L. Geeraert and M. Jocqué leg.; montane forest; pitfall trap; MACN-Ar 46476.

Description

Male (holotype, MACN-Ar 46476)
Body measurements. Total body length 2.41, carapace length 0.71, scutum magnum length 2.28, carapace maximum width 1.08, abdominal scutum maximum width 1.53. Appendage measurements in Table 4.

Dorsum. Outline hourglass-shaped with Eta (η) shape, with a slight constriction posteriorly at sulcus I level (Figs 21A, 22A). Carapace granulated, wider than long, anterior border convex, and unarmed (Figs 21A, 22A). Cheliceral sockets not marked (Fig. 22E). Eyes separated near sulcus I; interocular area granulated (Figs 21E, 22A). Carapace in lateral view straight in anterior region and slightly higher posteriorly (Fig. 21E). Abdominal scutum in lateral view convex (Fig. 21E). Sulcus I deep and complete, curving slightly posteriorly at midline in dorsal view (Fig. 22A). Mesotergal areas granulated and well-defined, with sulci II–V marked but shallower than sulcus I; sulci II–III slightly curved anteriorly; sulci IV–V straight. Mesotergal area V granulated (Figs 21A, 22A). Lateral margins of abdominal scutum with two rows of granules (Fig. 22A). Free tergites with two rows of granules (Figs 21E–F, 22A).

Venter. Coxa I with some small setiferous granules; coxa II incrassated, of same size as (or slightly smaller than) coxa IV (Fig. 21C); anteroposterior borders of coxa III with a row of strong granules connecting with coxae II and IV, respectively (Fig. 21C). Posterior border of spiracular area, free sternites I–V with a row of granules (Fig. 21D–F); anal operculum granulated (Fig. 21D–F). Spiracles not concealed (Fig. 21D).

Chelicera. Basichelicerite unarmed with a slightly marked bulla (Fig. 22E). Cheliceral hand with sparse setae (Fig. 22E–F). Fixed and movable fingers with small triangular-shaped teeth (Fig. 22F).

Pedipalp. Coxa elongated (i.e., remarkably longer than trochanter), dorsoproximally with one mesal and one ectal granule (Figs 21A, 22A). Trochanter unarmed. Femur straight, proximally with one small ventromesal spine (Fig. 22B–D). Patella elongated, club-shaped, and armed with a small distal ventromesal spine (Fig. 22B). Tibia with two ventromesal and two ventroectal spines, with distal ventroectal spine longest (Fig. 22B–C). Tarsus inflated, of spheroid shape, armed with two ventromesal

Fig. 21. *Metabiantes kaurii* sp. nov., holotype, ♂ (MACN-Ar 46476), habitus photos. **A**. Dorsal view. **B**. Ventral view. **C**. Ventral view with detail of coxae I–IV. **D**. Ventral view with detail of coxa IV and free sternites. **E**. Lateral view. **F**. Posterior view. Scale bars: A–B, E = 1 mm; C = 200 µm; D, F = 500 µm.

Table 4. Appendage measurements (in mm) of *Metabiantes kaurii* sp. nov. ***** = holotype. Abbreviations: Fe = femur; Mt = metatarsus; Pa = patella; T = total; Ta = tarsus; Ti = tibia; Tr = trochanter.

		Tr	Fe	Pa	Ti	Mt	Ta	T
♂ MACN-Ar 46476*	Pedipalp	0.25	1.20	0.65	0.55	–	0.62	3.27
	Leg I	0.26	0.94	0.39	0.69	1.01	0.73	4.02
	Leg II	0.32	1.59	0.62	1.24	1.42	1.36	6.55
	Leg III	0.24	1.17	0.47	0.89	1.14	0.73	4.64
	Leg IV	0.36	1.15	0.58	1.16	1.93	0.86	6.04

and two ventroectal spines; proximal spines longer than distal spines; ventroectal spine with the highest elevated socket; tarsus ventromedially with small granules (Fig. 22B–C).

Legs. Femur II unarmed, proximally thin, followed by an abrupt strong thickness, then tapering gradually (Fig. 23A–B). Patella II short and unarmed. Tibia II widened and unarmed (Fig. 23C–D). Metatarsus III with astragalus occupying the half region (Fig. 23E–G), ventrally with triangular-shaped tubercles (Fig. 23F–I). Calcaneus occupies half of metatarsus, with scattered low and rounded trichomes and long sensilla chaetica along the lateral surface (Fig. 23H–J). Tarsi III–IV with a dense scopula. Tarsal formula: 3(2):5(4):5:5.

Color (specimen preserved in 80% ethanol). Body brown yellowish (Fig. 21A–F); carapace with brown reticulations on anterior and lateral regions (Fig. 21A). Lateroanterior, lateral, and lateroposterior borders of mesotergal areas I–III and anal operculum dark brown (Fig. 21A, F); lateroanterior, lateral, and posterior borders of mesotergal area IV with dark brown patches (Fig. 21A). Mesotergal area V and

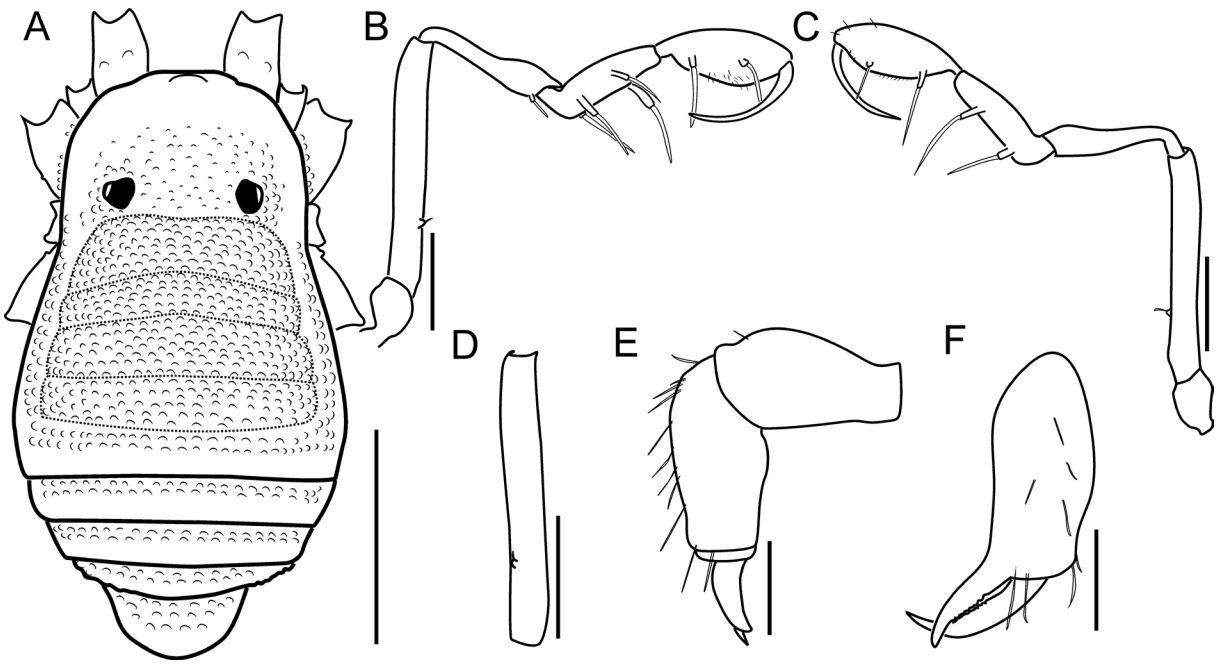

Fig. 22. *Metabiantes kaurii* sp. nov., holotype, ♂ (MACN-Ar 46476), drawings of habitus, pedipalp, and chelicera. **A**. Habitus, dorsal view. **B–D**. Left pedipalp. **B**. Mesal view. **C**. Ectal view. **D**. Femur, ventral view. **E–F**. Left chelicera. **E**. Ectal view. **F**. Frontal view. Scale bars: A = 1 mm; B–D = 500 μm; E–F = 250 μm.

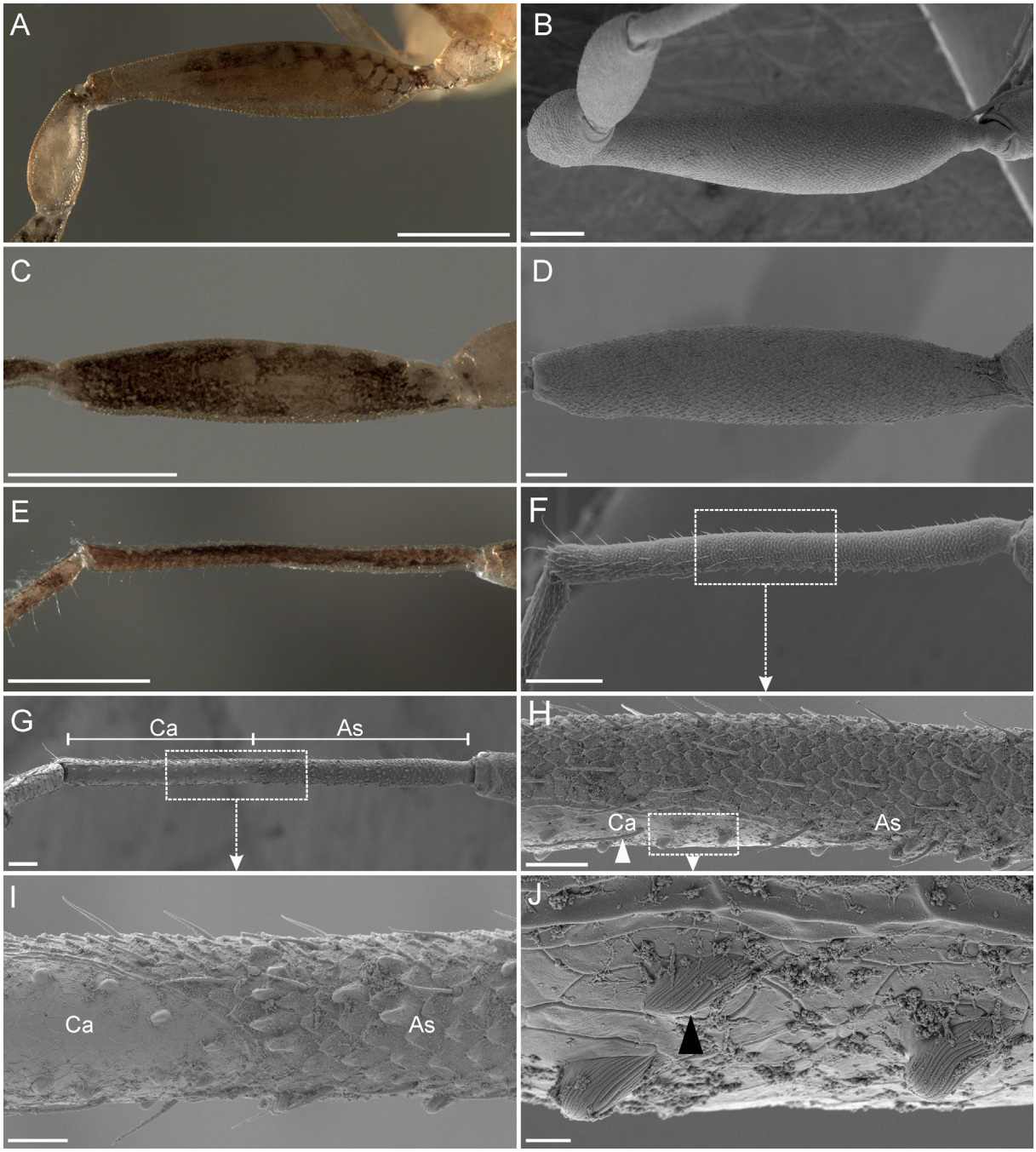

Fig. 23. *Metabiantes kaurii* sp. nov., holotype, ♂ (MACN-Ar 46476), photographs and scanning electron micrographs of left leg II. **A**. Femur, retrolateral view. **B**. Femur, ventral view. **C–D**. Tibia, retrolateral view. **E–F**. Metatarsus, retrolateral view. **G**. Metatarsus, ventral view. **H**. Detail of astragalus and calcaneus, retrolateral view. **I**. Detail of astragalus and calcaneus surface, ventral view. **J**. Detail of calcaneus surface, retrolateral view. Black triangle indicates a trichome; white triangle indicates a sensillum chaeticum. Abbreviations: As = astragalus; Ca = calcaneus. Scale bars: A, C, E = 500 µm; B, F = 200 µm; D, G = 100 µm; H = 40 µm; I = 30 µm; J = 5 µm.

free tergites with two lateral dark brown patches (Fig. 21A); coxae I–IV with brown reticulations; free sternites with anterior dark brown patches (Fig. 21B, D). Appendages with brown reticulations or dark patches (Fig. 21A–B, E).

Male genitalia. Pars basalis and pars distalis with indistinct boundaries, defined by the start of the most basal macrosetae marking the beginning of pars distalis (Fig. 24A–D). Pars basalis tubular, basally thin, gradually widening toward distal region (Fig. 24A); pars distalis slightly swollen, with maximum width at titillator level (Fig. 24B), and ventrally with slight angular lateral edges (Fig. 24D). Apical edge laminar (i.e., dorsoventrally flat) with a deep medial U-shaped cleft dividing it into two elongated, rounded halves, apically in contact (Fig. 24A–B, D). Pars distalis with a small distal depression in the ventromedial region (Fig. 24D). Each side of pars distalis bearing small conical microsetae irregularly arranged, extending from the dorsal to ventroapical region (Fig. 24B–D). Capsula externa with two broad titillators covering most of the capsula interna; titillators separated by a U-shaped cleft at the base, narrowing apically (Fig. 24B–C). Capsula interna formed by two laminar conductors and one stylus basally fused. Conductors apically curved toward medial region; conductor tips ventrally visible within U-shaped cleft. Stylus tubular, basally wide, apically thin, and with an irregular S-shaped curve in lateral view (Fig. 24C), with a rounded tip (Fig. 24B, D).

Female

Unknown.

Distribution

Known only from the type locality (Fig. 40).

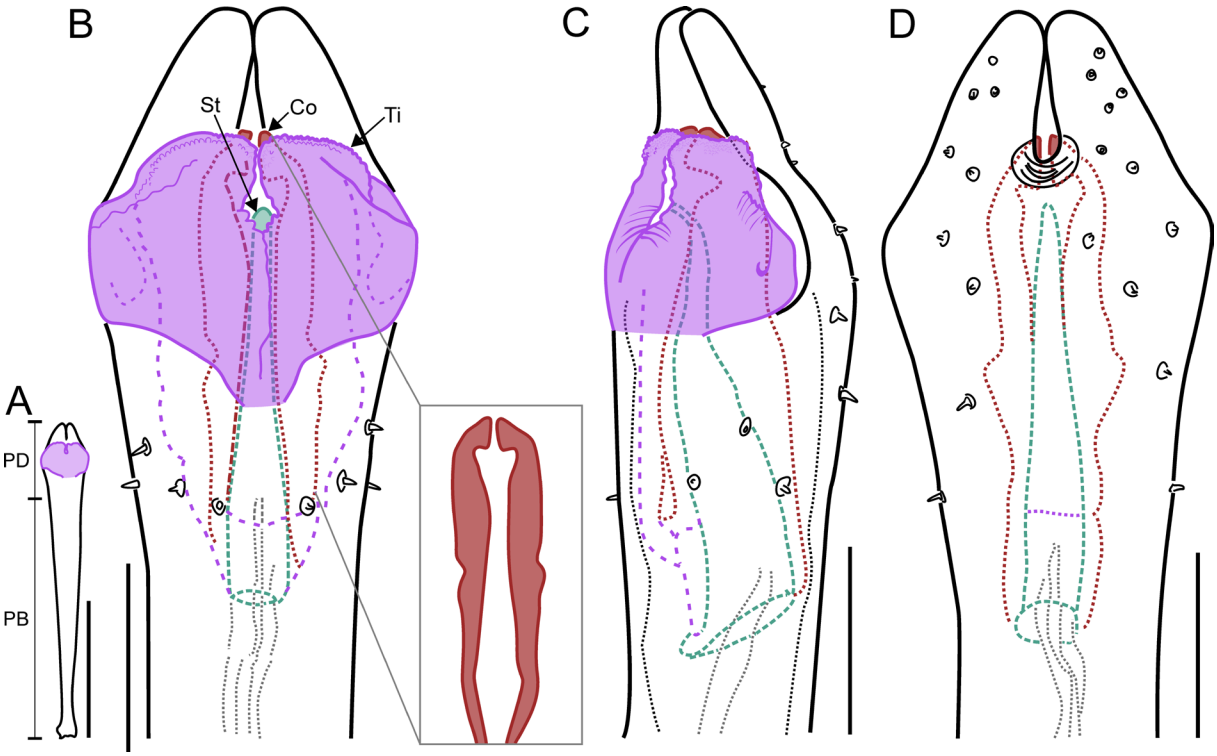

Fig. 24. *Metabiantes kaurii* sp. nov., holotype, ♂ (MACN-Ar 46476), penis drawings. **A–B**. Dorsal view (detail of conductors within box). **C**. Lateral view. **D**. Ventral view. Stylus in green, conductors in brownish red, titillators in magenta. Abbreviations: Co = conductor; PB = pars basalis; PD = pars distalis; St = stylus; Ti = titillator. Scale bars: A = 500 µm; B–D = 100 µm.

Metabiantes kivuensis sp. nov.
urn:lsid:zoobank.org:act:364EA7D6-9176-4A30-BE56-A53A50C64FD5
Figs 25–32; Table 5

Diagnosis

Major males and females (excluding minor males) of *Metabiantes kivuensis* sp. nov. can be distinguished from those of all other species of *Metabiantes* by the presence of a longitudinal division of mesotergal area IV into two halves (Figs 25A, 31A). Additionally, *M. kivuensis* differs from its congeners (except *M. herculeus* sp. nov., *M. kaurii* sp. nov., *M. machadoi*, *M. obscurus*, *M. pusulosus*, and *M. zuurbergianus*) by the following combination of traits: absence of tubercles on mesotergal areas III–V and free tergites; sexually dimorphic male leg II with a thickened femur, a broad tibia, and a metatarsus ventrally with tubercles (Figs 26A, 28A–F, 32B–C, E–F, H–I, K–L). Males of *M. kivuensis* differ from those of *M. herculeus* by the absence of ventral tubercles on tibia II, present in the latter species (Fig. 28C–D vs Fig. 17C–D). The penis of *M. kivuensis* sp. nov. is distinctive with closely together conductors and the presence of lateral projections, unlike the widely separated conductors in *M. kaurii* (Fig. 29B vs Fig. 24B) and the absence of lateral projections in *M. herculeus* (Fig. 29B vs Fig. 24B). Furthermore, males of *M. kivuensis* lack an enlarged trochanter II, distinguishing them from those of *M. pusulosus* (Fig. 25A, E vs Kauri 1961: fig. 5a). Also, major males of *M. kivuensis* are distinguished from those of *M. machadoi* by their abruptly thickened femur II (Fig. 25C vs Lawrence 1957: fig. 3b). The penis of *M. kivuensis* features a deeper U-shaped cleft of the lamina apicalis and smaller basal setae, which distinguish it from the shallow cleft and larger basal setae in *M. obscurus* and *M. zuurbergianus* (Fig. 29B–D vs Kauri 1961: figs 7a–b, 11a–b). Additionally, the rounded pars distalis in *M. kivuensis* differs from the stronger angular lateral edges of pars distalis in *M. pusulosus* (Fig. 29B–D vs Kauri 1961: fig. 1a–b).

Etymology

The species epithet '*kivuensis*' means 'of or from Kivu', a reference to the species type locality in North Kivu, a province of the Democratic Republic of the Congo.

Type material

Holotype

CONGO • major ♂; Kivu-N, Kilindera, "Face N. du Ruwenzori, camp de Kilindera" [North face of Ruwenzori, Kilindera camp]; 0.38333° N, 29.91667° E; 2950 m a.s.l.; Jul.–Aug. 1974; M. Lejeune leg.; "litière du bambusetum du Musoso" [litter of bamboo vegetation along the Musoso]; RMCA, BE_RMCA_ARA.Opi.154162.

Paratypes

CONGO • 1 major ♂, 1 minor ♂ (photo voucher), 1 ♀ (photo voucher); same data as for holotype; RMCA, BE_RMCA_ARA.Opi.247664 • 1 minor ♂ (SEM voucher); same data as for holotype; MACN-Ar 45445 • 1 major ♂; same data as for holotype; MACN-Ar 45437.

Other material examined

CONGO • 1 major ♂, 2 ♀♀, 2 juvs; Kivu-C, Kanzuiri, "Face N. du Ruwenzori, camp de Kanzuiri, crête du Kanzuiri" [North face of Ruwenzori, Kilindera camp, Kanzuiri Ridge]; 0.41667° N, 29.9° E; 3500 m a.s.l.; Jul.–Aug. 1974; M. Lejeune leg.; "dans mousses" [in mosses]; RMCA, BE_RMCA_ARA.Opi.154244 • 1 minor ♂, 1 ♀; same data as for preceding; MACN-Ar 45470.

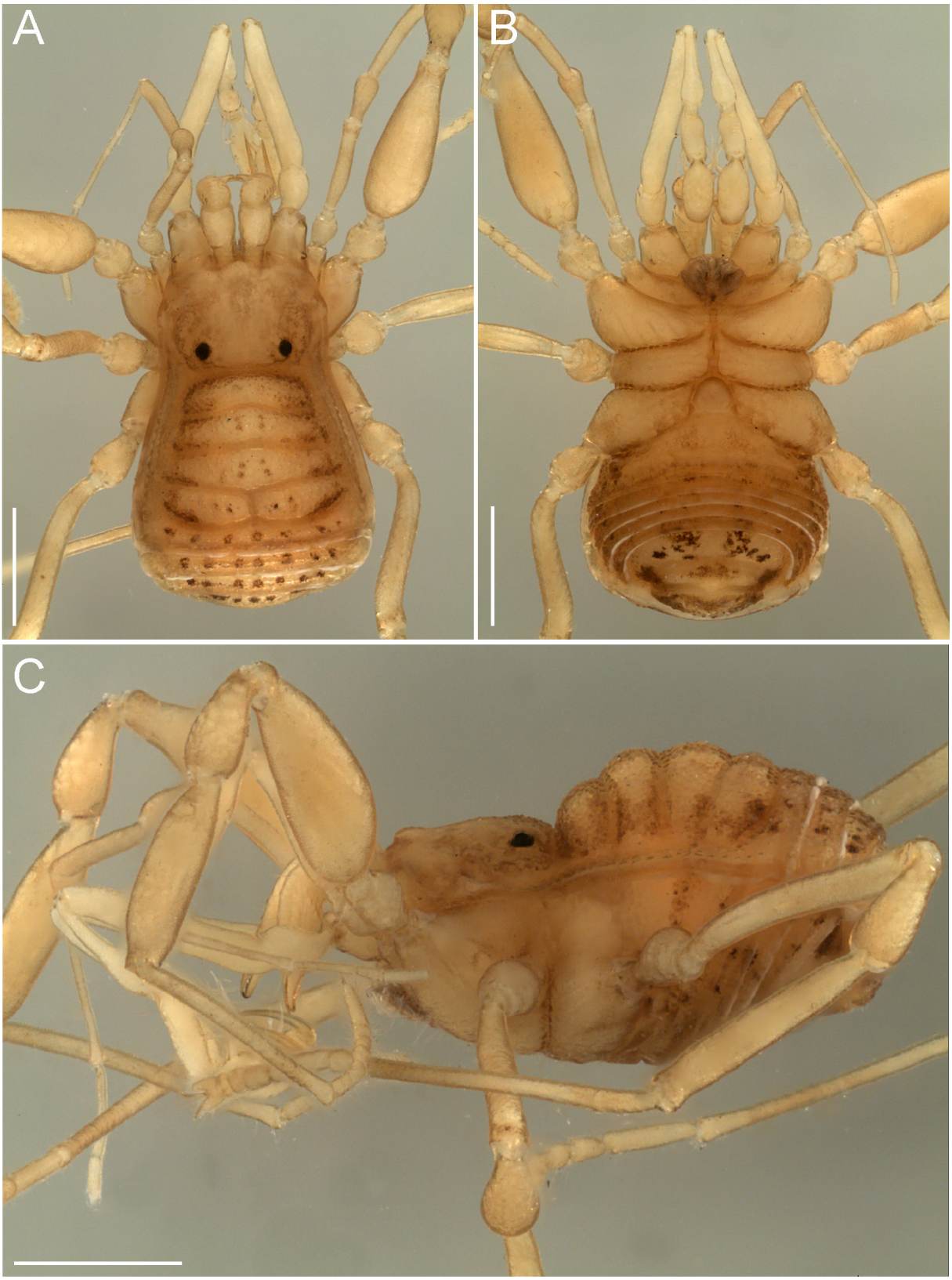

Fig. 25. *Metabiantes kivuensis* sp. nov., holotype, major ♂ (BE_RMCA_ARA.Opi. 154162), habitus photos. **A**. Dorsal view. **B**. Ventral view. **C**. Lateral view. Scale bars = 1 mm.

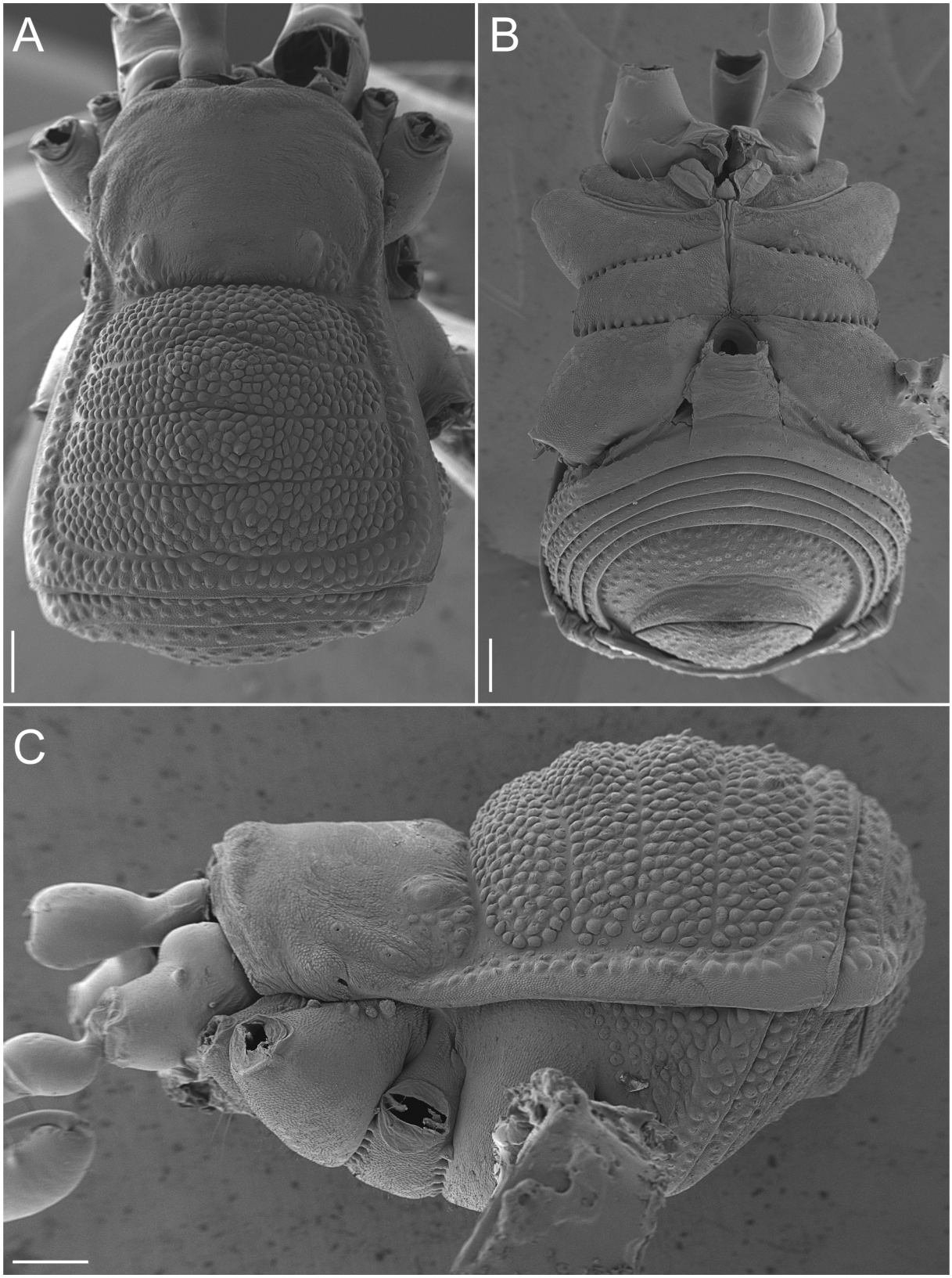

Fig. 26. *Metabiantes kivuensis* sp. nov., paratype, minor ♂ (MACN-Ar 45445), scanning electron micrographs of habitus. **A**. Dorsal view. **B**. Ventral view. **C**. Lateral view. Scale bars = 300 μm.

Description

Male (holotype, BE_RMCA_ARA.Opi.154162)

Body measurements. Total body length 2.95, carapace length 0.94, scutum magnum length 2.58, carapace maximum width 1.43, abdominal scutum maximum width 2.09. Appendage measurements in Table 5.

Dorsum. Outline slightly hourglass-shaped with Eta (η) shape, with a very slight constriction at sulcus I level (Figs 25A, 26A). Carapace wider than long with a row of granules on the posterior margin and granules concentrated laterally around eyes, anterior border slightly convex and unarmed (Fig. 26A); Cheliceral sockets not marked (Fig. 26A). Eyes separated near sulcus I; interocular area smooth (Figs 25A, 26A). Carapace in lateral view straight at anterior region and slightly higher posteriorly

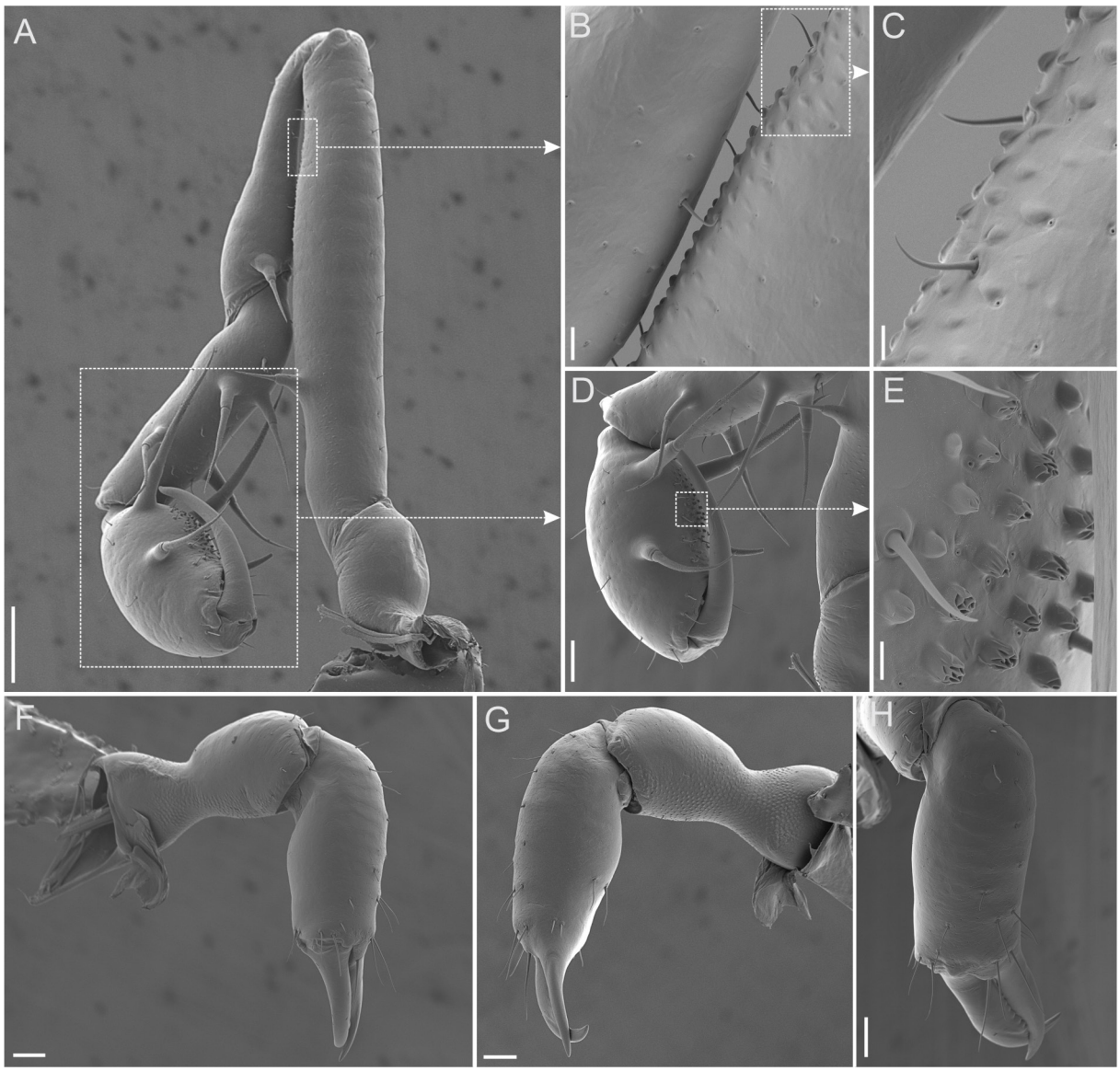

Fig. 27. *Metabiantes kivuensis* sp. nov., paratype, minor ♂ (MACN-Ar 45445), scanning electron micrographs of pedipalp and chelicera. **A–E**. Right pedipalp. **A**. Mesal view. **B**. Detail of femur. **C**. Detail of femoral granules. **D**. Tibia and tarsus, ventroectal view. **E**. Detail of aggregate pores of tarsus. **F–H**. Left chelicera. **F**. Mesal view. **G**. Ectal view. **H**. Frontal view. Scale bars: A = 200 μm; B = 20 μm; C, E = 10 μm; D, F–H = 100 μm.

(Figs 25C, 26C). Abdominal scutum in lateral view convex (Figs 25C, 26C). Sulcus I deep, complete, and slightly curved to the anterior body region (Figs 25A, 26A). Mesotergal areas granulated and well-defined, with sulci II–V marked but shallower than sulcus I; sulci II–III medially arched to the anterior body region; sulcus IV medially arched to posterior body region (Fig. 25A); sulcus V medially invaginated towards mesotergal area IV dividing it into two (Fig. 25A). Mesotergal area V with two rows of granules (Fig. 26A). Lateral borders of abdominal scutum with two rows of granules (Fig. 26A). Ozopore with an oval and narrow orifice with a descending channel that extends toward the ventroposterior region (Fig. 26C). Free tergites granulated (Fig. 26A, C).

Venter. Coxa I with few small medial setiferous granules (Fig. 26B); coxa II incrassated, slightly bigger than coxa IV (Fig. 25B); anteroposterior borders of coxa III with a row of strong granules connecting with coxae II and IV, respectively (Fig. 26B). Lateroposterior border of spiracular area and lateral border

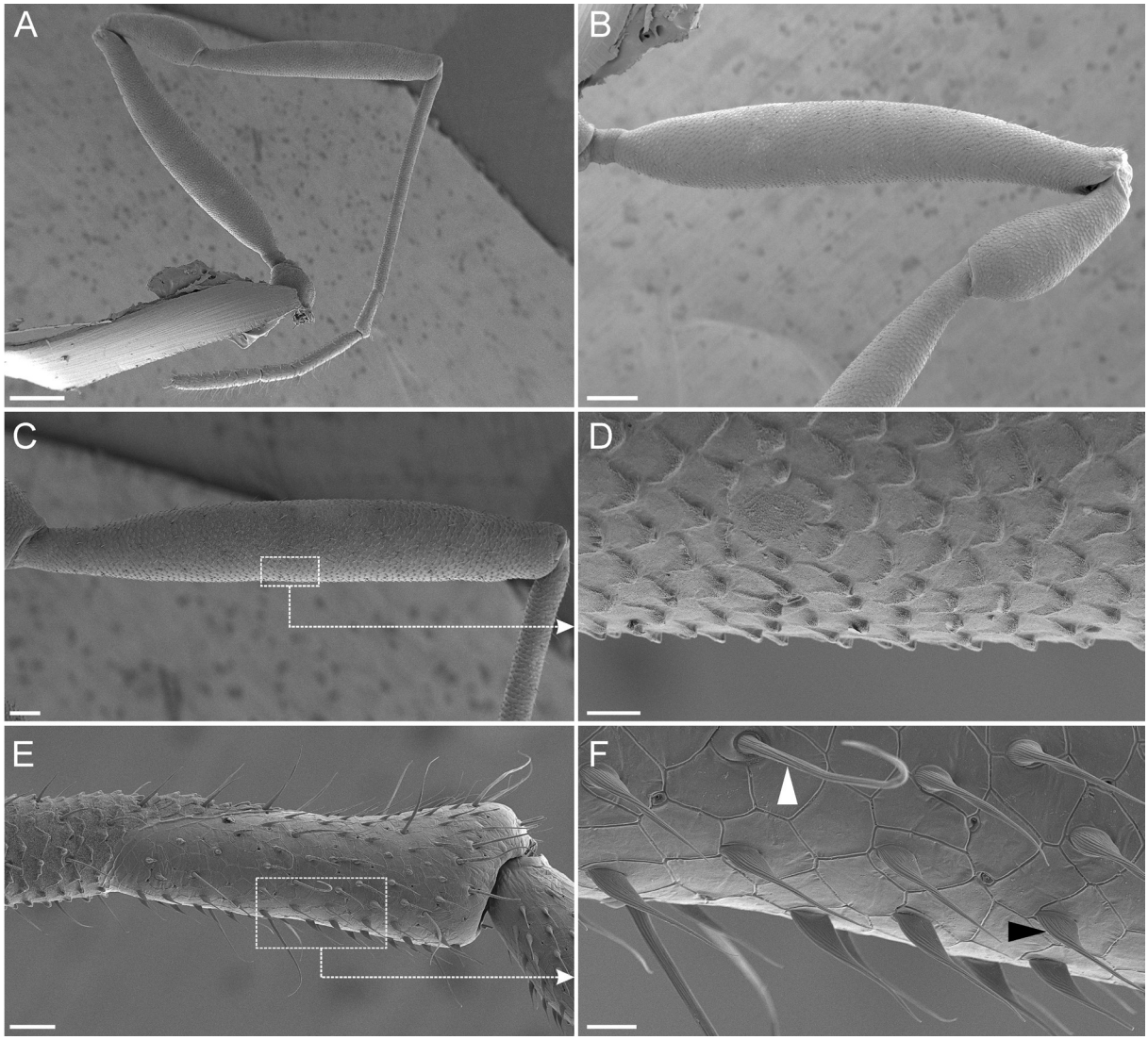

Fig. 28. *Metabiantes kivuensis* sp. nov., paratype, minor ♂ (MACN-Ar 45445), scanning electron micrographs of left leg II. **A**. Leg II, prolateral view. **B**. Femur, prolateral view. **C**. Tibia, prolateral view. **D**. Detail of tibia surface. **E**. Detail of astragalus and calcaneus, prolateral view. **F**. Detail of calcaneus surface. Black triangle indicates a trichome; white triangle indicates a sensillum chaeticum. Scale bars: A = 400 μm; B = 200 μm; C = 100 μm; D = 20 μm; E = 40 μm; F = 10 μm.

of free sternites I–V with rows of granules (Fig. 26B–C); anal operculum granulated (Fig. 26B–C). Spiracles not concealed (Fig. 26B).

Chelicera. Basichelicerite unarmed with a slightly marked bulla (Figs 26C, 27F–G). Cheliceral hand with sparse setae (Fig. 27F–H). Movable fingers with small, square-shaped teeth (Fig. 27H).

Pedipalp. Coxa elongated (i.e., remarkably longer than trochanter), proximally with one dorsoectal granule and three ventroectal granules – one proximal and two distal ones (Figs 25A, 26A–B). Trochanter unarmed (Fig. 27A). Femur robust, thick, and straight, ventroproximally with one mesal spine (Fig. 27A); ventral surface with small granules and scattered pores (Fig. 27B–C). Patella elongated, club-shaped, with a small mesodistal spine (Fig. 27A). Tibia with two ventroectal and two ventromesal spines (Fig. 27A). Tarsus inflated, spheroid in shape, with two ventromesal and two ventroectal spines; proximal spines longer than distal ones (Fig. 27A, D); ventral surface with conspicuous tubercles containing aggregate pores (Fig. 27D–E).

Legs. Coxa II with a row of dorsal granules (Fig. 26C). Femur II proximally thin, followed by an abrupt strong thickness, then tapering gradually (Figs 25C, 32C, F). Patella II short and thickened (Figs 25C, 32C, F). Tibia II dorsally widened (Figs 25C, 32C, I) and unarmed (Figs 28C–D, 32C, I). Metatarsus II with elongated astragalus, ventrally slightly swollen and armed with small triangular-shaped tubercles (Fig. 28A, E). Calcaneus occupies less than the last third of metatarsus, with trichomes and scattered

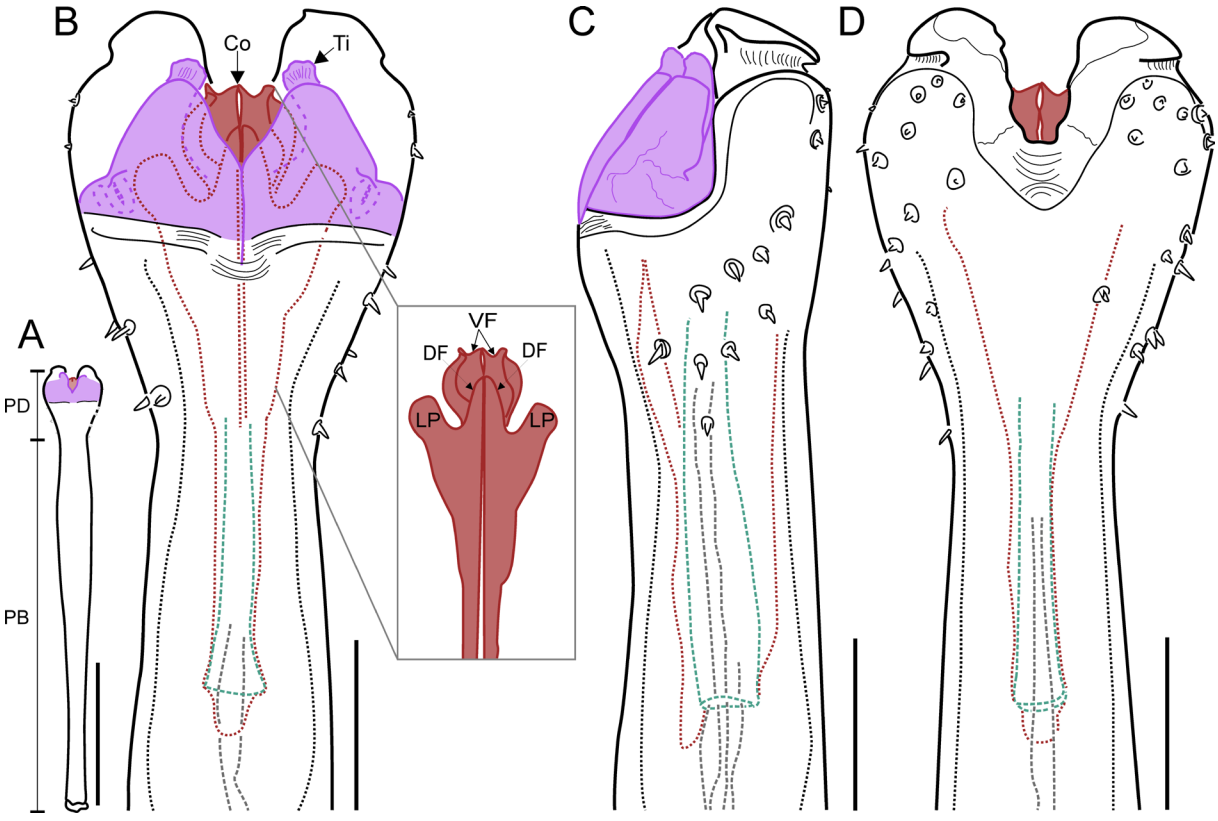

Fig. 29. *Metabiantes kivuensis* sp. nov., holotype, major ♂ (BE_RMCA_ARA.Opi. 154162), penis drawings. **A–B**. Dorsal view (detail of conductors within box). **C**. Lateral view. **D**. Ventral view. Stylus in green, conductors in brownish red, titillators in magenta. Abbreviations: Co = conductor; DF = dorsal fold; LP = lateral projection; PB = pars basalis; PD = pars distalis; Ti = titillator; VF = ventral fold. Scale bars: A = 500 µm; B–D = 100 µm.

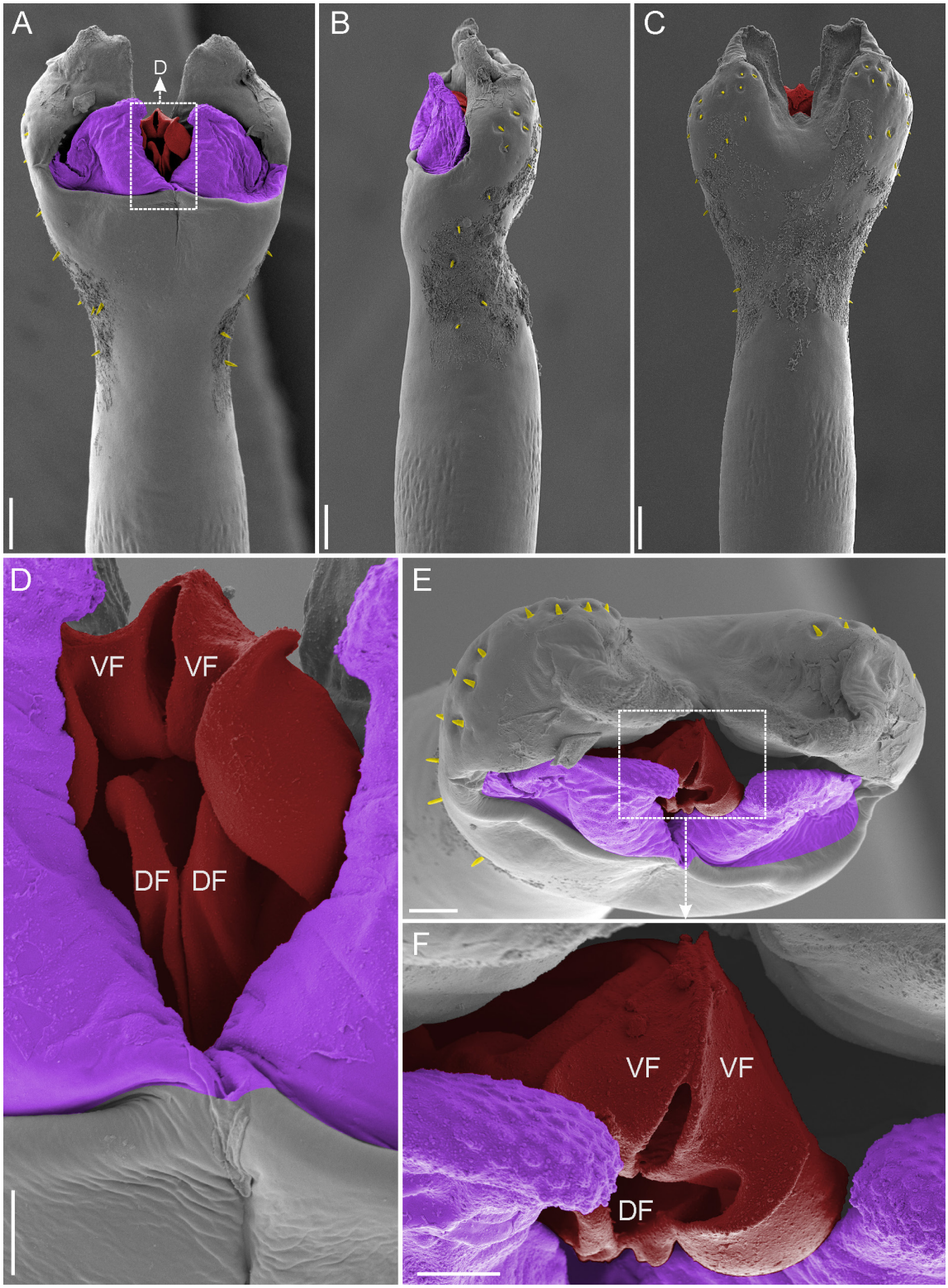

Fig. 30. *Metabiantes kivuensis* sp. nov., paratype, minor ♂ (MACN-Ar 45445), scanning electron micrographs of penis. **A**. Dorsal view. **B**. Lateral view. **C**. Ventral view. **D**. Detail of conductors, dorsal view. **E**. Anterior view. **F**. Detail of conductors, anterior view. Conductors in red, titillators in magenta, microsetae in yellow. Abbreviations: DF = dorsal fold; VF = ventral fold. Scale bars: A–C = 40 µm; D, F = 10 µm; E = 20 µm.

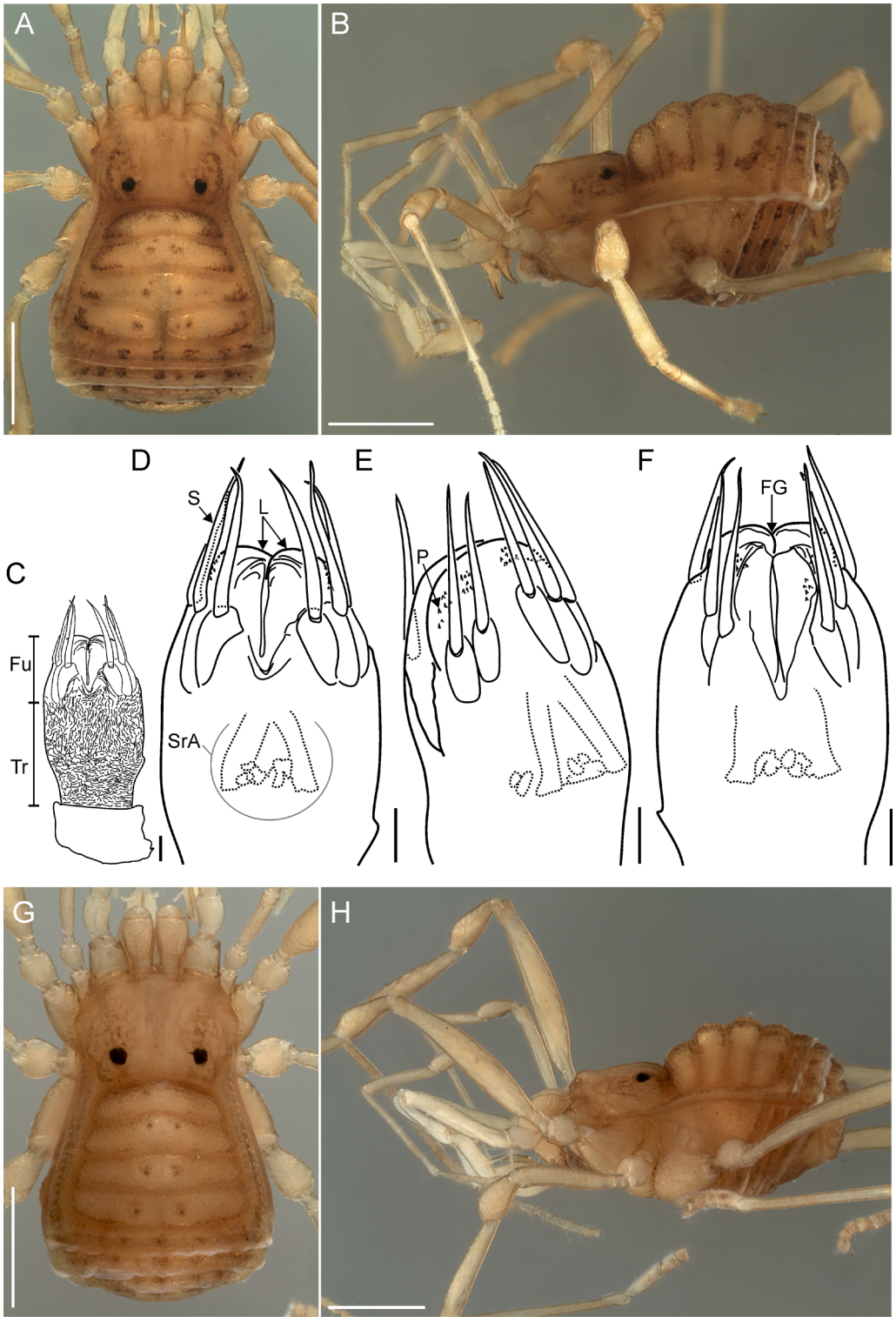

Fig. 31. *Metabiantes kivuensis* sp. nov., sexual dimorphism. **A–F**. Paratype, ♀ (BE_RMCA_ARA. Opi.247664). **A–B**. Habitus photos. **A**. Dorsal view. **B**. Lateral view. **C–F**. Ovipositor drawings. **C–D**. Dorsal view. **E**. Lateral view. **F**. Ventral view. **G–H**. Paratype, minor ♂ (BE_RMCA_ARA. Opi.247664), photo habitus. **G**. Dorsal view. **H**. Lateral view. Abbreviations: FG = furcal groove; Fu = furca; L = lobe; P = projection; S = seta; SrA = seminal receptacle area; Tr= truncus. Scale bars: A–B, G–H = 1 mm; C–F = 100 µm.

long sensilla chaetica distributed along all surfaces; trichomes with wider ovate-shaped bases, pointed tips, and variable length (Fig. 28E–F). Tarsi III–IV with a dense scopula. Tarsal formula: 3(2):5(4):5:5.

Color (specimen preserved in 80% ethanol). Body yellowish; carapace with light brown reticulations on the anterior and lateral sides (Fig. 25A, C). Anterior, lateral, and lateroposterior borders of mesotergal area I dark brown (Fig. 25A). Lateroanterior, lateral, and posterior borders of mesotergal area II dark brown (Fig. 25A). Lateroposterior border of mesotergal areas III–IV with dark brown patches. Mesotergal areas II–III medially with four medial dark points – two anterior and two posterior ones. Mesotergal area IV with two medial dark points in each half (Fig. 25A). Posterior border and free tergites with a row of dark points (Fig. 25A). Free sternite V and anal operculum with dark brown patches (Fig. 25B). Appendages with light brown reticulations (Figs 25A–C, 32C, F, I, L).

Male genitalia. Penis with distinguishable limits between pars basalis and pars distalis (Fig. 29A). Pars basalis tubular, thin at the base, slightly broadened apically, and ending in a slight constriction (Fig. 29A). Pars distalis swollen, with maximum width at titillator level (Figs 29B, D, 30A). Apical edge,

Fig. 32. *Metabiantes kivuensis* sp. nov., sexual dimorphism, left legs II photos. **A, D, G, J**. Paratype, ♀ (BE_RMCA_ARA.Opi.247664). **B, E, H, K**. Paratype, minor ♂ (BE_RMCA_ARA.Opi.247664). **C, F, I, L**. Holotype, major ♂ (BE_RMCA_ARA.Opi.154162). **A–C**. Leg II, retrolateral view. **D–F**. Femur and patella, retrolateral view. **G–I**. Tibia, retrolateral view. **J–L**. Metatarsus and tarsus, retrolateral view. Scale bars = 500 µm.

Table 5. Appendage measurements (in mm) of *Metabiantes kivuensis* sp. nov. ***** = holotype. Abbreviations: Fe = femur; Mt = metatarsus; Pa = patella; T = total; Ta = tarsus; Ti = tibia; Tr = trochanter.

		Tr	Fe	Pa	Ti	Mt	Ta	T
Major ♂ RMCA 154162*	Pedipalp	0.40	1.38	0.76	0.78	–	0.60	3.92
	Leg I	0.24	1.13	0.45	0.78	1.24	0.86	4.70
	Leg II	0.45	1.84	0.70	1.37	1.87	1.32	7.55
	Leg III	0.41	1.54	0.61	1.05	1.95	0.98	6.54
	Leg IV	0.50	1.96	0.79	1.51	2.70	1.17	8.63
Minor ♂ RMCA 247664	Pedipalp	0.37	1.33	0.69	0.67	–	0.55	3.61
	Leg I	0.29	1.07	0.42	0.78	1.17	0.80	4.53
	Leg II	0.43	1.98	0.77	1.56	1.86	1.49	8.09
	Leg III	0.38	1.58	0.57	1.14	1.86	0.99	6.52
	Leg IV	0.51	2.07	0.73	1.52	2.60	1.12	8.55
♀ RMCA 247664	Pedipalp	0.35	1.21	0.68	0.60	–	0.48	3.32
	Leg I	0.29	0.96	0.42	0.73	1.08	0.76	4.24
	Leg II	0.35	1.53	0.51	1.30	1.43	1.15	6.27
	Leg III	0.38	1.30	0.52	1.06	1.68	0.94	5.88
	Leg IV	0.52	1.68	0.74	1.41	2.24	1.05	7.64

laminar (i.e., dorsoventrally flat) with a large, open U-shaped cleft medially dividing into two rounded halves (Figs 29B, D, 30A, C); halves apically curved ventrally, less chitinous, and potentially inflatable by hemolymph pressure (Fig. 30C). Pars distalis with a small apical depression in the ventromedial region (Figs 29D, 30C). Each side of pars distalis armed with irregularly arranged microsetae, extending from dorsolateral to the ventrodistal region (Figs 29B–D, 30A–C). Capsula externa with two broad titillators ending in rounded tips, separated by a close U-shaped cleft; tips with inner rounded projections (Fig. 30E–F). Capsula interna formed by two complex conductors, each one with one laminar medial small dorsal fold and one longer ventral fold, with a lateral extension covering partially the dorsal fold, visible within the U-shaped cleft (Figs 29B, 30A, D–F); each conductor also with one broad lateral projection (Fig. 29B); stylus long and tubular, with its tip covered by conductors (Fig. 29B–D).

Minor male (paratype, BE_RMCA_ARA.Opi.247664)

Body measurements. Total body length 2.74, carapace length 0.96, scutum magnum length 2.5, carapace maximum width 1.4, abdominal scutum maximum width 1.98. Appendage measurements in Table 5.

Body. Minor male resembles major male in the armature of the scutum magnum, except for mesotergal area IV, which is not divided (Figs 26A, 31G vs Fig. 25A). Minor male has a dimorphic leg II but differs from major male by having remarkably thinner femur, patella, and tibia (Figs 31H, 32B, E, H vs Figs 25C, 32C, F, I); metatarsus II slightly thinner than that of major males (Fig. 32K vs Fig. 32L). Tarsal formula: 3(2):5(3):5:5.

Female (paratype, BE_RMCA_ARA.Opi.247664)

Body measurements. Total body length 2.91, carapace length 0.89, scutum magnum length 2.56, carapace maximum width 1.4, abdominal scutum maximum width 2.2. Appendage measurements in Table 5.

Body. Female resembles both minor and major males in the armature of the scutum magnum (Fig. 31A–B vs Figs 25A, C, 31G–H). Female differs from the minor male, but not from the major male, by having the mesotergal area IV divided (Fig. 31A vs Figs 26A, 31G). Female differs from both major and minor males by having a thin pedipalp tarsus and lacking a dimorphic leg II (Fig. 31B vs Figs 25C, 31H), with femur and patella thinner than in minor and major males (Fig. 32D vs Fig. 32E–F); tibia with similar width to that of the minor male and thinner than in the major male (Fig. 32G vs Fig. 32H–I); metatarsus II slightly thinner than that of minor and major males (Fig. 32J vs Fig. 32K–L). Tarsal formula 3(2):5(4):5:5.

Female genitalia. Ovipositor cylindrical (Fig. 31C), distally bearing two lobes (furca) (Fig. 31C–D, F). Each furcal lobe with five long, pointed setae (Fig. 31E) – three dorsal and two ventral ones – resulting in a total of six setae on the dorsal region (Fig. 31D) and four on the ventral region (Fig. 31F). External surface of furcal lobes with several short, pointed lateral projections, irregularly distributed (Fig. 31E). Receptacle chambers located near the base of the furcal groove (Fig. 31D–F).

Distribution

Known only from the type locality (Fig. 40).

Metabiantes serratus sp. nov.
urn:lsid:zoobank.org:act:99512C0D-7DDB-411F-BA7F-57D07D853187
Figs 33–39; Table 6

Diagnosis

Metabiantes serratus sp. nov. differs from the rest of the species of *Metabiantes* (except *M. elongatus* sp. nov., *M. litoralis* and *M. zuluanus*) by the following combination of characteristics: presence of tubercles on mesotergal areas III–V and sexually dimorphic male leg II with thickened femur, and metatarsus with tubercles on the ventral region (Figs 33A, C, 34A, C, 38A–B, 36A–H, 39B, D, F, H). *Metabiantes serratus* and *M. elongatus* share a remarkably similar male genital morphology, but *M. serratus* can be easily differentiated from *M. elongatus* by the presence of tubercles on free tergites I–II in contrast with granules in *M. elongatus* (Fig. 34A, C vs Fig. 7C); *M. serratus* also differs from *M. elongatus* by having a strong, thickened femur and swollen tibia and metatarsus of leg II (Figs 36A–C, E, 39B, D, F, H vs Figs 10A, C, E, 14B, D, F, H). Additionally, *M. serratus* has a pronounced constriction at the astragalus-calcaneus junction, which is absent in *M. elongatus* (Figs 36E–F, 39H vs Figs 10E–F, 14H). Males of *Metabiantes serratus* lack an enlarged trochanter II, distinguishing them from those of *M. zuluanus* (Fig. 33A, C vs Lawrence 1937a: fig. 26). Regarding male genital morphology, *M. serratus* has the penis with a deeper U-shaped cleft of lamina apicalis, wider titillators, and remarkably smaller basal setae, easily differentiated from the penis of *M. litoralis* and *M. zuluanus* with shallow cleft, narrow titillators, and larger basal setae (Fig. 37B–H vs Kauri 1961: fig. 34a–b, 22a–b).

Etymology

The species epithet '*serratus*', from the Latin meaning 'toothed like a saw' refers to the serrated ventral transverse rows of triangular tubercles of the metatarsus II in males of this species.

Type material

Holotype

CONGO • ♂; Bas-Congo, Mayombe, Luki Forest Reserve; 5.63333° S, 13.06667° E; 27 Sep. 2007; D. De Bakker and J.P. Michiels leg.; along trail in primary rainforest; sieving; RMCA, BE_RMCA_ARA.Opi.223705.

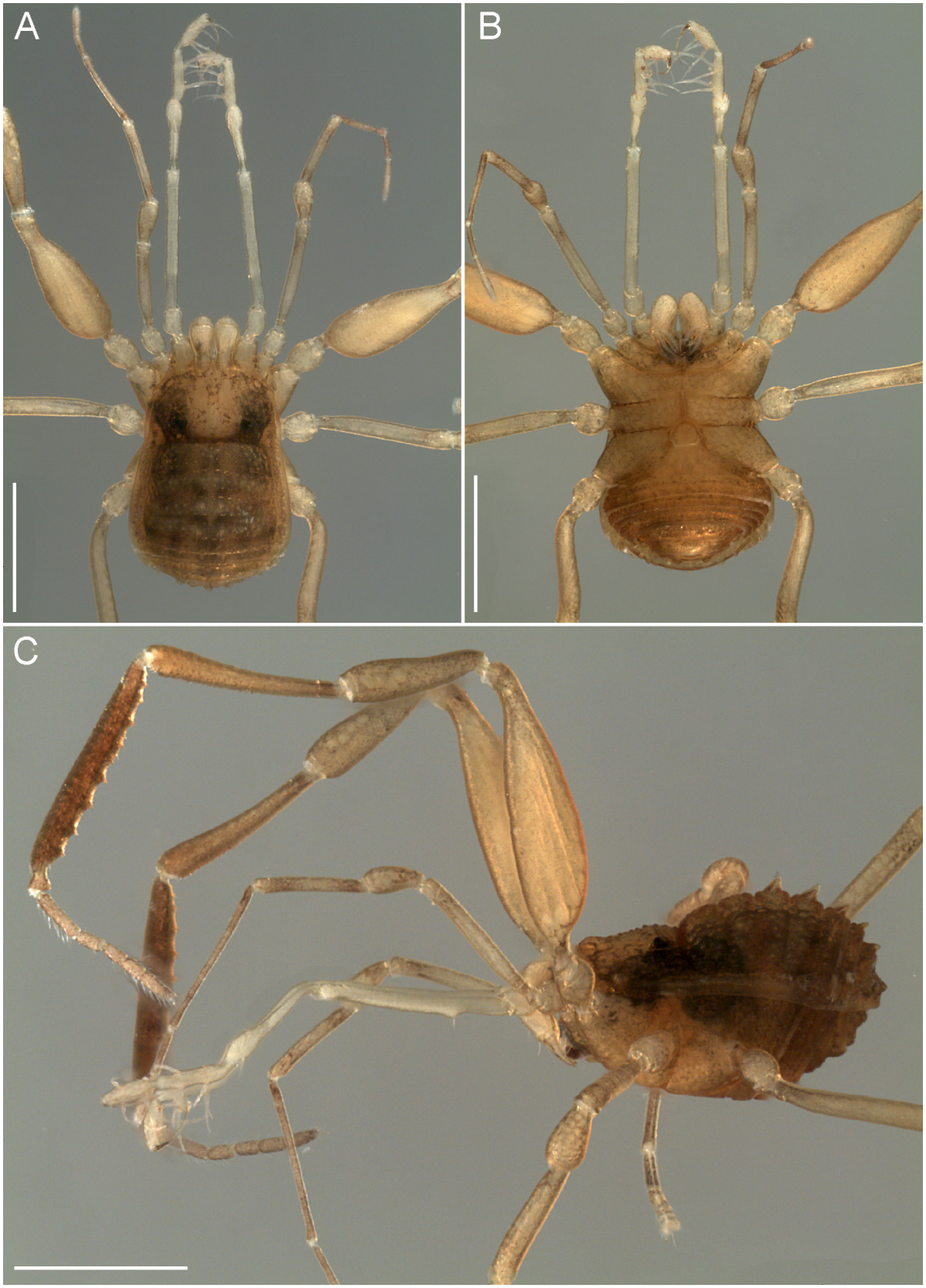

Fig. 33. *Metabiantes serratus* sp. nov., holotype, ♂ (BE_RMCA_ARA.Opi.223705), habitus photos. **A**. Dorsal view. **B**. Ventral view. **C**. Lateral view. Scale bars = 1 mm.

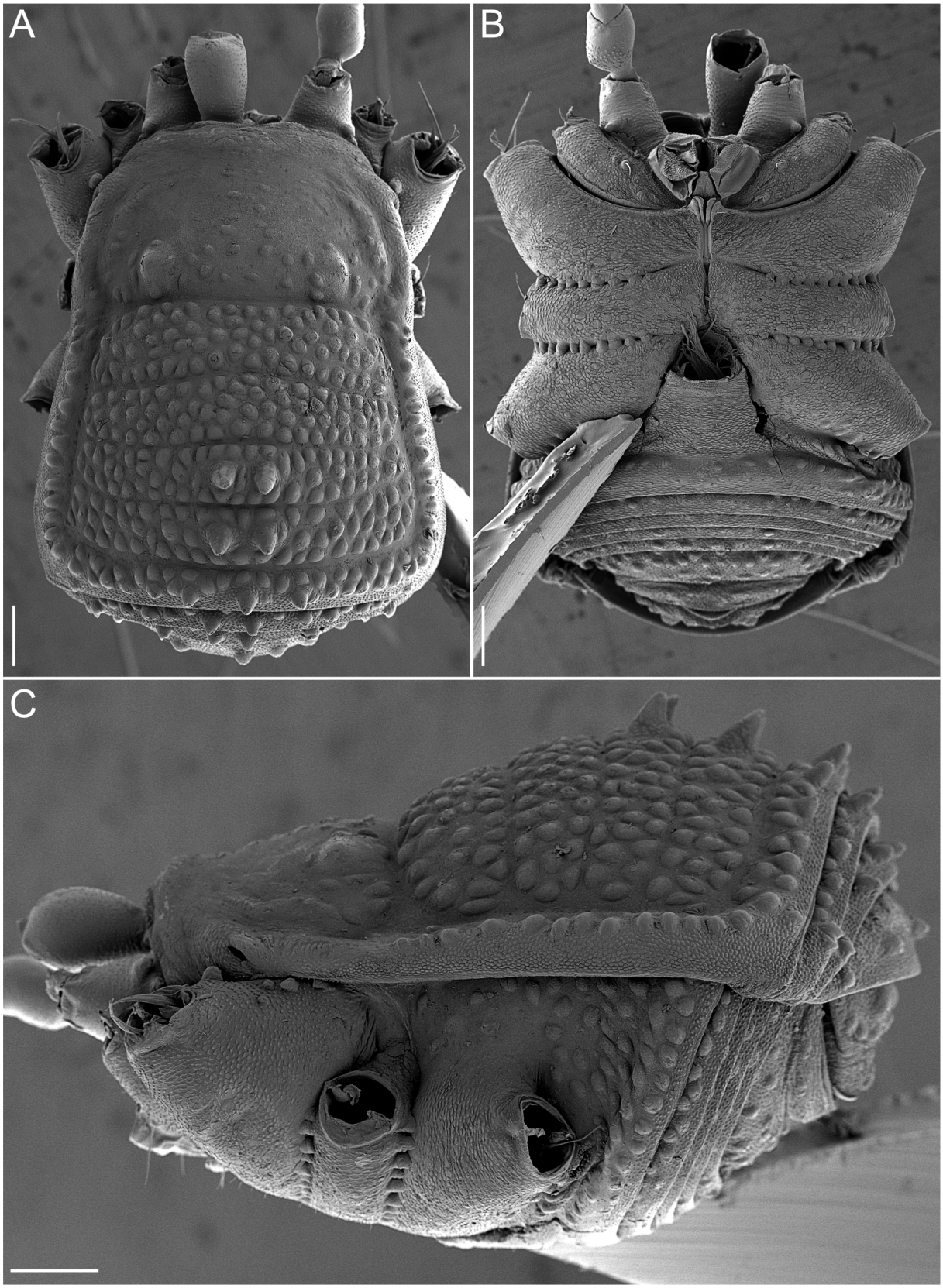

Fig. 34. *Metabiantes serratus* sp. nov., paratype, ♂ (MACN-Ar 45472), scanning electron micrographs of habitus. **A**. Dorsal view. **B**. Ventral view. **C**. Lateral view. Scale bars = 200 µm.

Paratypes

CONGO • 1 ♂, 3 ♀♀; same data as for holotype; RMCA, BE_RMCA_ARA.Opi.247665 • 1 ♂ (SEM voucher); same data as for holotype; MACN-Ar 45472 • 2 ♂♂ (1 SEM voucher), 1 ♀ (photo voucher); same data as for holotype; MACN-Ar 45474 • 6 ♂♂, 6 ♀♀; same data as for holotype; 1 Oct. 2007; RMCA, BE_RMCA_ARA.Opi.223775

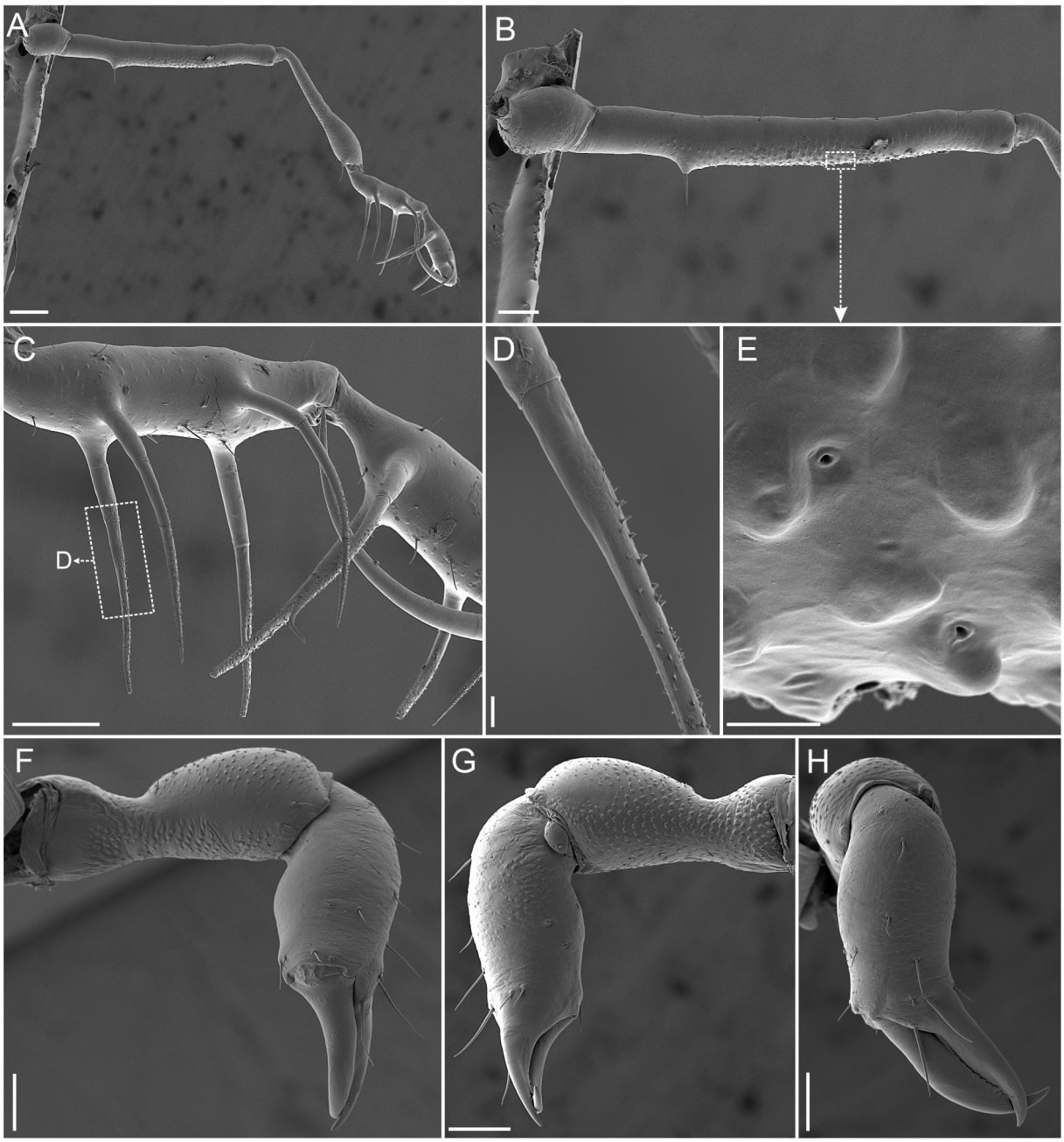

Fig. 35. *Metabiantes serratus* sp. nov., paratype, ♂ (MACN-Ar 45472), scanning electron micrographs of pedipalp and chelicera. **A–E**. Left pedipalp. **A**. Mesal view. **B**. Trochanter and femur, mesal view. **C**. Tibia, ventromesal view. **D**. Detail of ectoproximal tibial spine. **E**. Detail of femur surface. **F–H**. Right chelicera. **F**. Ectal view. **G**. Mesal view. **H**. Frontal view. Scale bars: A = 200 µm; B–C, F–H = 100 µm; D–E = 10 µm.

Description

Male (holotype, BE_RMCA_ARA.Opi.223705)

Body measurements. Total body length 1.73, carapace length 0.61, scutum magnum length 1.56, carapace maximum width 0.97, abdominal scutum maximum width 1.27. Appendage measurements in Table 6.

Dorsum. Outline slightly hourglass-shaped with Eta (η) shape, with a very slight constriction at sulcus I level (Figs 33A, 34A). Carapace with scattered medial granules, wider than long, anterior border slightly

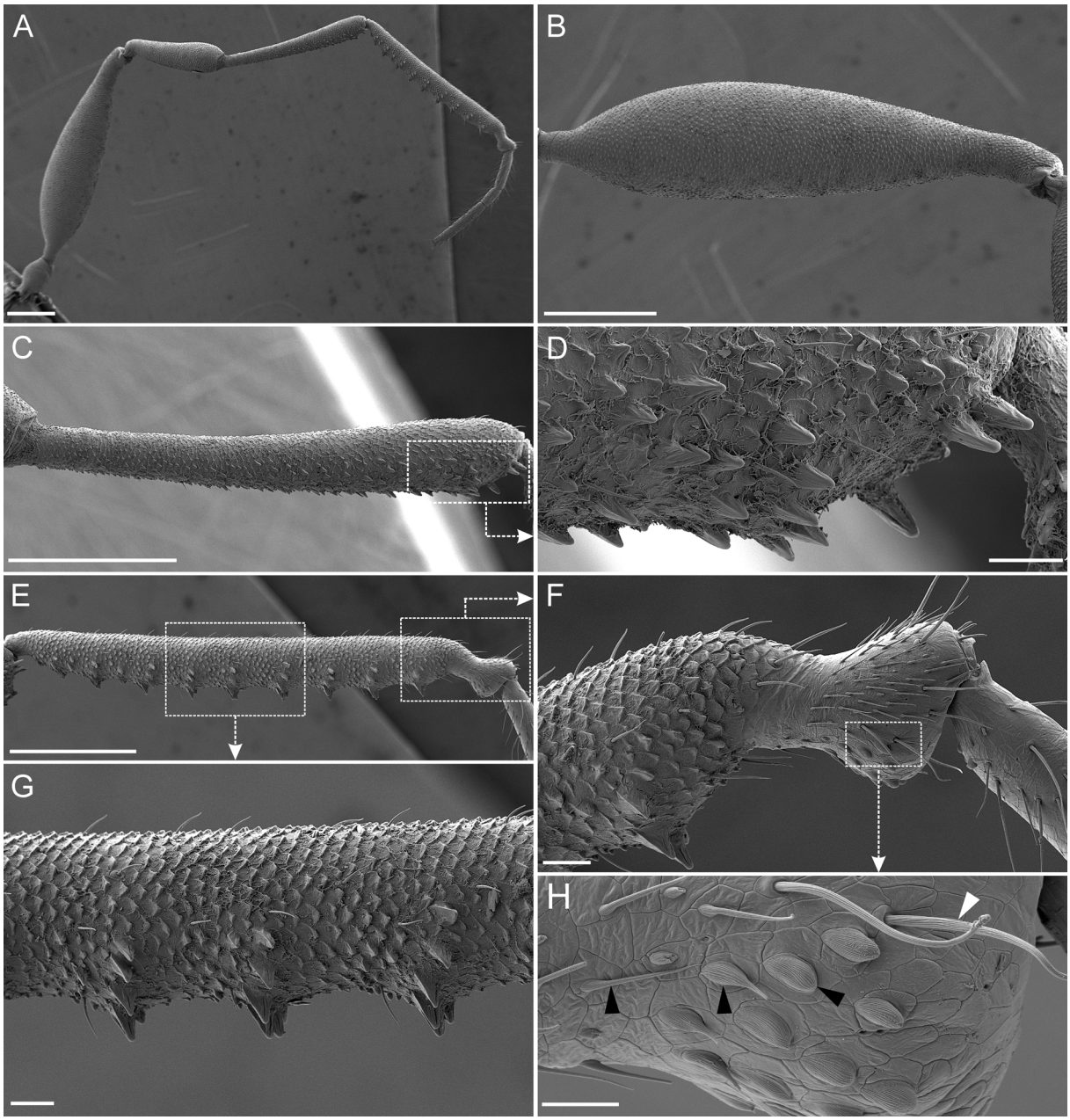

Fig. 36. *Metabiantes serratus* sp. nov., paratype, ♂ (MACN-Ar 45472), scanning electron micrographs of left leg II. **A**. Leg II, prolateral view. **B**. Femur, prolateral view. **C**. Tibia, prolateral view. **D**. Detail of tibia surface. **E**. Metatarsus, prolateral view. **F**. Detail of calcaneus. **G**. Detail of astragalus. **H**. Detail of calcaneus surface. Black triangles indicate trichomes; white triangle indicates a sensillum chaeticum. Scale bars: A–C, E = 400 μm; D, F–G = 40 μm; H = 20 μm.

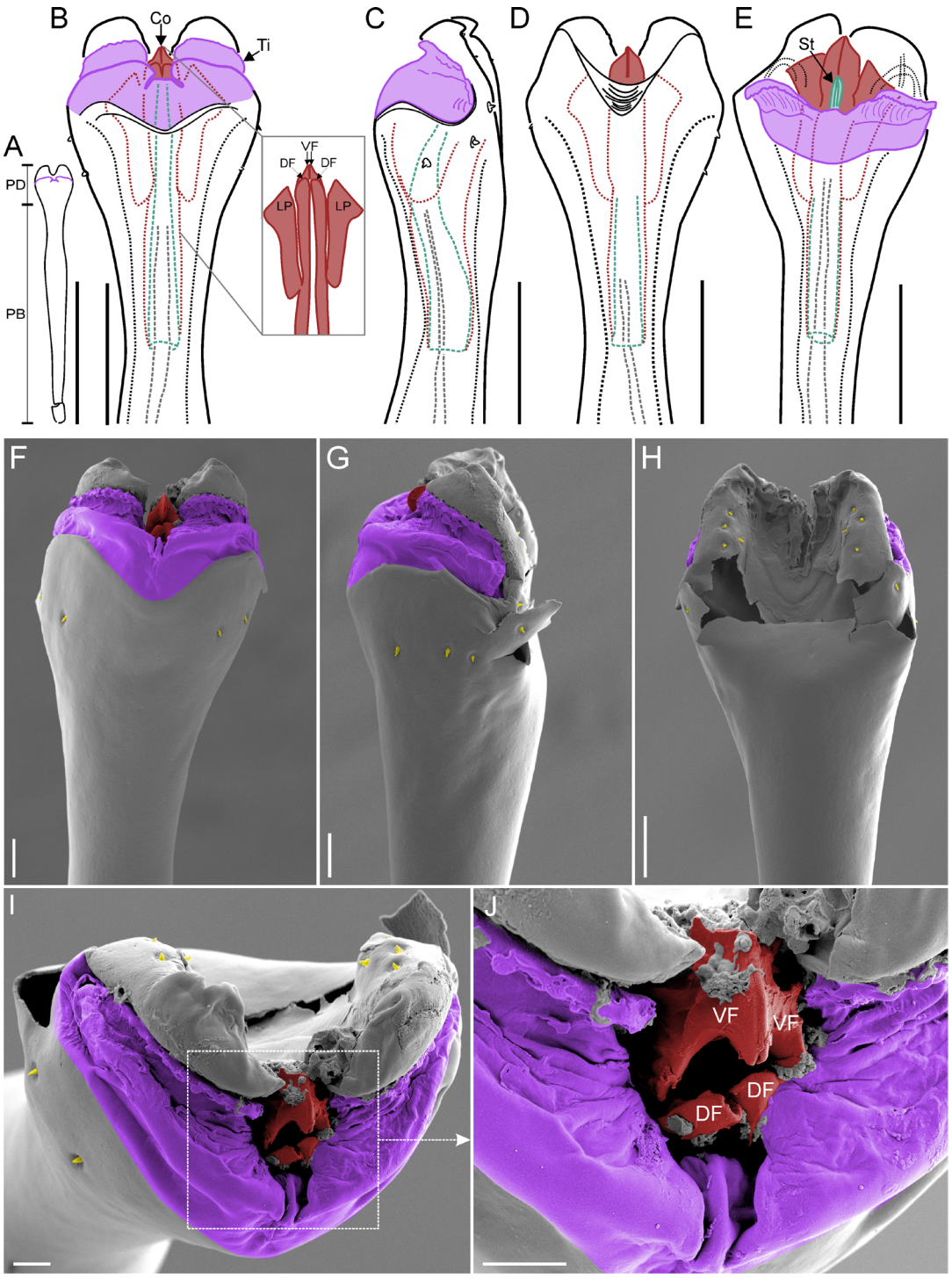

Fig. 37. *Metabiantes serratus* sp. nov., males, drawings and scanning electron micrographs of penis. **A–E**. Holotype (BE_RMCA_ARA.Opi.223705), penis drawings. **A–B**. Dorsal view (detail of conductors within box). **C**. Lateral view. **D**. Ventral view. **E**. Everted penis, dorsal view. **F–J**. Paratype (MACN-Ar 45474), scanning electron micrographs of penis. **F**. Dorsal view. **G**. Lateral view. **H**. Ventral view. **I**. Anterior view. **J**. Detail of conductors, anterior view. Stylus in green, conductors in brownish red, titillators in magenta, microsetae in yellow. Abbreviations: Co = conductor; DF = dorsal fold; LP = lateral projection; PB = pars basalis; PD = pars distalis; St = stylus; Ti = titillator; VF = ventral fold. Scale bars: A = 500 µm; B–E = 100 µm; F–G = 20 µm; H = 30 µm; I–J = 10 µm.

convex and unarmed, with a small and rounded frontal hump (Figs 33C, 34C); interocular area with scattered granules (Fig. 34A). Cheliceral sockets not marked (Fig. 34A). Eyes separated near sulcus I. Carapace in lateral view straight posterior to frontal hump and becoming slightly higher toward the posterior region (Figs 33C, 34C). Abdominal scutum in lateral view convex (Figs 33C, 34C). Sulcus I deep, complete, and straight (Fig. 34A). Mesotergal areas granulated and well-defined; sulci II–III medially curved to the anterior body region; sulci IV–V straight (Fig. 34A). Mesotergal areas III–IV medially with two conical and pointed tubercles (Figs 33A, C, 34A, C). Mesotergal area V with two irregular rows of granules and medially with three conical tubercles (Figs 33C, 34A, C). Lateral borders of abdominal scutum with a row of granules (Fig. 34A, C). Ozopore with an oval and narrow orifice with

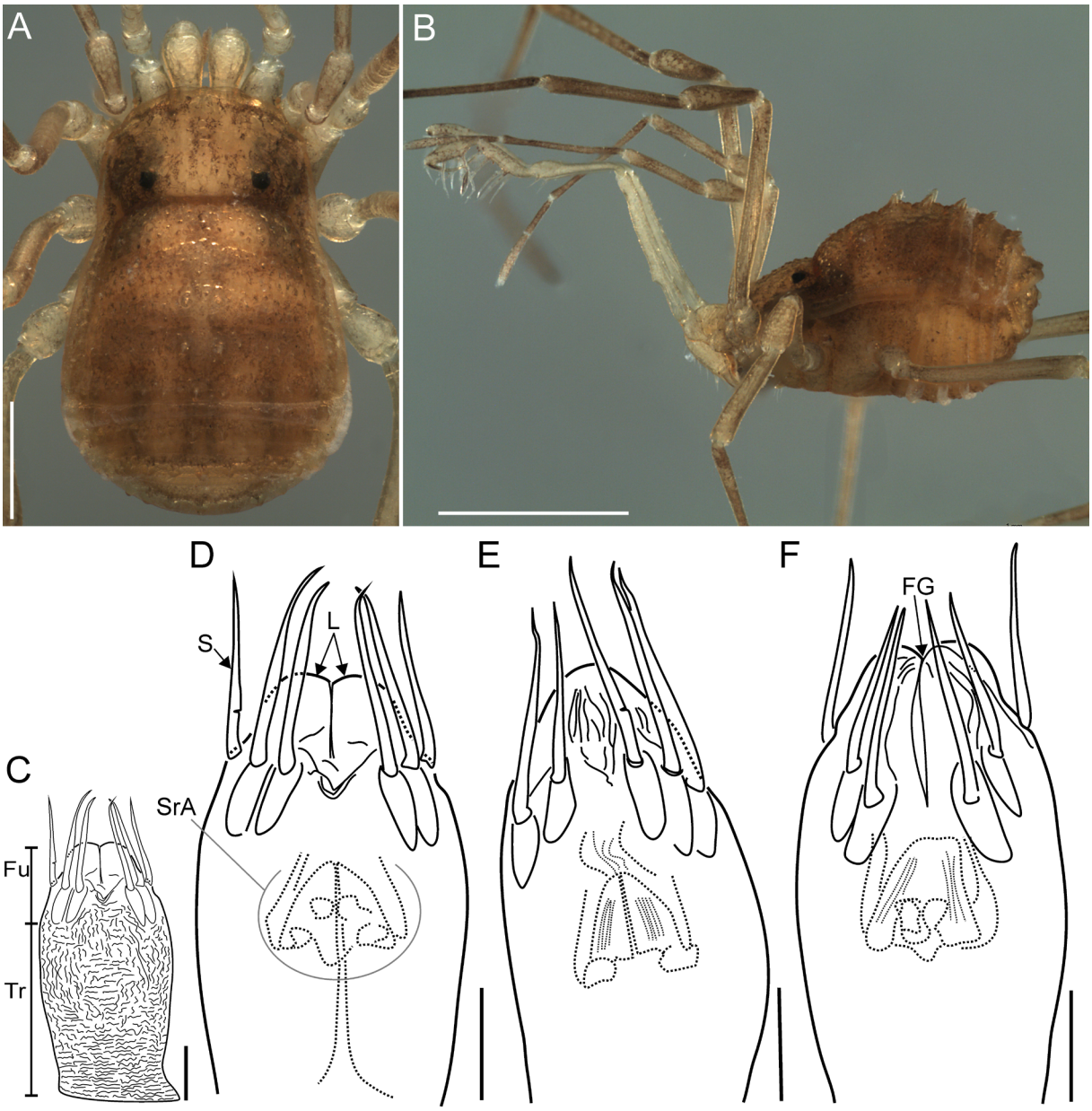

Fig. 38. *Metabiantes serratus* sp. nov., paratype, ♀ (MACN-Ar 45474). **A–B**. Habitus photos. **A**. Dorsal view. **B**. Lateral view. **C–F**. Ovipositor drawings. **C–D**. Dorsal view. **E**. Lateral view. **F**. Ventral view. Abbreviations: FG = furcal groove; Fu = furca; L = lobe; S = seta; SrA = seminal receptacle area; Tr = truncus. Scale bars: A–B = 1 mm; C–F = 100 µm.

a descending channel that extends toward the ventroposterior region (Fig. 34C). Free tergite I with a row of granules; free tergites I–II medially with three conical tubercles; free tergite III with a row of medial conspicuous granules (Fig. 34A).

Venter. Coxa I with few small medial granules (Fig. 34B); coxa II incrassated, of same size as (or slightly larger than) coxa IV (Figs 33B, 34B); anteroposterior borders of coxa III with a row of strong granules connecting with coxae II and IV, respectively (Figs 33B, 34B). Posterior border of spiracular area and free sternites I–V with a row of granules (Fig. 34B); anal operculum granulated (Fig. 34B–C). Spiracles not concealed (Fig. 34B).

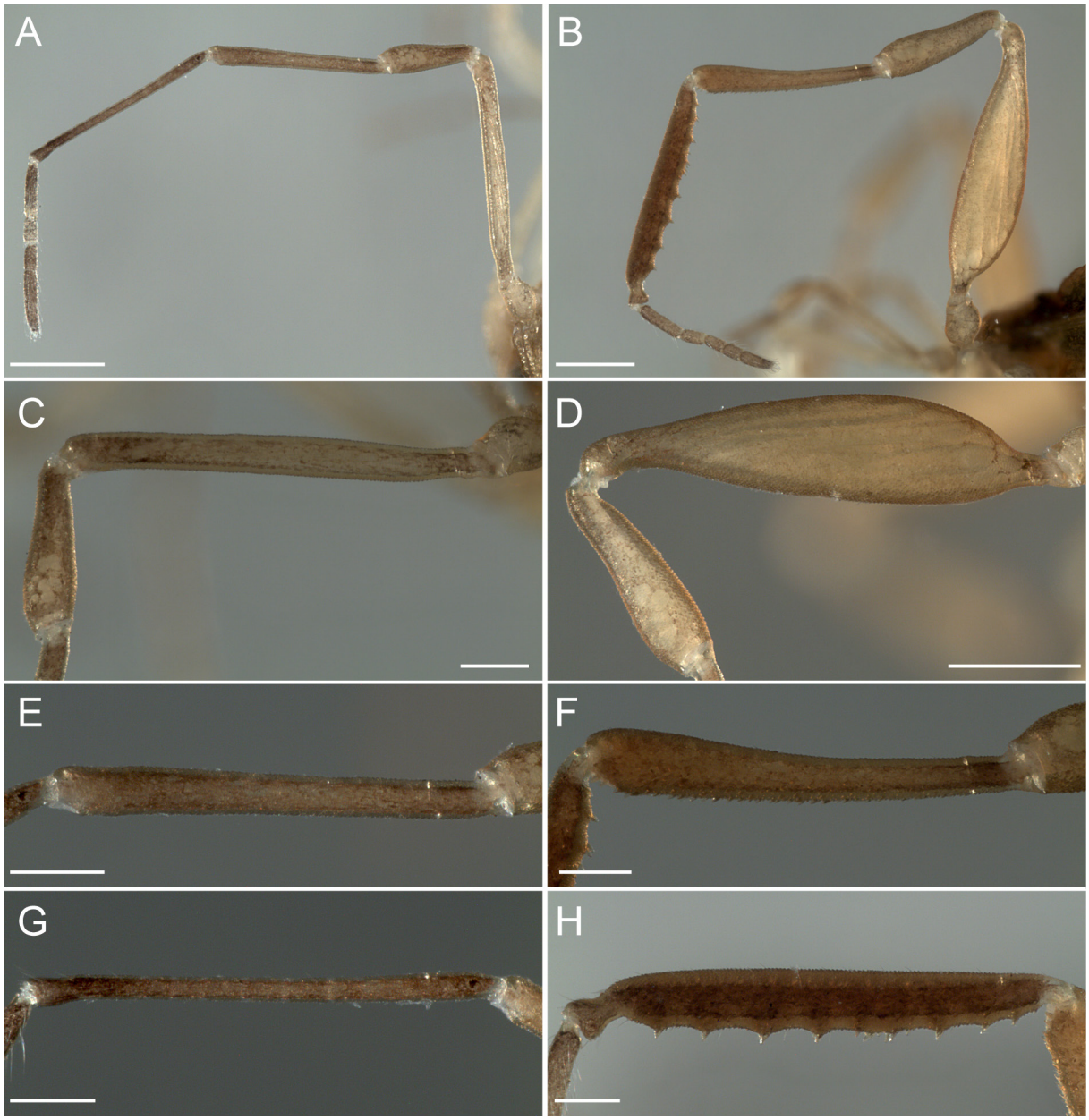

Fig. 39. *Metabiantes serratus* sp. nov., sexual dimorphism, photos of left legs II. **A, C, E, G**. Paratype, ♀ (MACN-Ar 45474). **B, D, F, H**. Holotype, ♂ (BE_RMCA_ARA.Opi.223705). **A–B**. Leg II, retrolateral view. **C–D**. Detail of femur and patella, retrolateral view. **E–F**. Detail of tibia, retrolateral view. **G–H**. Detail of metatarsus, retrolateral view. Scale bars: A–B, D = 500 µm; C, E–H = 200 µm.

Table 6. Appendage measurements (in mm) of *Metabiantes serratus* sp. nov. ***** = holotype. Abbreviations: Fe = femur; Mt = metatarsus; Pa = patella; T = total; Ta = tarsus; Ti = tibia; Tr = trochanter.

		Tr	Fe	Pa	Ti	Mt	Ta	T
♂ RMCA 223705*	Pedipalp	0.22	1.09	0.76	0.45	–	0.38	2.90
	Leg I	0.23	0.87	0.36	0.66	0.98	0.63	3.73
	Leg II	0.33	1.82	0.84	1.18	1.53	0.97	6.67
	Leg III	0.23	1.14	0.40	0.83	1.44	0.59	4.63
	Leg IV	0.26	1.36	0.49	1.01	1.89	0.70	5.71
♀ MACN-Ar 45474	Pedipalp	0.20	0.93	0.55	0.39	–	0.35	2.42
	Leg I	0.19	0.71	0.30	0.52	0.74	0.58	3.04
	Leg II	0.24	1.26	0.51	0.97	1.11	0.94	5.03
	Leg III	0.21	0.87	0.30	0.66	1.11	0.55	3.70
	Leg IV	0.28	1.09	0.41	0.83	1.47	0.65	4.73

Chelicera. Basichelicerite unarmed, with a slightly marked bulla (Fig. 35F–G). Cheliceral hand with sparse setae (Fig. 35F–H). Movable fingers with small square-shaped teeth (Fig. 35H).

Pedipalp. Coxa elongated (i.e., remarkably longer than trochanter), proximally with two granules – one dorsoectally and one ventroectally (Fig. 34A–B). Trochanter unarmed (Fig. 35A–B). Femur straight, proximally with a slight ventral narrowing followed by a small ventromesal spine (Fig. 35A–B), ventral surface with granules and pores (Fig. 35B, E). Patella elongated, club-shaped, and armed with a small mesodistal spine (Fig. 35A). Tibia with two ventromesal and two ventroectal long spines (Fig. 35A). Tarsus thin, with two ventromesal and two ventroectal spines; proximal spines longer than distal spines (Fig. 35A, C). Setae of spines proximally smooth, then covered by scattered microtrichia (Fig. 35C–D).

Legs. Femur II unarmed, thin proximally, followed by an abrupt thickness, and then tapering gradually (Figs 33C, 36A–B, 39B, D). Patella II long, thickened, and unarmed (Figs 33C, 36A, 39B, D). Tibia II distally widened, with ventral triangular-shaped tubercles that increase in size towards the distal region (Figs 33C, 36C–D, 39B, F). Metatarsus II with astragalus ventrally swollen and armed with equidistant transverse rows of triangular-shaped tubercles (Figs 33C, 36E–G, 39B, H). Limit astragalus-calcaneus defined by a strong constriction with a slightly incrassate calcaneus giving a peculiar form to distal region of the metatarsus (Figs 33C, 36E–F, 39H). Calcaneus ventrally mostly with ovate-shaped trichomes and some ovate-shaped base and pointed tip trichomes of variable length; lateral and dorsal surfaces of calcaneus with long thin-pointed trichomes and scattered sensilla chaetica and glandular pores (Fig. 36F, H). Tarsi III–IV with a dense scopula. Tarsal formula: 3(2):5(4):5:5.

Color (specimen preserved in 80% ethanol). Body dark brown; medial and posterior regions of carapace yellowish (Fig. 33A); ventral body region and appendages brown-yellowish with light brown reticulations (Fig. 33B–C); metatarsus II dark brown (Figs 33C, 39B, H).

Male genitalia. Penis with distinct boundaries between pars basalis and pars distalis (Fig. 37A). Pars basalis tubular, slightly broadened apically, and ends in a constriction (Fig. 37A). Pars distalis swollen with maximum width at basal level of titillators (Fig. 37B, D, F). Apical edge, laminar (i.e., dorsoventrally flat), with a medial U-shaped cleft dividing into two rounded halves (Fig. 37B, D, F, H); halves apically less chitinous and curved ventrally (Fig. 37C, G–H). Pars distalis with a distal depression in the ventromedial region (Fig. 37D, H). Each side of pars distalis armed with short, conical microsetae, irregularly arranged, extending basally from dorsolateral to the ventrodistal region (Fig. 37B, C, F–H). Capsula externa with two broad titillators separated by a narrow cleft (Fig. 37B–C, E–G). Capsula

interna is formed by two complex conductors and one stylus, basally fused. Each conductor apically with one small medial dorsal fold and one longer ventral fold, ventrally visible within the U-shaped cleft (Fig. 37B, D, I–J); each conductor also with one broad lateral projection, visible in the everted condition (Fig. 37B, D–E). Stylus with a rounded tip (Fig. 37E), wider basally, narrow distally, and with an irregular S-shaped curve in lateral view (Fig. 37B–E).

Female (paratype, MACN-Ar 45474)

Body measurements. Total body length 1.83, carapace length 0.52, scutum magnum length 1.5, carapace maximum width 0.89, abdominal scutum maximum width 1.24. Appendage measurements in Table 6.

Body. Female resembles males in the armature of the scutum magnum (Fig. 38A–B vs Fig. 33A, C) but differs by lacking dimorphic leg II; femur and patella not swollen as in male (Fig. 39A, C vs Fig. 39B, D); tibia thinner and unarmed (Fig. 39E vs Fig. 39F); metatarsus not swollen and unarmed (Fig. 39G vs Fig. 39H). Tarsal formula 3(2):4(3):5:5.

Female ovipositor. Ovipositor cylindrical (Fig. 38C), distally bearing two lobes (furca) (Fig. 38C–D, F). Each furcal lobe with five long, pointed setae (Fig. 38E) – three dorsal and two ventral – resulting in a total of six setae on the dorsal region (Fig. 38D) and four on the ventral region (Fig. 38F). Receptacle chambers located near the base of the furcal groove (Fig. 38D–F).

Distribution

Known only from the type locality (Fig. 40).

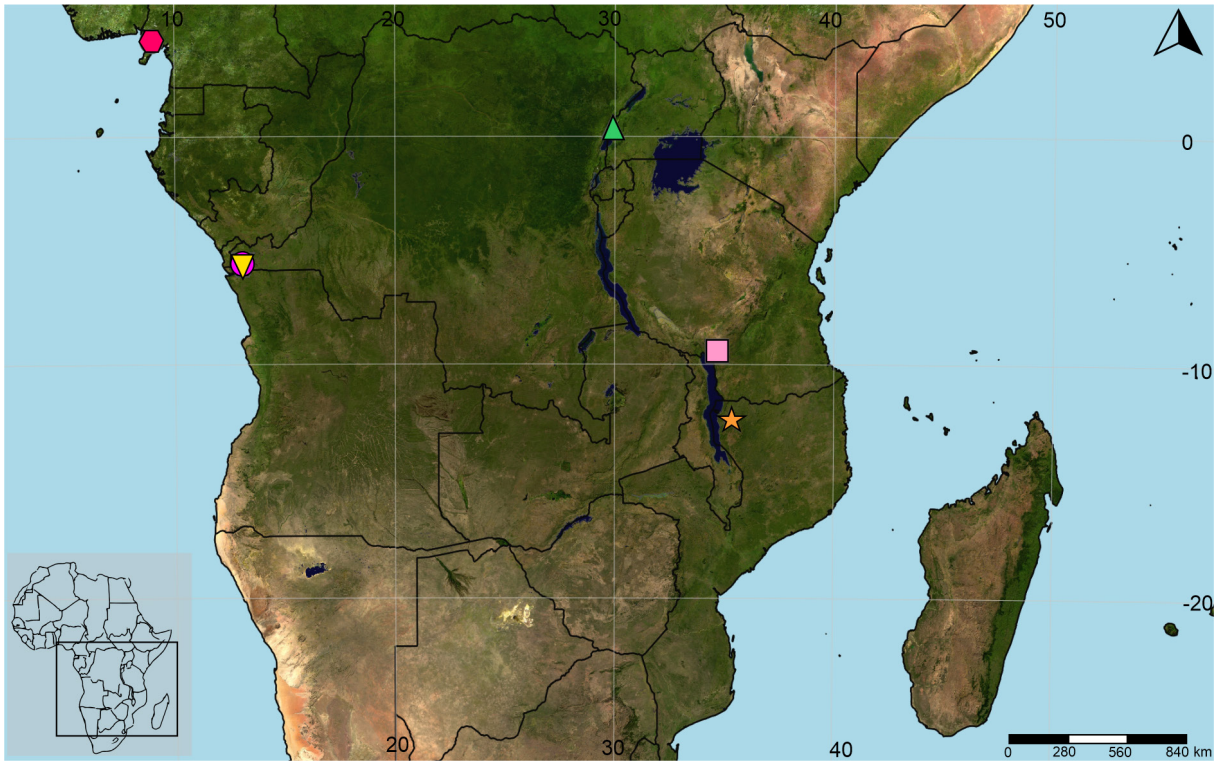

Fig. 40. Geographical distribution of *Clinobiantes paradoxus* Roewer, 1927 and the new species of *Metabiantes* Roewer, 1915 herein described. *Clinobiantes paradoxus* (red hexagon) in Cameroon; *M. kivuensis* sp. nov. (green triangle), *M. serratus* sp. nov. (magenta circle), and *M. elongatus* sp. nov. (yellow inverted triangle) in Democratic Republic of Congo; *M. herculeus* sp. nov. (pink square) in Tanzania; *M. kaurii* sp. nov. (orange star) in Mozambique.

Discussion

Over the years, the Afrotropical fauna of Biantinae has been insufficiently studied, resulting in a substantial lack of understanding its diversity. While South Africa and Madagascar boast the highest number of recorded species (e.g., Lawrence 1959; Kauri 1961), most African countries have only one or two documented biantin species (Fig. 41), highlighting a significant bias. Consequently, the discovery of numerous new species in previously unstudied collections is not uncommon, making the finding of five new species of *Metabiantes* in this study an unsurprising outcome.

Despite the shared trait of dimorphic legs II among all new species of *Metabiantes* and *Clinobiantes paradoxus*, we identified distinguishing characteristics that allow for a differentiation between species distributed farther west and those distributed farther east in continental Africa. Western species, such as *Metabiantes elongatus* sp. nov. (Bas-Congo), *Metabiantes serratus* sp. nov. (Bas-Congo), and *Clinobiantes paradoxus* (Cameroon), share common traits, including a conspicuous armature on mesotergal areas III–V. Additionally, both *Metabiantes serratus* and *Clinobiantes paradoxus* exhibit a marked constriction demarcating the limits of the astragalus and a reduced calcaneus in metatarsus II, a trait that is less pronounced in *Metabiantes elongatus*, conceivably due to the species' distinctly elongated appendages (see subsequent discussion). Further, *Metabiantes serratus* and *Metabiantes elongatus* are distinguished by the presence of trichomes with a wider ovate-shaped base on the calcaneus surface, visible only in SEM images (Figs 10H, 36H). Also, the pedipalp tarsus lacks a spheroid shape (Figs 7C, 35A vs Figs 15E, 21E, 27A), and the male genitalia in all these species feature rounded and short laminae apicalis, which are spaced apart, along with conductors that exhibit lateral projections (Figs 11B, 37B).

In contrast, the most easternward distributed species, such as *Metabiantes herculeus* sp. nov. (Tanzania) and *Metabiantes kaurii* sp. nov. (Mozambique), lack armature in the mesotergal areas III–V. These

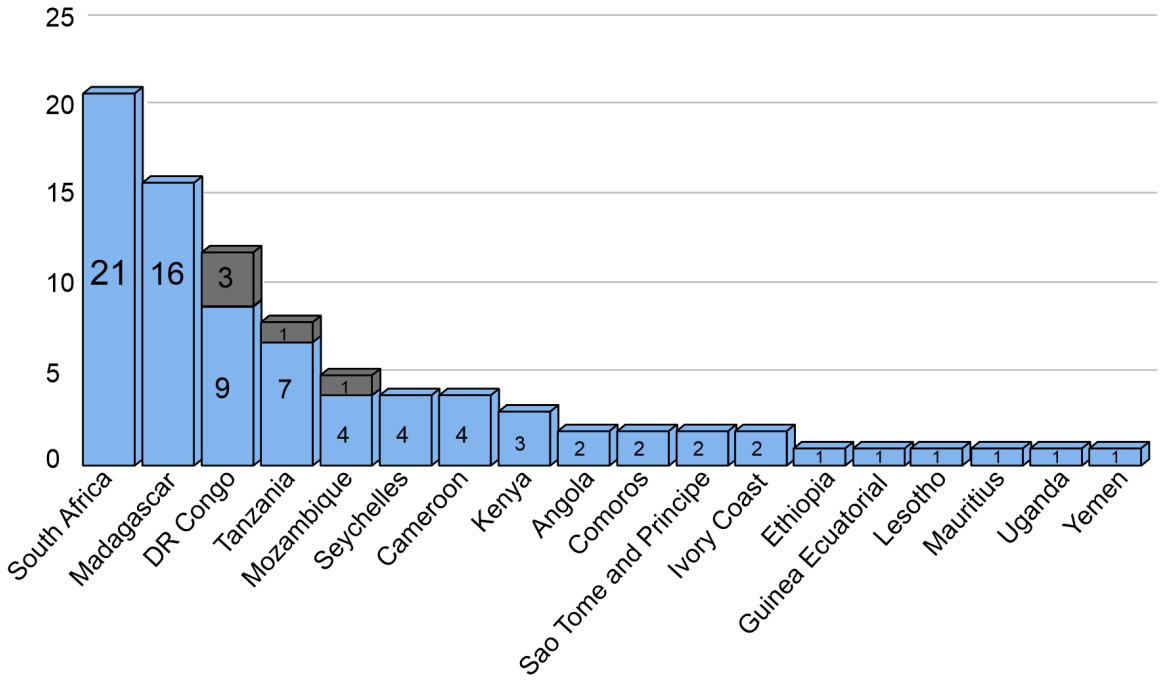

Fig. 41. Total number of recorded species of Biantinae Thorell, 1889 per African country and Yemen (bright-blue) and number of new species of Biantinae described in this work (gray).

species do not exhibit a strong constriction, demarcating the astragalus-calcaneus boundary in metatarsus II; in contrast, these species exhibit the calcaneus occupying approximately half the length of the podomere (Figs 17E, 23G). Additionally, the metatarsal calcaneus II features rounded and short trichomes (Figs 17F, 23F), and the pedipalp tarsus has a spheroid shape (Figs 15E, 21E). The male genitalia of both species are characterized by a prominent lamina apicalis with a long, narrow medial cleft and closely aligned thin halves (Figs 18B, 24B). Furthermore, the capsula interna lacks the two broad lateral projections observed in other species (Figs 18B, 24B vs Figs 4B, 11B, 29B).

Metabiantes kivuensis sp. nov., centrally distributed, exhibits intermediate exo-morphological and male genital characteristics. It shares with the western group (*M. elongatus* sp. nov., *M. serratus* sp. nov., and *Clinobiantes paradoxus*) the presence of trichomes with a wider ovate-shaped base on the metatarsal calcaneus II, which, though relatively short, lacks a distinct delimiting constriction (Fig. 28E). The male genitalia feature a rounded and short lamina apicalis, which is spaced apart, alongside conductors with lateral projections (Fig. 29B). Conversely, *M. kivuensis* shares with the eastern species (*M. herculeus* sp. nov. and *M. kaurii* sp. nov.) the absence of armature on areas III–V (Fig. 26A). Only *Metabiantes kivuensis* exhibits a medially divided area IV and includes tubercles with aggregate pores on the ventral surface of the pedipalp tarsus, but the presence of this last trait needs to be verified in *M. herculeus* and *M. kaurii*. The limited understanding of the central African biantid fauna suggests that additional morphologically intermediate species remain undiscovered. These findings are critical for elucidating the evolution of morphology in this group. However, the lack of molecular data is a limitation of this study, and further integrative taxonomic and systematic revisions incorporating both detailed morphological analyses and molecular data are essential for determining if both genera are synonyms and to testing the monophyly of the current *Metabiantes* concept.

Finally, we emphasize that sympatric *Metabiantes elongatus* sp. nov. and *Metabiantes serratus* sp. nov. may exhibit specific microhabitat preferences. At the same locality, specimens of *M. elongatus* were collected by fogging, while those of *M. serratus* were gathered by sieving forest litter. Although their male genitalia are strikingly similar, likely indicating a close phylogenetic relationship, the external morphology differs markedly, potentially reflecting microhabitat adaptations. The leaf-dwelling *M. elongatus* is characterized by thinner and longer legs – especially leg IV – and a light-yellow body coloration. In contrast, the leaf-litter-dwelling *M. serratus* displays shorter legs and a darker body and appendages. Such morphological differences may be strongly linked to microhabitat preferences, as observed in other arthropods, including Sclerosomatidae Simon, 1879 harvestmen (Curtis & Machado 2007; Proud *et al.* 2012), Pholcidae C.L. Koch, 1851 spiders (Eberle *et al.* 2018; Huber *et al.* 2019), Acrididae MacLeay, 1821 grasshoppers (García-Navas *et al.* 2017), and Ceratocanthidae Martínez, 1968 beetles (Ballerio & Wagner 2005; Ballerio & Grebennikov 2016). In these groups, longer legs and lighter coloration are typically associated with arboreal species, while shorter legs and darker coloration are traits of ground or leaf-litter-dwelling species. In the case of our biantid species, this pattern presents an intriguing hypothesis deserving a robust phylogenetic framework to better understand the evolutionary implications of these adaptations.

Acknowledgments

VM acknowledges the PhD fellowship of the Consejo Nacional de Investigaciones Científicas y Técnicas (CONICET), Argentina. This research was supported by the SYNTHESYS+ project (http://www.synthesys.info/), funded by the European Community Research Infrastructure Action under the H2020 Integrating Activities Programme, Project number 823827 (to APG), and by the Fondo para la Investigación Científica y Tecnológica (projects PICT 2015-2202 and PICT-2019-2745), and Consejo Nacional de Investigaciones Científicas y Técnicas (project PUE 098), Argentina. APG extends sincere thanks to Didier Van den Spiegel, Arnaud Henrard, Christophe Allard, and Larissa Smirnova for their assistance and hospitality during the visit to the RMCA. Special gratitude is owed to Dr Peter

Jäger, Julia Altman, and Jana Grueger (Senckenberg Museum Frankfurt) for loaning the *Clinobiantes paradoxus* syntypes. We are deeply thankful to Fabián Tricárico for his kind support and assistance during the Scanning Electron Microscopy sessions at MACN. We also express gratitude to Alberto Ballerio and Alexander Riedel, who generously shared information and references on morphological traits distinguishing canopy and ground-dwelling Coleoptera. Fieldwork in Mozambique was supported by the Critical Ecosystem Partnership Fund (Afromontane Hotspots Fund), the Royal Geographical Society (with IBG) through a Neville Shulman Challenge Award, The Rift Valley Corporation, and World Wildlife Fund Belgium. We sincerely appreciate the two reviewers for their detailed and thorough reviews, which significantly improved the manuscript.

References

Acosta L.E., Pérez-González A. & Tourinho A.L. 2007. Methods for taxonomic study. *In*: Pinto-da-Rocha R., Machado G. & Giribet G. (eds) *Harvestmen: The Biology of Opiliones*: 494–510. Harvard University Press, Cambridge.

Ballerio A. & Grebennikov V. 2016. Rolling into a ball: Phylogeny of the Ceratocanthinae (Coleoptera: Hybosoridae) inferred from adult morphology and origin of a unique body enrollment coaptation in terrestrial arthropods. *Arthropod Systematics & Phylogeny* 74 (1): 23–52. https://doi.org/10.3897/asp.74.e31837

Ballerio A. & Wagner T. 2005. Ecology and diversity of canopy associated Ceratocanthidae (Insecta: Coleoptera, Scarabaeoidea) in an Afrotropical rainforest. *In*: Huber B.A., Sinclair B.J. & Lampe K.-H. (eds) *African Biodiversity. Molecules, Organisms, Ecosystems*: 125–132. Springer US, Boston, MA. https://doi.org/10.1007/0-387-24320-8_8

Buzatto B.A. & Machado G. 2014. Male dimorphism and alternative reproductive tactics in harvestmen (Arachnida: Opiliones). *Behavioural Processes* 109: 2–13. https://doi.org/10.1016/j.beproc.2014.06.008

Curtis D.J. & Machado G. 2007. Ecology. *In*: Pinto-da-Rocha R., Machado G. & Giribet G. (eds) *Harvestmen: The Biology of Opiliones*: 280−308. Harvard University Press, Cambridge.

Eberle J., Dimitrov D., Valdez-Mondragón A. & Huber B.A. 2018. Microhabitat change drives diversification in pholcid spiders. *BMC Evolutionary Biology* 18 (1): 141. https://doi.org/10.1186/s12862-018-1244-8

García-Navas V., Noguerales V., Cordero P.J. & Ortego J. 2017. Phenotypic disparity in Iberian short-horned grasshoppers (Acrididae): The role of ecology and phylogeny. *BMC Evolutionary Biology* 17 (1): 109. https://doi.org/10.1186/s12862-017-0954-7

Gnaspini P. & Rodrigues G.C.S. 2011. Comparative study of the morphology of the gland opening area among Grassatores harvestmen (Arachnida, Opiliones, Laniatores). *Journal of Zoological Systematics and Evolutionary Research* 49 (4): 273–284. https://doi.org/10.1111/j.1439-0469.2011.00626.x

Gong X., Martens J. & Zhang C. 2018. Two new species of *Biantes* from China and Malaysia (Opiliones: Laniatores: Biantidae). *Zootaxa* 4461 (4): 587–599. https://doi.org/10.11646/zootaxa.4461.4.8

Huber B.A., Caspar K.R. & Eberle J. 2019. New species reveal unexpected interspecific microhabitat diversity in the genus *Uthina* Simon, 1893 (Araneae: Pholcidae). *Invertebrate Systematics* 33 (1): 181–207. https://doi.org/10.1071/IS18002

Kauri H. 1961. Opiliones. *In*: Hanström B., Brinck P. & Rudebeck G. (eds) *South African Animal Life. Results of the Lund University Expedition in 1950–1951*: 9–197. Almquist & Wiksell, Uppsala.

Kauri H. 1985. Opiliones from central Africa. *Annalen Zoologische Wetenschappen* 245: 1–168.

Kury A.B. & Medrano M. 2016. Review of terminology for the outline of dorsal scutum in Laniatores (Arachnida, Opiliones). *Zootaxa* 4097 (1): 130–134. https://doi.org/10.11646/zootaxa.4097.1.9

Kury A.B. & Pérez-González A. 2007. Biantidae Thorell, 1889. *In*: Pinto-da-Rocha R., Machado G. & Giribet G. (eds) *Harvestmen: The Biology of Opiliones*: 176–179. Harvard University Press, Cambridge.

Kury A.B., Mendes A.C., Cardoso L., Kury M.S., Granado A.A., Cruz-López J.A., Longhorn S.J., Medrano M., Kury I.S. & Souza-Kury M.A. 2022. World Catalogue of Opiliones. WCO-Lite Version 2.5.0. Available from https://wcolite.com/ [accessed 5 Mar. 2024].

Lawrence R.F. 1931. The harvest-spiders (Opiliones) of South Africa. *Annals of the South African Museum* 29: 341–508. Available from https://www.biodiversitylibrary.org/page/40891864 [accessed 5 Mar. 2024].

Lawrence R.F. 1933. The harvest-spiders (Opiliones) of Natal. *Annals of the Natal Museum* 7 (2): 211–241.

Lawrence R.F. 1937a. A collection of Arachnida from Zululand. *Annals of the Natal Museum* 8: 211–273.

Lawrence R.F. 1937b. The external sexual characteristics of South African harvest-spiders. *Transactions of the Royal Society of South Africa* 24: 331–337.

Lawrence R.F. 1949. A collection of Opiliones and scorpions from North-East Angola made by Dr A. de Barros Machado in 1948. *Publicacões culturais da Companhia de Diamantes de Angola* 6: 1–20.

Lawrence R.F. 1957. A third collection of Opiliones from Angola. *Publicacões culturais da Companhia de Diamantes de Angola* 34.

Lawrence R.F. 1959. *Arachnides-Opilions*. Faune de Madagascar 9. Publications de l'Institut de Recherche scientifique, Tananarive – Tsimbazaza.

Lawrence R.F. 1962. LXXIV.– Opiliones. *In*: *Résultats scientifiques des Missions zoologiques de l`IRSAC en Afrique orientale – (P. Basilewsky et N. Leleup, 1957)*: 9–89. Annales du Musée royal de l'Afrique centrale (Sciences zoologiques) 110.

Lawrence R.F. 1963. The Opiliones of the Transvaal. *Annals of the Transvaal Museum* 24: 275–304.

Loman J.C.C. 1898. Beiträge zur Kenntniss der Fauna von Süd-Afrika. Ergebnisse einer Reise von Prof. Max Weber im Jahre 1894. IV. Neue Opilioniden von Süd-Afrika und Madagaskar. *Zoologische Jahrbücher, Abteilung für Systematik, Geographie und Biologie der Thiere* 11: 515–531. https://www.biodiversitylibrary.org/page/9984174 [accessed 5 Mar. 2024].

Pérez-González A. & Werneck R.M. 2018. A fresh look over the genital morphology of *Triaenonychoides* (Opiliones: Laniatores: Triaenonychidae) unravelling for the first time the functional morphology of male genitalia. *Zoologischer Anzeiger* 272: 81–92. https://doi.org/10.1016/j.jcz.2017.12.010

Pocock R.I. 1902. On some new harvest-spiders of the order Opiliones from the southern continents. *Procceedings of the Zoological Society of London* 1902 (2): 392–413.
Available from https://www.biodiversitylibrary.org/page/31543511 [accessed 5 Mar. 2024].

Proud D.N., Felgenhauer B.E., Townsend V.R., Osula D.O., Gilmore W.O., Napier Z.L. & Van Zandt P.A. 2012. Diversity and habitat use of Neotropical harvestmen (Arachnida: Opiliones) in a Costa Rican Rainforest. *ISRN Zoology* 2012: 1–16. https://doi.org/10.5402/2012/549765

Roewer C.F. 1912. Die Familie der Cosmetiden Opiliones-Laniatores. *Archiv für Naturgeschichte, Abteilung A* 78 (10): 1–122. Available from https://www.biodiversitylibrary.org/page/13317265 [accessed 5 Mar. 2024].

Roewer C.F. 1913. Arachnides. I. Opiliones. *In*: *Voyage de Ch. Alluaud et R. Jeannel en Afrique orientale (1911–1912). Résultats scientifiques* 2: 1–22. A. Schultz, Paris.

Roewer C.F. 1915. 106 neue Opilioniden. *Archiv für Naturgeschichte, Abteilung A* 81 (3): 1–152. Available from https://www.biodiversitylibrary.org/page/13218633 [accessed 5 Mar. 2024].

Roewer C.F. 1923. Die Weberknechte der Erde. *Systematische Bearbeitung der bisher bekannten Opiliones*. Gustav Fischer, Jena.

Roewer C.F. 1927. Weitere Weberknechte I. *Abhandlungen des Naturwissenschaftlichen Vereins zu Bremen* 26 (2): 261–402.

Roewer C.F. 1949. Über Phalangodidae II. Weitere Weberknechte XIV. *Senckenbergiana* 30 (4): 247–289.

Roewer C.F. 1961. Opilioniden aus Ost-Congo und Ruanda-Urundi. *Annalen Zoologische Wetenschappen, Koninklijk Museum voor Midden-Afrika* 95: 1–48.

Santos R. & Prieto C.E. 2009. Los Assamiidae (Opiliones: Assamiidae) de Río Muni (Guinea Ecuatorial), con la descripción de ocho nuevas especies. *Revista de Biología Tropical* 58 (1): 203–243. https://doi.org/10.15517/rbt.v58i1.5205

Schwendinger P.J. & Martens J. 2002. A taxonomic revision of the family Oncopodidae III. Further new species of *Gnomulus* Thorell (Opiliones, Laniatores). *Revue suisse de Zoologie* 109: 47–113. https://doi.org/10.5962/bhl.part.79580

Shorthouse D.P. 2010. SimpleMappr, an online tool to produce publication-quality point maps. Available from http://simplemappr.net [accessed 6 Mar. 2024].

Shultz J.W & Pinto-da-Rocha R. 2007. Morphology and functional anatomy. *In*: Pinto-da-Rocha R., Machado G. & Giribet G. (eds) *Harvestmen: The Biology of Opiliones*: 14–61. Harvard University Press, Cambridge.

Sørensen W. E. 1910. Opiliones. *In*: Sjöstedt Y. (ed.) *Wissenschaftliche Ergebnisse der Schwedischen Zoologischen Expedition nach dem Kilimandjaro, dem Meru und den umgebenden Massaisteppen Deutsch-Ostafrikas 1905–1906* 3 (20): 59–82. pl. 4. P. Palmquist, Stockholm. https://doi.org/10.5962/bhl.title.1805

Staręga W. 1992. An annotated check-list of Afrotropical harvestmen, excluding the Phalangiidae (Opiliones). *Annals of the Natal Museum* 33 (2): 271–336.

Thorell T.T.T. 1889. Viaggio di Leonardo Fea in Birmania e regione vicine. XXI. Aracnidi Artrogastri Birmani raccolti da L. Fea nel 1885–1887. *Annali del Museo Civico di Storia Naturale di Genova* 27: 521–729. Available from https://www.biodiversitylibrary.org/page/35996191 [accessed 5 Mar. 2024].

Wolff J.O., Schönhofer A.L., Martens J., Wijnhoven H., Taylor C.K. & Gorb S.N. 2016. The evolution of pedipalps and glandular hairs as predatory devices in harvestmen (Arachnida, Opiliones). *Zoological Journal of the Linnean Society* 177 (3): 558–601. https://doi.org/10.1111/zoj.12375

Printed versions of all papers are deposited in the libraries of four of the institutes that are members of the *EJT* consortium: Muséum national d'Histoire naturelle, Paris, France; Meise Botanic Garden, Belgium; Royal Museum for Central Africa, Tervuren, Belgium; Royal Belgian Institute of Natural Sciences, Brussels, Belgium. The other members of the consortium are: Natural History Museum of Denmark, Copenhagen, Denmark; Naturalis Biodiversity Center, Leiden, the Netherlands; Museo Nacional de Ciencias Naturales-CSIC, Madrid, Spain; Leibniz Institute for the Analysis of Biodiversity Change, Bonn – Hamburg, Germany; National Museum of the Czech Republic, Prague, Czech Republic; The Steinhardt Museum of Natural History, Tel Aviv, Israël.